EXPLORING THE TRANSCRIPTIONAL AND TRANSLATIONAL PROFILES OF CELLS ACROSS THE OLIGODENDROCYTE LINEAGE

Antoinette Foster

A thesis submitted in fulfilment for the degree of Doctor of Philosophy

Presented to the Neuroscience Graduate Program and the Oregon Health & Science University
School of Medicine

Table of Contents

Acknowledgments

I would like to thank the many members of the Emery lab. First, I would like to thank Dr. Ben Emery for his scientific mentorship, guidance, and training, including rigorous experimentation, effective grant writing, presentation skills; you've greatly influenced the direction of my career. I would also like to thank past lab members Dr. Biliana Velva-Rotse, Dr. Helena Bujalka, and AeSoon Benson, particularly for their personal and emotional investment in my success. Lastly, I would like to thank the current members of the Emery Lab, Dr. Gregory Duncan, Michael McCane, Hannah Collins, and Dr. Tyrell Simkins. You all contribute to a healthy and productive lab environment and I appreciate your dedication to each other's success, as well as my own.

I owe many thanks to my dissertation advisory committee, Dr. Marc Freeman, Dr. Kelly Monk, Dr. Philip Stork, Dr. Gail Mandel, and my outside examiner, Dr. Anthony Barnes. You have all dedicated your personal time to ensuring my success inside and outside of DAC meetings. I greatly appreciate your mentorship and guidance.

My gratitude towards those involved with the creation and support of the Alliance for Visible Science in Diversity goes beyond words. To the co-founders of the Alliance for Visible Diversity in Science, Dr. Kathleen Beeson, Dr. Letisha Wyatt, and Dr. Lucille Moore, key faculty members, Dr. Gary Westbrook, Dr. Peter Barr-Gillepse, Dr. Kelly Monk, and Dr. Marc Freeman, as well as the ***many*** others who made AVDS possible- thank you. To AVDS members- you all have the ability to change the world and I am beyond honored to have worked with you. Regardless if it is appreciated, implemented, or accepted, the broader impact that you made will continue to affect change longer after you are gone. I deeply value what we've created. I would also like to thank the broader social justice community for your continuous and undervalued

dedication to radical change. I also give thanks to the culture-because everything that there is came from you, and without you, there is nothing. I would also like to thank my parents, my family, and my extended family, including the Williams family, for your continued support throughout this process.

Finally, no experimental work is completed in isolation. I would like to acknowledge the following scientific and intellectual contributions:

1) Sophie Johnson for her dedication to monotonous cell counting. Although the final cell quantifications obtained by Sophie were not used in the final version of this thesis, Sophie's dedication and work verified results important to our final conclusions regarding cell specificity in the INTACT and RiboTag lines.
2) Dr. Jonathan Nelson for his intellectual contributions regarding RNA-sequencing analysis outlined in Chapter 3. He generously offered his time, intellect, and guidance and became an invaluable resource to me.
3) Dr. James McGann for personally training and assisting me in establishing the INTACT method discussed throughout this thesis. Thank you for your kindness and interest in my success. Additionally, I would like to thank Dr. Gail Mandel for assisting our lab in establishing the INTACT method.
4) Dr. Ben Emery for performing the RiboTag immunopurification described in Chapter 3 and Chapter 4.
5) Dr. Rory Morgan for his extensive contributions, including zebrafish breeding, husbandry, CRISPR injections, and imaging (Chapter 3, Fig. 5 & Fig. S5). Dr. Morgan also dedicated his personal time to teach me several aspects of sg-design and synthesis. Your work helped me graduate. I deeply appreciate your contribution. I would like to

additionally acknowledge Dr. Kelly Monk for her personal dedication to the completion of this work.

6) Dr. Carlie Cullen for performing all iTBS manipulations outlined in Chapter 4.

Abstract

Oligodendrocytes are specialized central nervous glia that progress through distinct cellular stages, each with its own specific morphological features, specific proteins, and function. Oligodendrocyte progenitor cells (OPCs) represent the proliferative stem cell population that acts to maintain homeostatic oligodendrocyte numbers and have been shown to respond to neural activity as well as injury and disease. The role that oligodendrocytes play in signal propagation by wrapping axons in a non-conducting sheath represents the most well-known function of myelinating oligodendrocytes. A more recent focus on oligodendrocyte's potential for plasticity and metabolic support expands the possible functions for these dynamic cells, but also leaves major gaps in our understanding of potential mechanisms underlying these newly proposed functions. The overall goal of this dissertation is to study oligodendrocyte gene expression as a pathway towards understanding potentially relevant mechanisms regulating oligodendrocyte biology. Towards this goal, our first aim compared the transcriptome and translatome of OPCs and mature oligodendrocytes by taking advantage of the recent RNA immunopurification approaches, INTACT and RiboTag. Our second aim attemped to assess the oligodendrocyte transcriptional and translational response to increased neuronal activity. Together, the data presented here advances the understanding of the transcriptional and translational states of OPCs and mature oligodendrocytes within and outside of the context of increased activity.

Chapter 1- Introduction to Oligodendroglia: Function, Development, and RNA Profiling

1.1 Introduction to Oligodendroglia

1.1.1 Evolution and Function

Over the course of evolutionary history species evolved from small invertebrates to comparatively giant vertebrates. Species within each group are taxed with the challenge of transporting information from neuron to neuron on a functionally relevant time scale. The modulation of this time scale, or conduction velocity, is hugely important for coordinated responses and information processing. Axons in both invertebrates and vertebrates achieve suitable conduction velocities; however, the way by which this happens is quite different.

There are two basic mechanisms that nervous systems evolved to optimize conduction velocity. Many invertebrates, such as tube worms, squid, lobsters, and crayfish exhibit axonal giantism (Hartline and Colman, 2007). Increasing axonal diameter increases conduction velocity, therefore, many invertebrates tend to have larger-diameter axons for signals that require fast transmission. For example, the giant squid axon is used as part of the escape response and is roughly 1-1.5 mm in diameter, while the median size of an axonal diameter in invertebrates falls around 0.5 µm (Caldwell, 2009; Perge et al., 2012). Locusts demonstrate the same trend; the largest axons in a locust are interneurons that trigger the escape response (Bräunig and Burrows, 2004). However, there are limits to this solution. In vertebrate animals, long range axons such as those from dorsal root ganglion neurons can run from the base of the spinal cord to the most dorsal point of the body. Even more challenging, many of these long-range axons exist within the bony structures of the brain and spinal cord in vertebrates, making the solution of simply increasing axonal diameter a limited solution. How can such large animals maintain efficient conduction speeds over such long distances? Specialized cells called Schwann cells within the peripheral nervous system, and oligodendrocytes within the central nervous system, tightly wrap specific

segments of the axon in a structure called the myelin sheath. This insulation by the non-conducting myelin sheath increases membrane resistance by preventing the movement of free ions and reduces the axons membrane capacitance (Hartline and Colman, 2007; Hodgkin, 1954; Moore et al., 1978). The increase in resistance and decrease in capacitance reduces the flow of ionic current within the internodal space, speeds ion charging within the internode, and lowers the change in ion concentration required for an action potential (Hartline and Colman, 2007; Hodgkin, 1954; Moore et al., 1978).

Broadly speaking, invertebrates evolved more towards axonal giantism and vertebrates evolved more towards insulation otherwise known as myelination, however, this is a generalization. Myelination is observed in both invertebrates and vertebrates; likewise, both invertebrates and vertebrates have axons several times larger than other axons within an individual organism (Hartline and Colman, 2007). Regardless, the physical limitations of increasing axonal caliber makes myelination a brilliant solution. Indeed, myelination allows for humans and other species to maintain similar axonal diameters and rapid conduction velocities over vastly larger body sizes.

1.1.1.2 Oligodendrocyte function: Saltatory conduction

The role of oligodendrocytes in the propagation of electrical signals represents the most well studied oligodendrocyte function. Initially, neuronal axons are unmyelinated with voltage-gated sodium channels distributed over the length of the axon. Once an oligodendrocyte deposits and wraps myelin around the axon, to form the structure known as the internode, voltage-gated sodium channels are clustered into a restricted space called the node of Ranvier (Michalski and Kothary, 2015). Once the electrical signal moves through the myelinated region, it activates and

opens the high-density sodium channels. This sodium influx adds to the current electrical signal, allowing for the further prorogation of the electrical signal, a process known as saltatory conduction (Michalski and Kothary, 2015). Axonal myelination not only increases conduction over long distances, but also allows for the fine tuning of these electrical signals (see section 1.6.2 for further discussion). This timing and fine tuning of signaling is critically important for complex synchronization along the neuronal network (Fields, 2008). Until recently, the known function of oligodendrocytes was mainly restricted to their myelinating capacity, with their ability to increase axonal conduction speeds representing their only function. Recent research expanded the role of oligodendrocytes away from their sole role as myelination machines to active contributors to neuronal health via trophic and metabolic support.

1.1.1.3 Oligodendrocyte function: Metabolic support

Besides their importance in saltatory conduction, oligodendrocytes also play a role in the survival of myelinated axons (Griffiths et al., 1998; Kassmann et al., 2007; Lappe-Siefke et al., 2003). Recently, the discovery of metabolic coupling between oligodendrocytes and neurons shed light on potential mechanisms underlying oligodendrocytes' influence on the survival of neurons (For a detailed review on this topic see (Saab and Nave, 2017)). This body of research demonstrates that oligodendrocytes are capable of supplying lactate/pyruvate to neurons as a form of energy support, a mechanism potentially employed during times of high neuronal energy demand.

Two important pathways are used for the production of ATP: glycolysis, which occurs in the cytoplasm, and the Krebs cycle, which produces ATP within the mitochondria. In 2012, Fünfschilling and colleagues utilized a conditional knockout mouse line lacking the *Cox10* gene in postmitotic oligodendrocytes to test the relative importance of mitochondrial ATP to

oligodendrocytes and Schwann cells (Fünfschilling et al., 2012). The *Cox10* gene encodes for Cytochrome C oxidase (COX), which is an essential component in the electron transport chain within the mitochondria. If oligodendrocytes depend on mitochondrial ATP, the absence of COX will likely result in glial cell death. Mutant mice displayed no detectable signs of white matter pathology and no observable demyelination or changes to axonal integrity. Interestingly, both the cortex and white matter showed increased brain lactate via magnetic resonance spectroscopy only during anesthesia. Lactate levels quickly fell after removal of anesthesia, indicating that this increased concentration of lactate was not released in the blood stream but locally metabolized. This research suggests a model where oligodendrocytes produce lactate via aerobic glycolysis and are capable to transferring this potential energy source to other cells.

Within only a few months, Lee and colleagues showed that the monocarboxylate transporter MCT1, which rapidly transports many monocarboxylates such as lactate and pyruvate, is expressed in mature oligodendrocytes *in vivo* (Lee et al., 2012b). Previously published work demonstrated the expression of MCT2 in neurons (Pierre et al., 2000; Rafiki et al., 2003), suggesting MCT1/MCT2 may play a role in shuttling lactate from oligodendrocytes to neurons. Using various *in-vitro* and *in vivo* methods to disrupt MCT1 expression, researchers showed that neuronal survival depends on the oligodendrocyte expression of MCT1, lending credence to the notion that oligodendrocytes are capable of metabolically supporting neurons (Lee et al., 2012b). Considering that excessive lactate leads to lactic acidosis suggests regulated signaling must occur between neurons and oligodendrocytes to avoid a constant supply of lactate. In an interesting and more recent publication, Meyer et al. showed that oligodendrocytes in the corpus callosum provide energy to axons through the delivery of glucose, not lactate, suggesting a separate mechanism

employed by cells in the white matter region (Meyer et al., 2018). Together, these mechanisms have been proposed to occur along the axons to help meet the energy demand of the axon.

1.1.1.4 Oligodendrocyte function: Trophic Support

Several early studies suggest that oligodendrocytes secrete soluble factors that influence neuronal differentiation, growth, and survival (Colello et al., 1994; Griffiths et al., 1998; Meyer-Franke et al., 1995). Indeed, oligodendrocytes express many known trophic factors such as nerve growth factor (NGF) (Byravan et al., 1994; Dai et al., 2003) , EGF-like growth factor (Nakagawa et al., 1998), insulin growth factor (IGF) (Evercooren et al., 1991; Wilkins et al., 2001) , glial-derived nerve growth factor (GDNF) (Strelau and Unsicker, 1999; Wilkins et al., 2003), brain-dervied nerve growth factor (BDNF) (Dai et al., 2003), and neutrotrophin-3 (NT-3) (Dai et al., 2003). Of these many trophic factors, IGF-1, GDNF and BDNF have been shown to be functional important to neurons.

In 2001, Wilkins et al. demonstrated that conditioned media from oligodendrocyte progenitor cells promotes the survival of cultured neurons (Wilkins et al., 2001). Additionally, neutralizing antibodies against IGF-1 blocked this survival effect while the addition of recombinant IGF-1 promoted neuronal survival. In a follow-up study, Wilkins et al. showed that both oligodendrocyte progenitor cell and mature oligodendrocyte conditioned media promotes the survival of neuronal cells in culture working through a phosphatidylinositol 3'-kinase (PI3kinase)/Akt-dependent mechanism (Wilkins et al., 2003). Interestingly, conditioned media from mature oligodendrocytes, but not oligodendrocyte progenitor cells, increased axon length. This indicated the involvement of additional important oligodendrocyte derived trophic factors and involved the MAPK/Erk1/2 signaling pathway. Wilkins et al. showed differentiated

oligodendrocytes express GDN and neutralizing antibodies against GDNF resulted in the reduction of axon length. Additionally, GDNF was shown to activate the MAPK/Erk1/2 signaling pathway indicating that the oligodendrocyte derived trophic factors play a role in axonal growth apart from the survival effects seen with IGF-1.

Similarly, oligodendrocyte derived BDNF and NT-3 increase the survival and activity of cultured basal forebrain cholinergic neurons (Dai et al., 2003). Dai et al. demonstrated that oligodendrocytes express BDNF, NT-3, and NGF (Dai et al., 2003). However, neutralizing antibodies against both BDNF and NT-3, but not NGF, significantly reduced cholinergic neuronal activity. Whether additional oligodendrocyte expressed trophic factors affect neuronal functioning remains to be seen.

1.2 Oligodendrocyte development

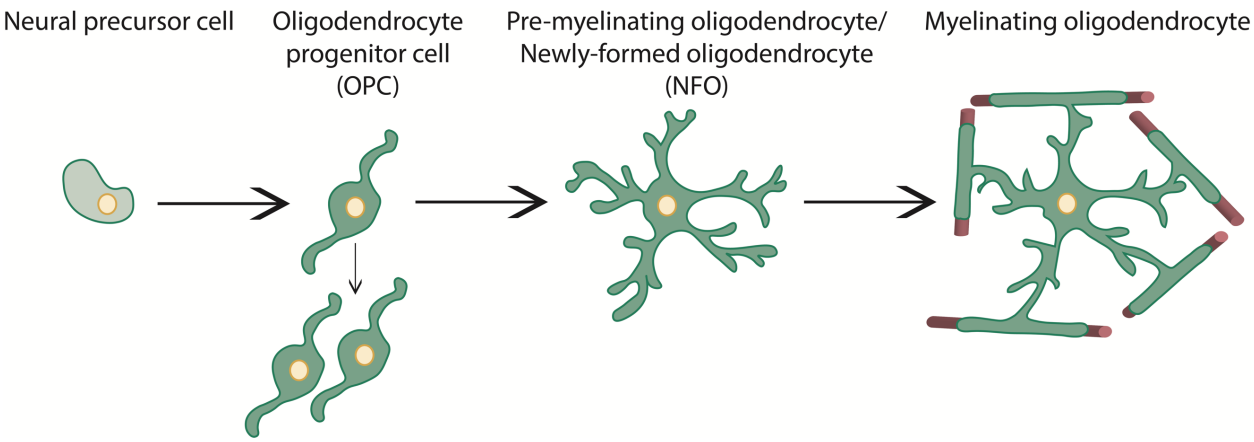

Figure 1: Oligodendroglial lineage progression

Oligodendrocytes move through distinct stages of development. Oligodendrocyte progenitor cells (OPCs) are derived from neural progenitor cells and are the resident oligodendrocyte progenitor population. These migratory cells can either proliferate to form additional OPCs or make the terminal decision to become newly-formed oligodendrocytes (NFOs). As pre-myelinating oligodendrocytes mature, they upregulate essential lipids and proteins required for the process of

myelination and use exploratory processes to select axons. In the final stage of maturation, myelinating oligodendrocytes ensheath axons by wrapping a lipid-rich membrane around the axon.

1.2.1 Origins

Oligodendrocyte lineage cells progress through distinct cellular states defined by specific morphological features and proteins; the progenitor state, otherwise known as oligodendrocyte progenitor cells (OPCs), pre-myelinating oligodendrocytes, and finally, myelinating oligodendrocytes (Fig. 1). OPCs are stellate in appearance and exist through the entire CNS (Michalski and Kothary, 2015). Within the spinal cord, brainstem, and the forebrain, oligodendrocytes arise from both ventral and dorsal sources. Within the forebrain, OPCs first arise from the medial ganglionic eminence (MGE), where they migrate both dorsally and laterally. In mouse, these cells are found within the cortex by E16 and populate the area by E18. They are joined by a secondary wave of progenitors from the lateral/caudal ganglionic eminence, with a final wave of progenitors derived from the cortical areas (Richardson et al., 2006). OPCs are highly motile cells that send out fine processes that survey surrounding areas while determining the location of their final position. OPCs are evenly distributed across the brain; a tiling behavior dependent on self-repulsion cues (Castro and Bribián, 2005). Given their wide distribution, OPCs may travel great distances to reach their final destination.

To ensure appropriate coverage, an excess number of OPCs are produced (Kessaris et al., 2005; Viganò et al., 2016). This is followed by a subsequent elimination process thought to be mediated by competition for the limited amounts of target-derived growth and survival factors such as platelet-derived growth factor alpha (PDGFα), fibroblast growth factor (FGF)-2, insulin-

like growth factor (IGF)-1, neurotrophin (NT)-3, and ciliary neurotrophic factor (CNTF) (Barres and Raff, 1994; Calver et al., 1998; Fruttiger et al., 1999; Miller, 2002).

OPCs represent the largest population of proliferating cells in the adult brain, constituting roughly 5% of total CNS cells (Dawson et al., 2003). OPCs continue to proliferate well into adulthood, although the rate declines with age and differ depending on the brain region (Young et al., 2013). OPCs either remain in the progenitor state, giving rise to additional OPCs, or the cell differentiates into a pre-myelinating oligodendrocyte (Fig. 1). Interestingly, the subventricular zone can give rise to new OPCs in adulthood, especially in the context of demyelination, as they can acutely respond and migrate to lesion areas (Nait-Oumesmar et al., 2007; Nakatani et al., 2013; Serwanski et al., 2018; Xing et al., 2014)

1.2.2 Migration

How is it possible for cells to move across such a complex landscape to reach their final destination? Interactions with the extracellular matrix, cell-surface proteins, and secreted molecules from various cell types impact OPC migration during development. Extracellular proteins such as fibronectin and merosin promote OPC migration, while tenascin-C selectively inhibits the fibronectin, but not the merosin, response to migration (Frost et al., 1996). Membrane expression of proteins such as N-CADHERIN allow OPCs to adhere to the surface of other cells, and the OPC expression of the membrane-anchored Ephrin ligands, ephrin B2/B3, interact with the axonal expression of the EPHRINB$_2$ receptor to impact the distribution of OPCs (Prestoz et al., 2004). Secreted growth factors such as FGF-2 and PDGF promote the migration of OPCs (Armstrong et al., 1990; Milner et al., 1997; Simpson and Armstrong, 1999), and studies suggest that Netrin and the various proteins within the semaphorin family act as both an attractive and

repulsive cue depending on the stage of development and brain region (Deiner and Sretavan, 1999; Jarjour et al., 2003; Sugimoto et al., 2001; Tsai et al., 2003).

In addition to the aforementioned mechanisms OPCs use for migration, Tsai and collogues recently demonstrated that OPCs also migrate along the vasculature matrices during development in both mice and humans (Tsai et al., 2016). Using a combination of mouse Cre-lines and *in-vitro* slice culture, researchers showed that OPCs associate with the vascular scaffold as they emerge from the MGE. As early as E12, 58% of OPCs position their cells bodies directly onto a blood vessel, and 67% show at least one process associated with a blood vessel. OPCs were observed to either trail along the vessel, or extend a process from one blood vessel to jump to a new vessel. Additionally, mutant mice that display defective vascular architecture also showed abnormal OPC accumulation near ventricular zones, resulting in 70% fewer OPCs within the surrounding gray matter (Tsai et al., 2016). The Wnt pathway, which inhibits OPC differentiation, also seems to play a role in the disassociation of OPC from its vessel, as inactivation of the Wnt pathway resulted in OPC clustering. OPCs express CXCR4, a Wnt-activated chemokine receptor, and CXCR4 antagonists result in a reversal of the OPC clustering (Tsai et al., 2016). Together, this research suggests that Wnt activation may drive a CXCR4-dependent mechanism that enables OPCs to attach to the vascular scaffold; a mechanism that is downregulated during differentiation.

Although OPCs may remain in their immature state for a significant amount of time, cells quickly move through the process of differentiation and subsequent myelination (see section 1.2.3 for further discussion). This seemingly simple three-step process is anything but; proliferation, differentiation, and myelination are controlled by several intrinsic and extrinsic factors acting to either move cells away from or towards maturity.

1.2.3 Differentiation and maturation

As oligodendrocytes mature and prepare for the process of myelination, vast quantities of lipids and several hundred types of membrane proteins are synthesized, transported, and inserted into the myelin sheath (Dhaunchak et al., 2010; Ishii et al., 2009; Werner et al., 2007). OPCs undergo a series of morphological changes during differentiation and subsequent myelination: 1) the extension of exploratory motile processes; 2) contact and initial ensheathment of axons; 3) forward spiral expansion of myelin membrane; 4) simultaneous lateral expansion of myelin membrane; and 5) the final compaction of myelin (Fig. 2) (Snaidero and Simons, 2014; Zuchero et al., 2015). Although many aspects of this major cellular event require further investigation, this last decade has shed light on mechanisms driving this striking process. These developments required the use of many techniques including *in vitro* methods, mouse and zebrafish genetics, and electron microscopy (specifically the use of high-pressure freezing), which allows for optimal tissue preservation and deeper investigation into the physical structure of myelin.

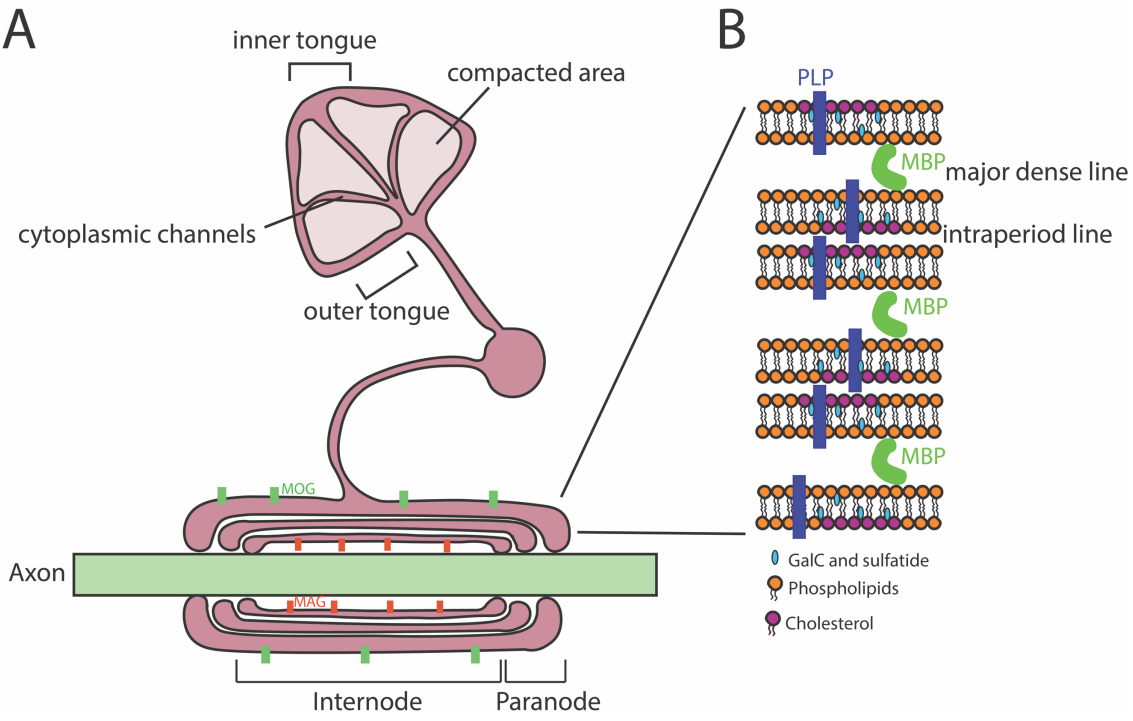

Figure 2: Myelin structure

A) Schematic depicting the developing myelin sheath, unwrapped to visualize the structure. The inner tongue or leading edge grows along the inside of the myelin spiral. The internode is formed during compaction and sub-domains of cytoplasmic channels move laterally forming the paranode region. Myelin Oligodendrocyte Glycoprotein (MOG) is localized on the outer-most lamellae of the sheath, whereas Myelin-associated glycoprotein (MAG) is localized to the inner-most membrane. B) A detailed schematic depicting the organization of the myelin membrane including high-abundance proteins, PLP and MBP, and lipids, including GalC, phospholipids, and cholesterol. PLP is inserted within the membrane and MBP is found between membranes. Together, these structures form the major dense and intraperiod lines seen by electron microscopy. This figure was adapted from (Ozgen et al., 2016).

1.2.3.1 From initial axonal contact to mature myelin

Upon axonal selection oligodendrocytes extend and broaden an exploratory motile process, now termed the inner tongue or leading edge, which encircles the axon (Hughes et al., 2013; Kirby et al., 2006; Snaidero and Simons, 2014). Myelination occurs in an 'inside-out' fashion meaning the inner tongue continues to grow along the inside of the myelin spiral, while laterally expanding the region of the membrane in contact with the axon (Fig. 2A) (Snaidero and Simons, 2014). Recently both Zuchero et al. and Nawaz et al. (Nawaz et al., 2015; Zuchero et al., 2015) demonstrated that this process is driven by the assembly and disassembly of F-actin. The ARP2/3-dependent assembly of F-actin acts as a protrusive force expanding the non-adhesive leading edge while the oligodendrocyte circles the axon. The subsequent ARP/cofilin1-dependent depolymerization of F-ACTIN collapses this structure, reduces the surface tension, and increases adhesion and lateral membrane spreading (Nawaz et al., 2015; Zuchero et al., 2015).

The final product is a multilayered stack of uncompacted membrane. Membrane expansion that occurs in this 'inside-out' fashion poses a particular problem: the expanding leading edge

requires transport of newly synthesized myelin proteins but counterproductively continues to increase the distance from the cell body where this synthesis occurs (Fig. 2A). How can such a large cell continue to expand its myelin at the leading edge? A landmark paper published by Snaidero et al. (Snaidero et al., 2014) elucidated how oligodendrocytes solve this dilemma. Interestingly, Snaidero and colleagues found that uncompact myelin uses cytoplasmic channels that connect the outer and inner layers to deliver vesicles containing essential myelin components, such as myelin basic protein (MBP), thereby shortening the distance to the leading edge. This group also showed that the number of cytoplasmic channels decreases as the oligodendrocyte matures, a process controlled by PI(3,4,5)P3. However, a region of cytoplasmic subdomain remains in close contact with the axon and moves laterally towards the eventual node, forming the paranodal loop which establishes a specialized junction with the axon (Fig. 2A). These cytoplasmic rich domains provide a functional location where mature oligodendrocytes remain connected with the axon and may share metabolites such as lactate (Saab et al., 2013).

The last step in establishing a mature myelin sheath occurs as the inner layer fills with myelin proteins and myelin compaction takes place. MBP binds two opposing membranes and drives myelin compaction by drawing the two membranes close together. MBP is crucial to membrane compaction, as *mbp* null mice do not produce compact myelin, display severe hypomyelination, and develop a shivering gait after a few weeks of age (Readhead et al., 1987; Roach et al., 1983). Myelin compaction reduces the amount of physical space and available cytoplasm, which restricts protein trafficking and creates a domain with little remaining cytoskeleton (Aggarwal et al., 2011, 2013; Bakhti et al., 2014; Snaidero et al., 2014). Caludin-11 securely connects the edge of the myelin lamellae by creating autotypic tight junctions (Gow et al., 1999) and compact myelin is formed. The final structure consists of alternating structures of

electron light and dense layers named “intraperiod line” and the “major dense line” that are easily observed with transmisison electron microscopy (Fig. 2B). Compaction is fast and happens early in development (Readhead et al., 1987) creating the region of high electrical resistance and low capacitance crucial for saltatory conduction. The rate at which this complex cellular event occurs can be astonishing. Using zebrafish, Czopka et al. demonstrated that oligodendrocytes are able to establish new myelin sheaths within as little as 5 hours (Czopka et al., 2013).

1.4 Myelination

1.4.1 Myelin components and organization

The insulating capacity of myelin suggests that the composition of this highly specialized membrane is unique. Indeed, myelin is unique compared to the other membrane cell types. Compared to the well hydrated membranes of the gray matter which contain 80% water, myelin only contains 40% water (Nave, 2010). Myelin membrane also differs from other cell types in that approximately 70% of their dry weight consists of lipids and 30% consists of proteins; a lipid-to-protein ration that is generally reversed in other cellular membranes (Baumann and Pham-Dinh, 2001; Ozgen et al., 2016). The composition, localization, and interactions between lipids and proteins prove critically important for the regulation of myelin formation and maintenance. These components act in concert with one another; lipids control the sorting of myelin proteins and myelin proteins organize lipids. This interaction forms specialized microdomains called lipid rafts which appear dynamic and act as signaling platforms themselves (Baron and Hoekstra, 2010; FÜLLEKRUG and SIMONS, 2004; Gielen et al., 2006; Krämer et al., 2001). The biogenesis and interactions between each component require tight regulation in order to maintain proper functioning.

1.4.2 High abundance myelin lipid and proteins

Given the highly specialized structure of myelin, it may be surprising to note that all lipids found in the myelin sheath are found in other cell types with slight species variability between rats and humans (Baumann and Pham-Dinh, 2001). Major myelin lipids include phospholipids, cholesterol, galactolipids (mainly galactosylcermidase (GalC)), and to a lesser extent, sulfatides (Fig. 2B) (Baron and Hoekstra, 2010; Baumann and Pham-Dinh, 2001). Cholesterol, an important component for the insulating function of myelin, makes up roughly 28% of the total dry weight of myelin in both human and rats (Baumann and Pham-Dinh, 2001). Galactolipids, namely GalC, comprise roughly 23% of the total dry weight and play an important role in the long-term maintenance of the membrane as well as oligodendrocyte differentiation and maturation (Dupree et al., 1998a, 1998b; Hirahara et al., 2004). Surprisingly galactosyltransferase knock-out mice, which lack GalC as well as other sulfatides, show normal myelin biogenesis and compaction despite the important ultrastructural abnormalities. Aged mutant mice showed unstable myelin, axonal swellings, and disrupted paranodal compartments, arguing these major myelin lipids play a functional role in the overall stability of myelin (Dupree et al., 1998a; Marcus and Popko, 2002).

Although cell-specific lipids are not found within the myelin sheath, many of the major protein components are found specifically in mature oligodendrocytes and/or Schwann cells. The most abundant myelin proteins found in the CNS are MBP and Proteolipid Protein (PLP) and its isoform, DM-20 (Fig. 2B). These low molecular weight proteins constitute roughly 80% of total myelin proteins, with MBP constituting 30%, and PLP making up the remaining 50% (Baron and Hoekstra, 2010; Baumann and Pham-Dinh, 2001; Ozgen et al., 2016). MBP has a multitude of isoforms with a different number of isoforms found in rats, mice, and human (Ozgen et al., 2016).

Surprisingly, despite the high abundance of each protein within the myelin, MBP is the only known structural protein essential for the formation of myelin in the mature oligodendrocyte (Readhead et al., 1987). As previously discussed, the positively charged MBP is required for the compaction of myelin and MBP null-mice do not produce myelin(Readhead et al., 1987). Unlike MBP, PLP null mice show no disruption to the formation of myelin(Klugmann et al., 1997). However, the overexpression of PLP as well as mutations within the *Plp1* gene result in severe gain of function phenotypes (Simons et al., 2002). Mikael Simons and colleagues showed that duplication of PLP caused sequestration of cholesterol in late endosomes/lysosomes resulting mistrafficking of lipid raft components leading to improper myelin membrane assembly (Simons et al., 2002). This stresses the importance of regulating the correct amount and formation PLP, as these factors affect the proteins ability to assemble essential lipid microdomains critical for proper myelin assembly.

Lipid and protein composition differ between non-compact and compact myelin. The paranodal loop within the non-compacted myelin houses proteins such as neurofascin (NF155), a glial cell adhesion molecule important for the axo-glial junction(Tait et al., 2000), and the glycosphingolipid sulfatide (Baron and Hoekstra, 2010). Unlike non-compact myelin, compact myelin houses both MBP and PLP proteins as well as high concentrations of the lipid cholesterol and the glycosphingolipid GalC. MBP is found in between membranes and creates the major dense line easily seen by electron microscopy. PLP, with four membrane spanning domains, is found inserted within the membrane. GalC and cholesterol are both inserted into the outerleaflet of the membrane and help form the intraperiod line (Ozgen et al., 2016).

1.4.3 Low abundance myelin proteins

Other cell-specific proteins are found within myelin as well, albeit at much lower concentrations. 2',3'-Cyclic-nucleotide 3'-phosphodiesterase, or CNP, constitutes roughly 4% of myelin proteins and is localized inside of the cell in the cytoplasmic plasma membrane (Baumann and Pham-Dinh, 2001). Myelin-associated glycoprotein, or MAG, represents only 1% of the myelin total protein, and Myelin Oligodendrocyte Glycoprotein, or MOG, is localized to the plasma membrane and is in high abundance on the outer most lamellae of the myelin sheath (Fig. 2B) (Nave, 2010). Interestingly, proteins that are non-specific to oligodendrocytes are found within the myelin as well, including proteins associated with neuronal signaling and vesicle release (see section 1.6.6 for further discussion). These proteins may indicate oligodendrocytes unappreciated role in various forms of cell-to-cell communication.

1.5 Intrinsic control of the oligodendrocyte lineage

1.5.1 Introduction to Intrinsic control of the oligodendrocyte lineage

Given the relationship between neurons and mature oligodendrocytes, neuronal signaling would be predicted to play a large role in influencing oligodendrocyte lineage progression. Interestingly, previous studies instead support the importance of intrinsic mechanisms, including the observation that oligodendrocytes survive, proliferate, and differentiate in monoculture (Abney et al., 1981; Durand and Raff, 2000; Knapp et al., 1987; Zeller et al., 1985). In addition, oligodendrocytes form a sheath-like membrane when plated on flat coverslips, and show the ability ensheath inert nanofibers (Dugas et al., 2006; Lee et al., 2012a; Rosenberg et al., 2008). This not

only demonstrates oligodendrocytes ability to progress without neuronal signaling, but also that ensheathment does not solely depend on axonal surface expression or excreted ligands.

1.5.2 Transcriptional regulation of oligodendrocyte lineage cells

A review written by Emery and Lu provides a framework to understand the intrinsic mechanisms controlling oligodendrocyte lineage progression (Emery and Lu, 2015). A complex interplay of transcriptional and epigenetic regulation controls all stages of lineage progression: specification, maintenance, differentiation, and finally maturation and myelination.

1.5.2.1 OPC specification

After the initial wave of motor neurons emerge from the pre-motor neuron domain of the ventral spinal cord, OPCs begin to emerge. The expression of the pan-oligodendrocyte transcription factor, *Olig2*, is expressed early within OPCs (Fu et al., 2002; Lu et al., 2002; Novitch et al., 2001; Zhou and Anderson, 2002; Zhou et al., 2001). Interestingly, *Olig2* plays an important role in establishing both the motor neuron population as well as the oligodendrocyte population- a dual function executed through two separate mechanisms (Zhou et al., 2001). The generation of motor neurons occurs due to the phosphorylation of OLIG2 at serine 147, whereas dephosphorylation at this site allows for oligodendrogenesis (Tyler et al., 2011). Although OPCs express OLIG2 early and consistently throughout each stage of oligodendrocyte development, the function and importance of OLIG2 changes based on the region and stage of maturation. For example, constitutive deletion of *Olig2* in OPCs causes cell fate to switch from OPCs to astrocytes within the neocortex and corpus callosum, but not in the ventral forebrain (Zhu et al., 2012). Additionally, dorsally derived OPCs do not initially express *Olig2*, demonstrating *Olig2* is not

required for the initial specification of dorsally derived OPCs (Cai et al., 2005; Kessaris et al., 2005; Richardson et al., 2006; Vallstedt et al., 2005) . It is likely that the closely related *Olig1* may compensate for this lack of expression in OLIG2 (Zhou and Anderson, 2002).

1.5.2.2 OPC maintenance

As the progenitor population continues to proliferate and migrate, OLIG2 induces the expression of additional transcription factors. Forced expression of OLIG2 is not only sufficient to induce oligodendroglia specification, but it also induces the expression of NKX2.2 and SOX10 (Liu et al., 2007; Zhou et al., 2001). NKX2.2 and SOX10 demonstrate a challenge in identifying a transcription factor specific and necessary for maintenance; despite their early expression, neither genes seem necessary for OPC maintenance (Qi et al., 2001; Stolt et al., 2002). *Nkx2.2* null mice show a dramatic reduction in OPC differentiation but not specification (Qi et al., 2001). Similarly, *Sox10* null mice show a relatively normal progenitor population with a disruption in terminal differentiation (Stolt et al., 2002).

Despite the lack of a singular maintenance specific gene, the deletion of both *Sox10* and an additional transcription factor, *Sox9*, results in a reduction of OLIG2-positive OPCs due to increased apoptosis and aberrant migration (Finzsch et al., 2008). Additionally, this double deletion also causes decreased expression of PDGFRα in the remaining OLIG2 population, suggesting that PDGFRα is under the transcriptional control of SOX9 and SOX10 (Finzsch et al., 2008). Since PDGFRα is an important survival factor and used in OPC migration, SOX9 and SOX10 show redundancy for critical functions during OPC maintenance (Finzsch et al., 2008).

1.5.2.3 Terminal differentiation

Differentiation marks a major transitional phase for oligodendrocytes. Once differentiation occurs, oligodendrocytes exit the cell cycle, thereby losing their ability to proliferate, and quickly move towards maturity. This process occurs rapidly, occurring within a mere 5 hours in zebrafish (Czopka et al., 2013). In humans, pre-myelinating oligodendrocytes can be found several weeks before MBP+ segments are detected, indicating a slower and more protracted rate of differentiation (Back et al., 2001). The complexity involved in the timing and regulation of differentiation demonstrates the necessity to tightly control this event. Negative and positive regulators of differentiation act to ensure balance and control between the competing stages of proliferation and differentiation.

1.5.2.3.1 Negative regulation of terminal differentiation

OPCs inhibit differentiation through the expression of many transcription factors, including ID2, ID4, HES5, SOX5, and SOX6. These factors act in concert to control the extracellular signaling and prevent differentiation. Overexpression of ID2 inhibits OPC differentiation; conversely, the absence of ID2 allows for terminal differentiation *in vitro* (Wang et al., 2001). Both ID2 and ID4 act within the nucleus to inhibit differentiation and are translocated to the cytoplasm upon differentiation (Wang et al., 2001). Additionally, ID proteins physically bind and prevent both OLIG1 and OLIG2 activity, thereby preventing the induction of downstream pro-differentiating factors (Samanta and Kessler, 2004). The negative regulation of differentiation is also carried out through *Hes5* activity. Again, overexpression of HES5 *in vitro* blocks OPC differentiation, while deletion of HES5 *in vivo* leads to accelerated expression of mature oligodendrocyte markers such as MBP and PLP1 (Liu et al., 2006). HES5 is able to both bind and compete with the transcription factor SOX10, preventing the transcription of MBP (Liu et al.,

2006). Although SOX proteins regulate the progenitor population, the deletion of both *Sox5* and *Sox6* within the spinal cord allowed for the increased expression of both MBP and PLP1 (Stolt et al., 2006). Similar to HES5, both SOX5 and SOX6 prevent SOX10 activity demonstrated by their ability to bind the promotor region of the *Mbp* gene(Stolt et al., 2006).

1.5.2.3.2 Positive regulation of terminal differentiation

Key factors involved in differentiation proved challenging to resolve, as transcription factors may play roles in several stages of the oligodendrocyte lineage. As previously mentioned, *Olig2* plays an important role in specification and maintenance, although its expression continues in the differentiated and mature oligodendrocyte. In order to determine the function of *Olig2* in post-mitotic oligodendrocytes, researchers used a conditional knockout strategy which targeted the deletion of *Olig2* after oligodendrocyte differentiation (Cai et al., 2007; Mei et al., 2013). This resulted in a significant reduction in the density of mature oligodendrocytes and myelin, demonstrating the multiple roles that a single transcription factor may play throughout the multiple stages of oligodendrocyte development (Cai et al., 2007; Mei et al., 2013).

Since pro-differentiation and maturation factors such as OLIG2, SOX9, and SOX10 are expressed before differentiation but are inhibited by transcription factors such as the IDs and HES5, this led to the development of a 'derepression model' (Emery, 2010). The 'derepression model' suggests oligodendrocytes would default to differentiation and maturation, but negative regulation prevents this default mode. Therefore, in order to move towards differentiation and maturation, the negative regulation itself must be inhibited to allow for the positive regulation and progression towards maturation (Emery, 2010). The pathways involving ZFHX1B/SIP1 represents an elegant example of the alleviation of negative regulation that results in differentiation (Weng

et al., 2012). Both the WNT pathway, as discussed in section 1.2.2 and will be further discussed in section 1.5.4.1, and bone morphogenic protein (BMP) signaling inhibit OPC differentiation (Weng et al., 2012). During the stage of OPC maintenance, SIP1 expression remains low (Weng et al., 2012). During differentiation, OLIG1 and OLIG2 activate SIP1 production, which physically antagonizes BMP activity and promotes a critical differentiation activator, SMAD7. SMAD7 further blocks BMP and WNT signaling, leading to the suppression of negative regulators of differentiation such as the IDs and HES5. This alleviation will allow already present transcription factors such as OLIG1, OLIG2, and SOX10 to relocate and promote differentiation (Weng et al., 2012).

1.5.2.4 Maturation/myelination

Many of the transcription factors that control maturation and myelination are initially expressed at the earliest stages of development and continue their expression through maturation. As previously discussed, OLIG2 is an example of this. Other examples include NKX2.2, OLIG1, ASCL1, and SOX10. For example, loss of NKX2.2 function using a *Nkx2.2* null mutant results in a delay and reduction in oligodendrocytes, specifically oligodendrocytes expressing both MBP and PLP1 (Qi et al., 2001). NKX2.2 also drives GFP expression from the *Plp1* promoter, but may also reduce activity at the *Mbp* promoter (Gokhan et al., 2005; Wei et al., 2005). Despite this seemingly paradoxical result, NKX2.2 is required for proper differentiation and myelination.

Another example is ZFP191, also known as ZFP24. ZFP24 is a zinc finger protein which contains both DNA-binding zinc finger domains protein-protein interaction SCAN domains (Howng et al., 2010). ZFP24 is widely expressed in many cell types and is expressed through the stages of the oligodendrocyte lineage. *ZFP24* mutants show reduced expression of many myelin related genes, indicating a role in maturation, despites its early expression (Howng et al., 2010).

Recent work by Elbaz et. al demonstrated that ZFP24's role in maturation is controlled by its phosphorylation (Elbaz et al., 2018). Phosphorylated ZFP24 accumulates in OPCs and is unable to bind DNA. As cells mature, unphosphorylated ZFP24 accumulates and binds to a consensus DNA sequence proximal to many genes important for CNS myelination, such as MBP and SOX10, thereby enhancing target gene expression (Elbaz et al., 2018). Given that the knockouts of transcription factors are expressed throughout the stages of the oligodendrocyte lineage, yet still show stalling during differentiation of myelination, suggests that several transcription factors have non-redundant and essential functions over the course of oligodendrocyte development.

Currently, only one transcription factor shows induced expression during differentiation, rather than before, is essential to CNS myelination, and shows oligodendrocyte-specific expression amongst neural cells. Myelin Gene Regulatory Factor (*Myrf/gm98*) is a transcription factor that acts as a master regulator controlling oligodendrocyte maturation and myelination. Conditional knockouts of MYRF result in a severe failure to myelinate, eventually leading to postnatal death (Emery et al., 2009a). The expression of MYRF is induced by SOX10 and OLIG2 (Hornig et al., 2013; Yu et al., 2013) and MYRF subsequently drives maturation and myelination by directly targeting many genes essential for myelination, including *Cntn2*, *Trf*, *Mag*, *Mbp*, and *Plp1* (Bujalka et al., 2013). In addition, MYRF expression is also essential in the ongoing maintenance for mature oligodendrocytes (Koenning et al., 2012) .

1.5.3 Epigenetic Regulation of oligodendrocyte lineage cells

In addition to the intricate transcriptional network discussed previously, epigenetic regulation also influences the progression of oligodendrocytes. Epigenetic regulation is defined as

mechanisms that affect gene expression without altering the DNA sequence itself, and can occurs through DNA methylation, histone medication, and miRNAs (Emery and Lu, 2015).

1.5.3.1 DNA Methylation

The most well understood type of DNA methylation is CG methylation, where the addition of a cytosine base is added to a guanine nucleotide (Emery and Lu, 2015). This modification happens most commonly within the promoter regions of protein coding genes and the methylation of the CG sites is typically associated with the silencing of downstream genes (Tiane et al., 2019). DNA methyltransferases (DMNTs) add the methyl-group the cytosine, and ten-eleven translocation (TET) enzymes can remove the methyl-group (Tiane et al., 2019).

In an early study, neonatal rats treated with a DNMT-inhibitor displayed hypomyelination in 11-day old optic nerves accompanied by a reduction in the number of oligodendrocytes (Ransom et al., 1985). Similarly, deleting *Dnmt1* in progenitor cells results in OPC growth arrest and severe hypomyelination (Moyon et al., 2016). Just as DNA methylation affects the oligodendrocyte lineage, the removal of the methyl groups by TET enzymes also influences differentiation. Knock-down of *Tet* mRNA resulted in the increased expression of negative regulators of oligodendrocyte differentiation, such as ID2 and HES5 proteins (Zhao et al., 2014). DNA methylation may also influence the temporal expression of downstream genes, with PRMT5 serving as an example. PRMT5 is methyltransferase that binds CG-rich domains within the *Id2* and *Id4* genes, silencing their expression thereby relieving the inhibition of differentiation (Huang et al., 2011). Similarly, SIRT2 can translocate to the nucleus to methylate DNA regions upstream of *Pdgfrα,* subsequently initiating glial differentiation (Fang et al., 2019). Although PRMT5 and SIRT2 are classified as

histone-modification enzymes, they are also able to induce epigenetic changes via DNA methylation as well (Tiane et al., 2019).

1.5.3.2 Histone modification and chromatin remodeling

Histone modifications occurs through a variety of changes on the histone tail, including (de)acetylation, which is heavily involved in different aspects of oligodendrocyte development. Histone acetyltransferases (HATs) are responsible for histone acetylation, which relaxes the DNA into an 'open' structure allowing for easier accessibility to the DNA region (Tiane et al., 2019). Conversely, histone deacetylases (HDACs) remove the acetyl group, resulting in a 'closed' and less accessible DNA structure. While limited studies have assessed the role of HATs in oligodendrocyte development, HDACs clearly influence oligodendrocytes (Tiane et al., 2019). The conditional deletion of *Hdac1* and *Hdac2* in OPCs causes a reduction in the number of OPCs as well as a delay in differentiation and myelination (Ye et al., 2009), implicating HDAC involvement in both early and later stages within the oligodendrocyte lineage. The pharmacological inhibition of HDACs prevented the expression of inhibitory transcription factors, such as ID2 and SOX10 in rats and ID4, SOX2, and TCF4 in humans (Conway et al., 2012; Swiss et al., 2011). This suggests that HDACs promote differentiation by suppressing the expression of inhibitory genes that otherwise block differentiation.

In addition to direct histone modification, ATP-dependent chromatin remodeling complexes also influence the oligodendrocyte lineage. ATP-dependent chromatic remodeling complexes use ATP as an energy source in order to reposition nucleosomes, which alters histone accessibility and subsequent gene transcription (Tiane et al., 2019). Brahma-related 1 (BRG1) is a helicase component of the SWI/SNF-related complex and is expressed in throughout all stages of

the oligodendrocyte lineage, with OPCs showing the highest expression. BRG1 interacts with the *Olig2* promoter to induce its expression in OPCs (Matsumoto et al., 2016). Initial studies showed that BRG1 is then recruited by OLIG2 to enhance the expression of additional oligodendrocyte genes (Yu et al., 2013). Subsequent studies showed that the pair drives the expression of an additional ATP-dependent chromatin remodeler, CHD7 (He et al., 2016). During oligodendrocyte differentiation, when CHD7 expression is the highest, it acts with SOX10 to enhance the expression of genes essential for myelination, such as *Myrf* and *Sox10* (He et al., 2016).

1.5.3.3 Non-coding-RNAs

In addition to DNA methylation and histone modification, small non-coding RNAs also prove powerful and important epigenetic regulators of oligodendrocyte gene expression. Major types of non-coding RNAs include small interfering RNAs (siRNAs), Piwi-interacting RNAs (piRNAs), long non-coding RNAs (lnc-RNAs), and micro RNAs (miRNAs)(Tiane et al., 2019). Although lnc-RNAs, such as *Neat1*, demonstrate the ability to influence OPC genesis and myelin gene expression (Dong et al., 2015; Katsel et al., 2019) , miRNAs represent the most abundant and most well-studied non-coding RNA to influence the oligodendrocyte lineage. miRNAs are small molecules often transcribed from non-coding regions and coding protein introns and bind the seed sequence at the 3' untranslated region of target mRNA (Tiane et al., 2019). This binding results in either the repression of translation or the degradation of the target mRNA. Interestingly, miRNA with low base-pair complementarity may bind to several 3' UTR sequences resulting in the reduction of expression for several genes and may converge on a single pathway such as cell proliferation and differentiation (Tiane et al., 2019).

The expression profile of many miRNAs varies throughout the stages of oligodendrocyte development, indicating their possible importance in the regulation of cellular events. This

importance is underscored by mice lacking DICER1, an enzyme responsible for processing pre-miRNA into mature miRNA. Differentiating oligodendrocytes show greater DICER1 expression compared to OPCs, and conditional ablation of *Dicer1* severely disrupts differentiation in OPCs (Dugas et al., 2010; Shin et al., 2009). miR-219, miR-138, and miR-338 show a 10-100-fold increase during differentiation and have been show to play an important role in differentiation specifically (Dugas et al., 2010; Shin et al., 2009). miR-219 directly targets genes important for maintaining proliferation in OPCs such as *Sox6*, *Hes5*, and *Pdgfr*α (Dugas et al., 2010). Working in concert with miR-138, their increased expression during differentiation and suppression of genes important for OPCs indirectly increases the expression of monocarboxylate transporters, thereby increasing oligodendrocyte numbers and increasing the expression of MBP and CNP (Dugas and Notterpek, 2011; Wang et al., 2017). miR-219 also regulates the metabolic regulation of lipid formation and maintenance, demonstrating a role for miR-219 in both the beginning and later stages of differentiation(Shin et al., 2009).

While some miRNAs influence mRNA translation and oligodendrocyte differentiation by increasing their expression and RNA binding, other miRNAs affect differentiation via downregulated expression. For example, the expression of miRNA-9 decreases as oligodendrocytes differentiate and is concurrent with the increased expression of Serum response factor (SRF), a transcription factor that transactivates actin-associated genes important for oligodendrocyte differentiation (Buller et al., 2012). Overexpression of miR-9 in cultured OPCs suppresses SRF expression and inhibits OPC differentiation, while the depletion of miR-9 in OPCs stimulates OPC differentiation (Buller et al., 2012). In a recent finding, Kornfeld and collegues demonstrate that the high expression of miR-145-5p in OPCs prevents differentiation by binding *Myrf* transcripts, thereby inhibiting the expression of critical differentiation and myelination genes

(Kornfeld et al., 2020). Taken together, the various expression profiles of miRNAs strongly influence the oligodendrocyte state and prove important regulators of CNS myelination.

1.5.4 Important intracellular signaling pathways

As discussed, a complicated network of cellular events control oligodendrocyte lineage progression and myelination. Oftentimes, these cellular events converge on three main intracellular signaling pathways: the canonical wingless and integration site WNT-signaling pathway, the ERK/MAPK pathway, and the AKT/mTOR pathway (Fig. 3) (Gaesser and Fyffe-Maricich, 2016).

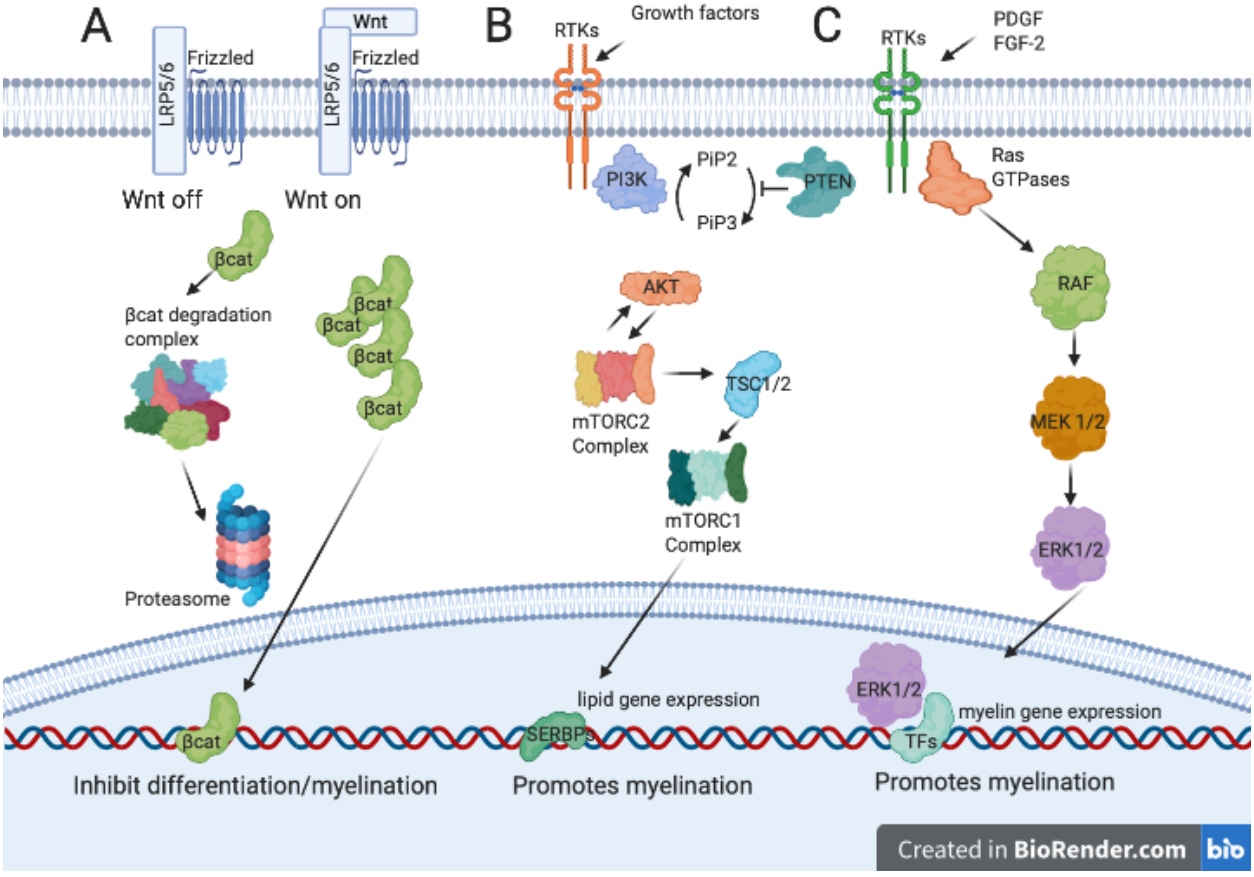

Figure 3-Major pathways influencing myelination.
Schematic depicting three major pathways important for myelination: Wnt/b-catenin (A), AKT/mTOR (B), and ERK/MAPK (C). Extracellular ligands are shown to bind their respective

receptors, activating downstream pathways either inhibiting (A) or enhancing (B&C) myelination. Growth factors such as brain-derived neurotrophic factor (BDNF), nerve growth factor (NGF) and neurotrophin 3 (NT3), bind receptor tyrosine kinases and activate the AKT/mTOR pathway (B). The figure was adapted from (Alcover-Sanchez et al., 2020). βcat: β-catenin, Lrp5/6: low density lipoprotein 5 and 6, RTKs: Receptor tyrosine kinases, PI3K: phosphoinositide-3-kinase, PIP2: phosphatidylinositol 4,5-bisphosphate, PIP3: phosphatidylinositol 3,4,5 trisphosphate, TSC2: tuberous sclerosis complex, SREBPs: Sterol regulatory element-binding proteins, mTOR: mechanistic target of rapamycin, mTORC: mechanistic target of rapamycin complex, PDGF: Platelet-derived growth factor, FGF-2: fibroblast growth factor 2, MEK: mitogen activated kinase kinase, ERK1/2: extracellular signal related kinase 1 and 2, TF: transcription factors.

1.5.4.1 Canonical Wnt signaling pathway

The WNT signaling pathway plays an important role in development, growth, metabolism, and maintenance of stem cells (van Amerongen and Nusse, 2009). WNT proteins are extracellular signaling molecules that bind the Frizzled membrane receptor and their co-receptors, including the intracellular signaling molecule, β-catenin (Fig. 3A) (Logan and Nusse, 2004). In the absence of WNT, β-catenin remains in a destruction complex with other proteins including adenomatous polycosis coli (APC), resulting in the continuous degradation of β-catenin (Clevers and Nusse, 2012). Upon WNT binding, β-catenin disassociates from the destruction complex, accumulates, and re-locates to the nucleus where it interacts with TCF/LEF family members to initiate target gene expression (Behrens et al., 1996). Although initially understood as an inhibitor of oligodendrocyte development, several seemingly contradictory studies suggest that WNT signaling influences oligodendrocyte lineage progression to both inhibit and promote myelination.

Although it is tempting to think of any signaling mechanisms as binary ‘on/off’ systems, somewhat paradoxical evidence suggests the WNT pathway does not neatly fit into this type of model. For example, activation of the WNT pathway via constitutive expression of β-catenin in

transgenic mice, using the *Olig1*-Cre driver, results in the inhibition of OPC generation (Fancy et al., 2009; Feigenson et al., 2009; Ye et al., 2009), while the repression of WNT signaling results in enhancement of OPC generation (Langseth et al., 2010). However, neonatal expression of constitutively active β-catenin using *Olig2*-Cre mice fails to alter OPC generation (Fancy et al., 2009). This may indicate the importance of timing for the expression of β-catenin, or may indicate the importance of appropriate β-catenin levels, given the difference in promoter strength used to drive β-catenin expression (Gaesser and Fyffe-Maricich, 2016).

In addition to the β-catenin's role in OPC generation, several studies demonstrate that WNT signaling inhibits differentiation and subsequent myelination. Activating this pathway via overexpression of a dominant-active β-catenin in all oligodendrocyte linage cells (*Olig2*-Cre/DA-Cat) (Fancy et al., 2009) or mature oligodendrocytes (*CNP*-Cre/DA-Cat) (Feigenson et al., 2009) results in a delay in OPC differentiation. Mutant mice displayed hypomyelination along with a decreased number of PLP1 expressing oligodendrocytes (Fancy et al., 2009; Feigenson et al., 2009). Importantly, *Olig2*-Cre/DA-Cat mice showed an increased proportion of oligodendrocytes that express TCF712, an important nuclear binding partner of β-catenin. This led to a model suggesting that β-catenin, along with TCF712, negatively regulate OPC differentiation by increasing the transcription of WNT pathway target genes (Fancy et al., 2009). In addition, other studies suggest a similar role for WNT/β-catenin signaling inhibiting differentiation in postnatal myelination. For example, increasing the expression of the extracellular agonist WNT3A resulted in an increase of OPC numbers and a decrease in mature oligodendrocytes in culture (Azim and Butt, 2011; Feigenson et al., 2011). Likewise, conditional ablation of the molecule responsible for the degradation of β-catenin, APC, decreases the number of mature oligodendrocytes (Lang et al.,

2013). Together, these data suggest that the WNT/β-catenin pathway negatively regulates differentiation and myelination.

Despite a clear role for the negative regulation of differentiation and myelination, other studies show that activation of the WNT/beta-catenin pathway pushes oligodendrocytes towards maturation. In culture, exogenous addition of WNT molecules increase OPC differentiation, *Plp1* promoter activity is enhanced with the overexpression of nuclear-localized beta-catenin, and knock down of β-catenin using siRNA decreases the expression of major myelin proteins and myelination (Gaesser and Fyffe-Maricich, 2016; Kalani et al., 2008; Ortega et al., 2013; Tawk et al., 2011). These seemingly conflicting results suggest a model where the timing and level of expression for molecules within the WNT/β-catenin pathway must be tightly controlled for proper OPC generation, differentiation, and myelination (Gaesser and Fyffe-Maricich, 2016).

1.5.4.2 AKT/mTOR signaling pathway

The serine/threonine kinase AKT acts as an important signaling molecule influencing cell growth, proliferation, and survival (Gaesser and Fyffe-Maricich, 2016). This pathway is activated by extracellular growth factors binding receptor tyrosine kinases on the cell surface, which trigger an intracellular cascade. Initially, activation of 3-Phosphoinositide 3 kinase (PI3K) converts PtdIns(4,5,)P2 (PIP2) to PtdIns(4,5,)P3 (PIP3) which leads to the partial activation of AKT via 3-phosphoinositide-dependent kinase I (PDK1) (Fig. 3B) (Gaesser and Fyffe-Maricich, 2016). Phosphorylation of AKT via the rapamycin complex mTORC2 completes the activation of AKT, creating a positive feedback loop for AKT activation. Upon complete activation, AKT phosphorylates tuberous sclerosis complex 2 (TSC2), which allows for the activation of mTORC1

activity and initiates important downstream cellular processes (Gaesser and Fyffe-Maricich, 2016). In oligodendrocytes, both differentiation and myelination involve AKT/mTOR signaling.

Both *in vitro* and *in vivo* studies indicate AKT signaling plays an important role in oligodendrocyte lineage cells. Phosphatase and tensin homologue (PTEN) inhibits PI3K/AKT; therefore, inhibition of PTEN results in activation of the AKT/mTOR pathway. In co-cultures of either rat or human OPCs and dorsal root ganglion neurons, the addition of the PTEN inhibitor, bisperoxovanadium, along with growth factor and receptor tyrosine kinase ligand IGF-1 results in increased MBP accumulation in OPCs (Paula et al., 2014). Further support of the AKT/mTOR pathway comes from several *in vivo* experiments. Deleting PTEN in all oligodendrocyte progenitor cells (using *Olig2*-Cre), or mature oligodendrocytes (using *CNP*-Cre or *Plp1*-Cre), results in increased levels of PIP3 and phosphorylated AKT, as well as significant CNS hypermyelination (Goebbels et al., 2010; Harrington et al., 2010). In addition, expression of constitutively active AKT in mature oligodendrocytes (using *Plp1*-AKT-DD) also results in hypermyelination and increases in both MBP expression and mTORC1 activity (Flores et al., 2008; Narayanan et al., 2009). Together, these studies implicate the AKT/mTOR pathway in myelination, but does this pathway also influence differentiation in OPCs?

Studies using the mTOR inhibitor rapamycin in cultured OPCs suggest this pathway may play a role in differentiation, as the addition of rapamycin results in decreased OPC differentiation and a reduction in myelin mRNA and protein (Guardiola-Diaz et al., 2012; Tyler et al., 2009, 2011). In addition, developmental exposure to rapamycin in wild-type mice leads to CNS hypomyelination (Narayanan et al., 2009). In order to better understand the mechanism underlying these effects, several studies targeted different components of the mTOR pathway, including targeting the immediate early gene that activates mTORC1, *Raptor*, the gene that encodes for a

subunit of mTORC2, *Rictor*, or both (Bercury et al., 2014; Lebrun-Julien et al., 2014; Wahl et al., 2014; Zou et al., 2014). Mutant mice lacking either *mTOR* (Wahl et al., 2014) or both *Raptor/Rictor* (Lebrun-Julien et al., 2014) in mature oligodendrocytes results in a decrease in mature oligodendrocytes, supporting the idea that mTOR signaling is important for OPC differentiation. Studies targeting mTORC1 or mTORC2 individually demonstrate that mTORC1 may play a more important role in oligodendrocytes, as inhibition of mTORC1 results in a more severe deficit in differentiation and myelination than inhibition of mTORC2 activity (Bercury et al., 2014; Lebrun-Julien et al., 2014; Zou et al., 2014).

It is well known that mTOR regulates gene expression in many cell types, but several studies indicate that the mTOR pathway may also play a role in mRNA translation (Bercury et al., 2014; Lebrun-Julien et al., 2014; Wahl et al., 2014; Zou et al., 2014). Although there is a reduction in the abundance of many myelin proteins following developmental impairment of mTOR signaling (Bercury et al., 2014; Wahl et al., 2014), MBP is the only myelin protein showing a long-term deficit (Wahl et al., 2014). For example, many studies demonstrate that inactivation of mTORC1 at several developmental timepoints leads to a reduction in MBP protein with no change to *Mbp* mRNA levels (Wahl et al., 2014). Therefore, mTOR activity, or more specifically mTORC1, may play an important role in the trafficking or translation of *Mbp* mRNA. Additionally, *Mbp* mRNA is known to be trafficked and locally translated in oligodendrocytes (Ainger et al., 1993; Wake et al., 2011). Although local translation occurs in other cell types, like the local translation of *Camk2α* mRNA in neuronal dendrites (Ainsley et al., 2014), *Mbp* remains the only known mRNA to undergo local translation in oligodendrocytes. Given the relationship between *Mbp* mRNA localization, local translation of *Mbp*, and mTORC1 activity, it is possible that mTORC1 may influence mRNA important for local translation. Local mRNA translation and

the role of mTORC1 in mRNA translation within oligodendrocytes remains an open area of investigation.

1.5.4.3 ERK/MAPK signaling pathway

The ubiquitous and well-conserved ERK/MAPK pathway influences the expression of many genes important for cell proliferation, differentiation, and survival. ERK1 and ERK2 are widely expressed protein kinases that act as intracellular signaling molecules that catalyze the phosphorylation of many proteins within the cytoplasm and the nucleus (Gaesser and Fyffe-Maricich, 2016). Both growth factors, like PDGFRα and FGF-2 (Fig. 3C) (Bansal et al., 2003; Bhat and Zhang, 2002; Yim et al., 2001), and neurotropic factors such as NGF, NT3, and BDNF (Althaus et al., 1997; Du et al., 2006), bind to tyrosine kinase receptors to initiate a downstream signaling events. Extracellular binding to the tyrosine kinase receptors activates the RAS family of GTPases, which in turn phosphorylates RAF (MAP3K) (Raman et al., 2007). RAF phosphorylates MEK1 and MEK2, which leads to the phosphorylation of ERK1 and ERK 2 (Raman et al., 2007). This triggers ERK1 and ERK2 to relocate to the nucleus in order to regulate the expression of a multitude of genes.

Within oligodendroglia, ERK1 and ERK2 may play a role in survival, proliferation, and differentiation, although determining whether their expression positively or negatively regulates these outcomes requires further investigation (Gonsalvez et al., 2016). For example, many studies suggest that the ERK/MAPK pathway plays a role in differentiation *in vitro* (Baron et al., 2000; Dai et al., 2014; Stariha et al., 2002; Younes-Rapozo et al., 2009). These studies suggest that the inhibition of ERK/MAPK signaling in either mouse or rat OPCs decreases OPC differentiation.

Although *in vitro* studies indicated the involvement of the ERK/MAPK pathway in differentiation, *in vivo* studies show mixed results.

Using a neural progenitor driver to conditionally knockout mouse *B-Raf*, an upstream kinase responsible of phosphorylating MEK, Galabova-Kovacs and colleagues showed an increase in the number of OPCs. This was accompanied by a decrease in OPC differentiation and a decreased number of mature oligodendrocytes early in development (P18) (Sobczak et al., 2008). In a separate study, Fyffe-Maricich and colleagues deleted *Erk2* from hGFAP+ radial glial cells which resulted in decreased MBP expression in the corpus callosum at P10 and inhibited OPC differentiation when grown in culture (Fyffe-Maricich et al., 2011). Similar to the *in vitro* studies, these studies support the role for the ERK/MAPK in oligodendrocyte differentiation. Conversely, experiments inhibiting both *Erk1* and *Erk2* specifically in OPCs fail to demonstrate the same effect of inhibiting differentiation (Ishii et al., 2012; Xiao et al., 2012). Likewise, *Erk1/2* double knockouts that conditionally delete *Erk2* in an *Erk1* null mice also fail to show any changes in OPC differentiation (Ishii et al., 2012). In addition, sustained activation of ERK1/2 in oligodendrocyte lineage cells does not increase differentiation (Fyffe-Maricich et al., 2013; Ishii et al., 2013; Xiao et al., 2012). These mixed results between *in-vitro* and *in vivo* studies may reflect a compensatory mechanism *in vivo* that prevents a disturbance in differentiation. These differences may reflect the difference between inhibiting the ERK/MAPK pathway in neural stem cells or radial glial populations versus inhibiting this pathway directly within the oligodendrocyte lineage, reflecting the importance of timing in ERK/MAPK pathway activation. Similarly, studies show mixed results regarding the role of the ERK/MAPK pathway regarding OPC proliferation and survival (Gaesser and Fyffe-Maricich, 2016).

Mature oligodendrocytes express both *Erk1/2* mRNA, with *Erk1* expression being much higher than *Erk2* (Cahoy et al., 2008). ERK1 and ERK2 proteins exhibit high sequence homology (>80%) and demonstrate very similar substrate specificity (Boulton et al., 1991). *Erk2* conditional knockout mice display transient hypomyelination (Fyffe-Maricich et al., 2013) and double knockout mice show more extreme hypomyelination, accompanied by a persistent decrease in myelin gene mRNA and protein expression (Ishii et al., 2013). Interestingly, deletion of both *Erk1/2* does not change the number of mature PLP+ oligodendrocytes, nor did it impact the axonal contact required for myelination or the initiation of myelination (Ishii et al., 2013). Sustained ERK1/2 activation via constitutively active MEK in CNP+ oligodendrocytes results in robust developmental increases in myelin thickness in transgenic mice (Fyffe-Maricich et al., 2013; Ishii et al., 2013), and myelinating co-cultures expressing constitutively active MEK display increased MAG and MBP expression (Xiao et al., 2012). Together, these data suggests ERK1/2 impacts myelination specifically by increasing myelin gene expression.

Clearly the ERK/MAPK pathways regulates myelination, but which upstream and downstream signaling molecules affect myelination? The neurotrophin receptor *TrkB* and growth factor receptor *Fgfr1/2* mediate myelination; oligodendrocyte specific knockout mice show no change in the total number of mature oligodendrocytes, the initial contact with axons, or ensheathment, but show a signification reduction in myelin thickness (Furusho et al., 2012; Wong et al., 2013). In a follow-up study, Furusho and colleagues further investigated the role of both FGFR1 and FGFR2 receptors in myelination (Furusho et al., 2017). FGFR2 is highly enriched within the paranodal region of myelin. Using a conditional ablation of FGFR2 or FGFR1 in CNP+ oligodendrocytes, only FGFR2 knockout mice display a myelination phenotype (Furusho et al., 2017). These mice show decreased myelin growth and myelin gene expression, decreased ERK1/2

activity, as well as decreased mRNA expression of the key transcription factor, *Myrf* (Furusho et al., 2017). Previous studies demonstrate the importance of ERK/MAPK signaling in myelin maintenance, supporting the finding that the ERK/MAPK pathway may partially drive MYRF expression (Ishii et al., 2013). Additionally, Furusho and colleagues showed that *Fgf2* KO mice show a downregulation in molecules important for mTOR signaling with no change in the amount of phosphorylated AKT (Furusho et al., 2017). Together, this suggests that FGFR2 signaling regulates myelin thickness through activation of the ERK/MAPK pathway, which promotes mTORC1 activity in an AKT-independent manner (Furusho et al., 2017). This illustrates how major pathways important for myelination such as ERK/MAPK and mTOR signaling may converge in non-conical ways to regulate oligodendrocyte lineage cells.

1.6 Extrinsic control of the oligodendrocyte lineage: the role of neuronal activity

Several sub-sections within "Extrinsic control of the oligodendrocyte lineage: the role of neuronal activity" section were adapted from the review article I wrote in collaboration with Helena Bujalka and Ben Emery: Foster AY, Bujalka H, Emery B. Axoglial interactions in myelin plasticity: Evaluating the relationship between neuronal activity and oligodendrocyte dynamics. Glia. 2019;1–12. ***https://doi.org/10.1002/glia.23629***

1.6.1 Introduction to Extrinsic Control of the Oligodendrocyte lineage

Oligodendrocytes exist in a complex environment, with astrocytes, microglia, neurons, and vascular/perivascular cells all navigating through and interacting with the extracellular matrix. Although external factors such as cell-cell interactions and excreted growth factors derived from many of the aforementioned cell types influence oligodendroglia (for a comprehensive and current review, see (Baydyuk et al., 2020)), the effect of neuronal activity on oligodendroglial cells

emerges as a central focus point. An early study published over five decades ago points to a connection between activity and oligodendroglia, showing that dark-reared mice display a delay in myelination within the optic nerve (Gyllensten and Malmfors, 1963). Over the last two decades, several studies have demonstrated the ability and importance of this type of neuronal-oligodendroglial communication. In adult humans, a number of neuroimaging studies show structural changes in white matter tracts in response to juggling, piano practicing, and working memory tasks, suggesting that changes in task-related neuronal activity may increase myelination (Bengtsson et al., 2005; Scholz et al., 2009; Takeuchi et al., 2010). Rodents also appear to demonstrate experience-dependent changes in myelination. Social isolation (Liu et al., 2012; Makinodan et al., 2012), environmental deprivation and enrichment (Hughes et al., 2018; Narducci et al., 2018), and motor training (Keiner et al., 2017; McKenzie et al., 2014; Xiao et al., 2016) have all been shown to impact oligodendroglia development or myelination. More specifically, directly blocking or stimulating neuronal activity in co-culture (Demerens et al., 1996; Lundgaard et al., 2013; Stevens et al., 2002), *in vivo* rodent models (Gibson et al., 2014; Gyllensten and Malmfors, 1963; Li et al., 2010; Mitew et al., 2018; Stedehouder et al., 2018), and zebrafish (Hines et al., 2015; Koudelka et al., 2016; Mensch et al., 2015) all support the connection between neuronal activity and myelination. This section focuses on the relationship between neuronal activity and myelination and discusses the emerging theory that describes activity-dependent changes to myelination, referred to as adaptive myelination.

1.6.2 Possible functions of adaptive myelination

Despite the piqued interest and clear indication that activity is capable of modulating myelination, one major question remains unresolved: What is the purpose? In other words, what

functional benefits exist for neurons to regulate or control myelination throughout life? One possibility is that activity-dependent changes to myelination represent a form of neuroplasticity; experience-dependent changes in activity influence the amount or placement of *de novo* myelin, resulting in modulated axonal conduction velocity and the fine-tuning of neuronal circuits (Almeida and Lyons, 2017; Fields, 2005; Fields et al., 2015; Foster et al., 2019; Gibson et al., 2014). Using adult mice, Tomassy et al. demonstrated that myelinated cortical neurons display long segments of unmyelinated regions throughout the length of the axon, lending credence to the possibility of *de novo* myelination past developmental myelination (Tomassy et al., 2014). Even after a period of developmental myelination and refinement, ~30-70% of the corpus callosum axons remain unmyelinated despite having axonal diameters receptive to myelination (>0.2 uM) (Olivares et al., 2001; Sturrock, 1980). Additionally, changes to internode length (the length of the myelin segment in between the nodes of Ranvier), myelin thickness, and nodal width can all modulate conduction velocity (Ford et al., 2015; Foster et al., 2019; Waxman, 1980; Wu et al., 2012). Together, this suggests that neurons may locally signal to oligodendrocytes to promote myelination of previously unmyelinated areas. It is possible that novel experiences or learning may prompt the addition of new myelin to strengthen specific connections similar or Hebbian plasticity or act to synchronize firing patterns across disperse brain regions (Hoz and Simons, 2015; Pajevic et al., 2013). In an example of synchronicity, although thalamocortical projections are derived from different cortical areas and display various fibers of different lengths, the arrival time of spikes are synchronous (Salami et al., 2003). As proposed by Hoz et al., different patterns of myelination may help synchronize the timing of this arrival across different axon lengths (Hoz and Simons, 2015).

Another proposed function of adaptive myelination is the metabolic support of neurons by oligodendrocytes. As previously mentioned (section 1.1.3), studies have recently shown that oligodendrocytes are capable of supplying energy in the form of lactate/pyruvate to neurons via MCT1/2 transporters, which is used in the production of ATP (Fünfschilling et al., 2012; Lee et al., 2012b). Interestingly, it is well known that short ranged interneurons are myelinated, which seems paradoxical if the sole purpose of myelination is to increase conduction and velocity (Micheva et al., 2016; Orduz et al., 2015; Stedehouder et al., 2018). In fact, one study suggests that ~25-50% of all myelinated cortical axons are from GABAergic interneurons (Orduz et al., 2015). If short ranged axons are less reliant on myelination for increasing conduction velocity, is it possible that rapidly firing interneurons rely on metabolic support from oligodendrocytes? Myelination is an energetically costly process and calculations show that axons may need to fire millions of times to offset the energy demand of myelination depending on the axons size, taking an estimated 1-2 months in the optic nerve (Harris and Attwell, 2012). Nevertheless, determining the net energetic cost/benefit to the entire organism becomes complicated when considering the additional energetic cost of maintaining the myelin sheath, as well as the energy cost of maintaining the resting membrane potential in oligodendrocytes (Harris and Attwell, 2012).

Determining the function of adaptive myelination, whether that is to influence additional *de novo* myelination in previously unmyelinated areas, fine-tune neuronal signaling, or provide metabolic support for rapidly firing axons is yet to be determined. Although the field is unclear as to why or how activity influences oligodendrocyte behavior, it is at least clear that modulating activity can affect the oligodendrocyte linage in several ways, including oligodendrogenesis, differentiation, and several aspects of myelination.

1.6.3 Activity-mediated oligodendrogenesis

A number of cellular processes dictate the available pool of differentiating oligodendrocytes available to myelinate. Generally speaking, proliferation of the OPC population increases the number of cells available to either continue proliferation or terminally differentiate into pre-myelinating oligodendrocytes. Live imaging studies within the adult mouse cortex found that the differentiation of one OPC tends to be associated with subsequent proliferation of an adjacent OPC in order to replace it (Hughes et al., 2013), so in practice the processes of differentiation and proliferation are tightly coupled. In addition to the differentiation of OPCs, cell death also contributes to the ultimate number and location of myelinating oligodendrocytes; a large proportion of the newly differentiated pre-myelinating oligodendrocytes undergo apoptosis during both development and adulthood (Barres et al., 1992; Hughes et al., 2018; Trapp et al., 1997). Genetically blocking apoptosis causes increased myelination, including of axonal populations that usually remain unmyelinated (Sun et al., 2018). Current evidence suggests that neuronal activity influences the final density of myelinating oligodendrocytes through all three of these processes; proliferation, differentiation, and cell death.

Substantial experimental evidence links stimulation of neuronal firing to OPC proliferation. For example, direct electrical stimulation of the corticospinal tract in adult mice leads to increased OPC proliferation (Li et al., 2010). Similarly, optogenetic stimulation of the premotor cortex leads to increased OPC proliferation 3 hours after stimulation within the cortex and underlying white matter; an increase that is reduced but still detectable 4 weeks after a week of stimulation (Gibson et al., 2014). Chemogenetic stimulation of cortical neurons using excitatory Designer Receptors Exclusively Activated by Designer Drugs (DREADDs) results in increased OPC proliferation within the corpus callosum, albeit with much longer latency between stimulation

and detectable increases in proliferation (Mitew et al., 2018). Some of these differences in timing may reflect the frequencies and activity patterns generated by the optogenetic and chemogenetic approaches, given the recent findings that high frequency stimulation (25–300 Hz) has greater effects on OPC proliferation within the corpus callosum than low-frequency stimulation (Nagy et al., 2017). Compared to these stimulation experiments, sensory deprivation experiments have yielded mixed results. An early study sought to examine the effect of decreased neuronal activity on oligodendrogenesis within the developing optic nerve of early postnatal rats using the Na+ channel blocker tetrodotxin (TTX) to block retinal ganglion cell action potentials. Injection of TTX into one eye resulted in a substantial decrease in the number of mitotic OPCs in the optic nerve after 2 days (Barres and Raff, 1993). A more recent study sutured the eye shut to reduce coordinated activity between P15 and P32 found only a minor decrease in OPC proliferation over this longer time period (Etxeberria et al., 2016); however, sensory deprivation via whisker trimming has been linked to increased OPC proliferation in the somatosensory cortex (Hill et al., 2014).

1.6.4 Activity-mediated differentiation, maturation, and survival

The differentiation of the progenitor population represents an important cellular process, as this newly differentiated pool may potentially myelinate previously unmyelinated regions of axons. The above studies show that increasing neuronal activity in the brain or corticospinal tract via electrical, optogenetic, or chemogenetic stimulation all result in increased differentiation of EdU or BrdU-labeled OPCs into postmitotic oligodendrocytes within the stimulated regions (Gibson et al., 2014; Li et al., 2010; Mitew et al., 2018; Nagy et al., 2017). In contrast, the effect of decreased firing of the retinal ganglion cells (RGCs) within the optic nerve during development suggests relatively limited influences of activity on differentiation. Reduced RGC firing at P4 via

TTX injections resulted in decreased myelin segments within the optic nerve when examined at P6 (Demerens et al., 1996), but the density of MBP expressing oligodendrocytes remained unchanged. This suggests that myelination but not the preceding step of differentiation was sensitive to activity. A recent monocular deprivation model examining the optic tract at P32 surprisingly reported an increase in mature oligodendrocytes generated between P15 and P32 in the deprived optic nerve and tract (Etxeberria et al., 2016). Given the strong apparent drive for the visual system to fully myelinate, these slightly disparate findings could perhaps be reconciled if an early decrease in myelin formation resulted in a compensatory increase in oligodendrocyte differentiation at later time points.

In other models, studies suggest that experience-driven oligodendrocyte differentiation precedes changes in proliferation. McKenzie et al. (McKenzie et al., 2014) and Xiao et al. (Xiao et al., 2016) provided mice with a complex running wheel task and found little change in OPC division in the first two days of running (measured by incorporation of EdU), though OPC proliferation was subsequently increased at four days. In subsequent experiments, OPCs were prelabeled with EdU prior to the introduction of the wheel. Researchers observed a reduction in the density of EdU-labeled OPCs at two days after introduction to the wheel, suggesting that they may have begun to differentiate. Using the expression of Ectonucleotide Pyrophosphatase/Phosphodiesterase 6 (*Enpp6*), a gene highly enriched in newly formed oligodendrocytes, they reported a significant increase in this population in as little as two hours after exposure to the running wheel, thereby confirming a rapid differentiation response. This result raises the possibility OPCs may typically respond to increases in activity first by differentiation, followed by a subsequent homeostatic proliferative response. A broadly similar

enhancement of differentiation (at the expense of OPC proliferation) has been reported in response to running on a noncomplex wheel (Simon et al., 2011) as well.

These studies show that changes to neuronal activity can lead to changes in the number of OPCs, newly formed oligodendrocytes, and mature oligodendrocytes. Are these newly generated pools transient or do they represent a cell population stabilized over time? Recently published work shows that the majority of oligodendrocytes that differentiate in the adult cortex fail to stably integrate; however, placing adult mice in an enriched environment that provides frequent whisker stimulation results in an increase in the of number of newly generated oligodendrocytes within the barrel cortex after 20 days (Hughes et al., 2018). Conversely, whisker trimmed mice show increased death of newly generated oligodendrocytes within the developing somatosensory cortex, without changes in the rate of cell death of mature oligodendrocytes (Hill et al., 2014). Collectively, these studies suggest that increases to neuronal activity can lead to an increased pool of newly generated oligodendrocytes, capable of surviving and myelinating.

1.6.5 Activity and myelin remodeling

Many studies cite an increase in proliferation, maturation, and *de novo* myelination after increases in activity, but can existing myelin segments undergo activity-dependent remodeling? The main aspects of myelin remodeling commonly examined are changes in myelin thickness and changes in internode length. Several genetic approaches demonstrate that mature oligodendrocytes can intrinsically regulate myelin thickness, as both the activation of the Erk1/2-MAPK (Ishii et al., 2012, 2013) and PI3K/AKT/mTOR pathway increase the myelin thickness by triggering additional wrapping in mature oligodendrocytes (Snaidero et al., 2014). Although stimulation of either pathway has yet to be liked to adaptive myelination, increases in myelin thickness are seen after

neuronal stimulation in both juvenile and adult mice (Gibson et al., 2014; Mitew et al., 2018). In the auditory system, Sinclair et al. asked whether raising the threshold in the auditory system changed aspects of myelination. Researchers provided mice between P55 and P66, a period after myelination reaches maturity in this region, with earplugs to raise the auditory threshold which resulted in a decrease in myelin thickness on large diameter axons. Although this study does not directly test adaptive myelination, it provides evidence that physiologic changes to activity are capable of remodeling myelin *in vivo* (Foster et al., 2019; Sinclair et al., 2017).

Changing the length of the myelin sheath or internode length may impact conduction speed. It may also change the length of the nodes of Ranvier and myelin coverage overall. Indeed, variable node lengths are observed in the optic nerve and cortex, and conduction velocity can theoretically change upon changes to nodal length (Hamilton et al., 2017). Whether nodal length is determined by axonal organization or myelination is yet to be determined (Williamson and Lyons, 2018). Technical limitations have hampered our ability to definitively address whether activity remodels existing internodes, as this requires observing the same internodes before and after stimulation.

In 2018, two separate studies used an *in vivo* two-photon imaging approach in mice to determine if sheath lengths were dynamically regulated. Hill et al. (Hill et al., 2018) looked in early adulthood (P90-120) and showed the majority (81%) of sheath lengths remained stable with age. Hughes et al. (Hughes et al., 2018) examined older animals (P365) and determined that 99% of sheaths remained stable, indicating that sheaths may become more stable with age. To determine if either increases or decreases in sensory stimulation effect this high level of stability, researchers used whisker stimulation (using hanging beads in the home cage) or whisker trimming and saw no change to the low level of remodeling. Together, these reports suggest that remodeling via alterations to existing internode length may not represent a major component to plasticity, but does

not rule out the possible influence on myelin thickness. Similar to the two-photon *in vivo* imaging studies, the same myelin segment would need to be examined over time in order to determine the potential impact of activity. Currently, the method of cross-sectional measurements via electron microscopy to measure myelin thickness limits the ability to examine sheath parameters longitudinally (Williamson and Lyons, 2018).

1.6.6 Mechanisms

Changes to neuronal activity influence oligodendrocyte dynamics, including alterations in proliferation, differentiation, survival, *de novo* myelination, and may remodel existing myelin segments. What possible signaling mechanisms underlie these changes to oligodendroglia?

1.6.6.1 Trophic factors

Several diffusible signaling molecules have been identified that may promote oligodendrocyte proliferation or differentiation within a brain region. Using a combined proteomics and optogenetics approach, Venkatesh et al. (Venkatesh et al., 2015) identified a series of proteins released by activated neurons, including Neuroligin-3 and BDNF. A role for Neuroligin-3 in myelination has not been shown, though Venkatesh et al. (Venkatesh et al., 2015) did find that it mediated much of the activity-induced proliferation of glioma cells in their model. Of the activity-induced proteins identified in that study, BDNF in particular represents an attractive candidate for mediating activity-induced oligodendrogenesis within active tracts, as it acts through oligodendroglial TrkB receptors to promote both OPC proliferation and subsequent myelination (Peckham et al., 2015; Wong et al., 2013; Xiao et al., 2011). In a recent animal study, Geraghty et al. specifically probed the connection between neuronal activity, BDNF, and the OPC TrkB

receptor and their roles in myelination (Geraghty et al., 2019). This study used optogenetics to stimulate neuronal activity in mice that either lacked activity-induced expression of *Bdnf* or lacked OPC-specific expression of TrkB. In the first strain, triple-site knock-in mutations in the BDNF protomer region prevents the binding of calcium-regulated factors essential for the activity-induced expression of *Bdnf* (particularly CREB). This allowed the activity-independent expression of *Bdnf* to continue while specifically inhibiting the activity-dependent expression. After optogenetic stimulation of the premotor cortex, control mice show an increase in OPC proliferation and thicker myelin, while mice lacking either the activity-dependent expression of BDNF and mice lacking the expression of OPC-derived TrkB expression show no change in proliferation or myelin thickness. These results suggest that neuronal activity mediates myelination through Bdnf-TrkB signaling in cortical projection neurons (Geraghty et al., 2019).

In addition to BDNF, a recent animal study implicated the secreted neuropeptide VGF in activity-mediated oligodendrogenesis. In a mouse genetic model of ataxia (Alvarez-Saavedra et al., 2016), voluntary exercise (running) both increased VGF expression and improved cerebellar myelination. VGF promoted oligodendrogenesis *in vitro* and viral expression of VGF increased myelination in the mouse ataxia model, suggesting it may contribute to the protective effects of exercise (Alvarez-Saavedra et al., 2016). As VGF is both downstream of BDNF and in turn modulates signaling through neurotrophic receptors (Alder et al., 2003; Bozdagi et al., 2008; Lin et al., 2015), considerable potential also exists for these two activity secreted factors to act in concert.

1.6.6.2 Neurotransmitters

Activity-regulated release of neurotransmitters demonstrate the potential to contribute to the activity-dependent myelination in either an axon-specific or at least highly localized level. In

addition to synaptic release at their terminals, axons release vesicular neurotransmitters along their length during action potentials (Kukley et al., 2007). OPCs express voltage gated ion channels and several neurotransmitter receptors including AMPA, NMDA, and GABA receptors (Biase et al., 2010). OPCs also receive direct synapse-like input from the axons of both excitatory and inhibitory neurons (Bergles et al., 2000; Lin and Bergles, 2003; Ziskin et al., 2007). The expression of many of these receptor subunits decreases in OPCs both during their differentiation and as the rate of myelination decreases with age (Biase et al., 2010; Spitzer et al., 2019). Interestingly, post-mitotic oligodendrocytes express detectable NMDA receptors, providing a potential mechanism to survey levels of activity in individual axons (Micu et al., 2016; Saab et al., 2016). Blocking axonal vesicular release in a subset of axons in the developing zebrafish reduces their myelin coverage (Hines et al., 2015; Mensch et al., 2015), a finding potentially attributable to the vesicular release of glutamate acting to promote the stabilization or extension of the developing myelin segments. Consistent with this possibility, blocking glutamate release from mouse RGC axons did not prevent their myelination but resulted in reduced internode length in the optic nerve (Etxeberria et al., 2016). Interestingly, studies show that *Mbp* mRNA travels to distal processes inside of RNA granules, awaiting translation (Ainger et al., 1993; Wake et al., 2011). Localized activity and synaptic release of glutamate also induces localized Ca^{2+} signaling and translation of MBP in oligodendrocyte processes (Krasnow et al., 2018; Wake et al., 2011), providing a localized cellular mechanism that could direct preferential myelin extension along active axons.

Nevertheless, the exact role of vesicular release of neurotransmitters in myelination remains unclear, with oligodendrocyte conditional knockouts of neurotransmitter receptor subunits showing only modest phenotypes. Myelination proceeds relatively normally in mice with deleted OPC specific NR1 subunit of NMDARs, with proliferation and differentiation remaining

unaffected and displaying only a minor delay in myelination (Biase et al., 2010; Saab et al., 2016). This argues for a modest role for NMDARs in myelination; so why express them at all? NMDA receptors demonstrate a higher affinity for glutamate than AMPA receptors. It is possible that these receptors act more as sensors prone to respond to smaller changes in glutamate levels or spillover from nearby active areas. Disruption of AMPARs in the oligodendrocyte lineage also results in relatively modest phenotypes, with a minor decrease in the myelinating oligodendrocytes caused by increased apoptosis of the differentiating cells (Kougioumtzidou et al., 2017). Although oligodendroglial NMDARs were not essential for myelination, Saab et al. (Saab et al., 2016) found NMDARs regulate the surface expression of glucose transporters. Additionally, researchers found mice without functional NMDARs in oligodendroglia develop a late onset axonal pathology (Saab et al., 2016). This supports the finding that oligodendrocyte glutamate signaling may be non-essential for myelination but an important mechanism regarding the metabolic support of axons by oligodendrocytes.

1.6.6.3 Contact mediated

During the exploratory phase of axonal selection and subsequent myelination, oligodendrocytes use motile processes to survey axons. Schwann cells, the resident myelinating cell in the periphrail nervous system (PNS), require the axonal expression of neuregulin-1 type III (NRG-1) (Taveggia et al., 2005) and the glial receptor expression of ERBB2/3 (Garratt et al., 2000) to determine the axon's myelination fate. The necessity of these molecules for myelination is more complicated in the CNS. Studies using NRG-1 mutants report regional differences in CNS myelination (Taveggia et al., 2007) or no difference in myelination (Brinkmann et al., 2008), and mice lacking the expression of ERBB3/ERBB4 in mature oligodendrocytes display normal CNS

myelination (Brinkmann et al., 2008). Despite the lack of clarity on the necessity of each molecule for CNS myelination, axonal NRG-1 and oligodendrocyte ERBB3 expression has been linked to activity-dependent myelination. Socially isolating juvenile mice during the critical period of development results in decreased myelination in the prefrontal cortex, as well as decreased expression of NRG-1 (Liu et al., 2012; Makinodan et al., 2012). Similarly, mutant mice lacking ERBB3 in OPC's during the critical period of development(Makinodan et al., 2012), as well as heterozygous NRG-1 mutants (Taveggia et al., 2007) show similar decreases in myelination in the prefrontal cortex, providing a possible link between the social-isolation induced hypomyelination and NRG-1 signaling. Outside of NRG-1/ERBB3, the axonal expression of N-cadherin, a cell adhesion molecule that promotes oligodendroglial-axonal interactions (Schnädelbach et al., 2001), increases along axons in an activity-dependent manner in the developing zebrafish (Chen et al., 2016). Conversely, inhibiting N-cadherin blocks the activity-induced change in myelination (Chen et al., 2016).

Linking contact-mediated mechanisms that regulate adaptive myelination within the CNS remains challenging, as essential cell surface molecules that regulate CNS myelination in general remain elusive. It is possible that CNS myelination depends on several contact-mediated mechanisms and that only a subset of these interactions is involved in adaptive myelination. Outside of specific molecules, it is well known that axonal diameter clearly influences CNS myelination, with a preference towards larger caliber axons (Goebbels et al., 2016; Lee et al., 2013; Mayoral et al., 2018). Interestingly, high-frequency signaling in neurons can transiently increase axonal diameter (Chéreau et al., 2017), providing a possible link between oligodendrocyte axonal selection and activity.

1.6.7 Synaptic connection between neurons and oligodendroglia

Cellular signaling between cells represents a fundamental aspect of nervous system communication. Within the CNS, our greatest understanding of the structural, molecular, and functional communication is between neurons via synapses. Our understanding of different types of cell to cell communication continues to develop, particularly our understanding of the synaptic or synapse-like connection between neurons and the oligodendroglia.

1.6.7.1 OPCs and neurons

The first reports of OPCs expressing molecules related to synaptic signaling, namely voltage-gated ion channels, occurred nearly three decades ago (Barres et al., 1990; Sontheimer et al., 1989) (Sontheimer, Barres 1990). Although an interesting finding, it took another decade to provide the first structural and physiological evidence of synaptic or synapse-like structures in OPCs (Bergles et al., 2000). Here, Bergles and colleagues used a combination of electrophysiological and electron microscopy techniques to demonstrate that neurons from the CA3 region of the hippocampus form synaptic connections with NG2+ oligodendrocyte progenitor cells (Bergles et al., 2000). Subsequently, two similar observations showed two separate populations, one expressing receptors for glutamate receptors and the other expressing glutamate transporters from NG2+ cells, receive synaptic input from neurons (Jabs et al., 2005; Matthias et al., 2003). Since initially discovered in the hippocampus, neuron-OPC synapses have been described in the cerebellum (Lin et al., 2005), corpus callosum (Kukley et al., 2007; Ziskin et al., 2007) and cortex, and have even been shown to maintain this connection throughout cell division (Ge et al., 2008; Kukley et al., 2008). Notably some, but not all, unmyelinated neurons release

glutamate along their axons, and some reports estimate the total number of synapses could be up to 70 from one cerebellar climbing fiber to one OPC (Lin et al., 2005).

The question of whether these connections are bona fide synapses or synapse-like structures continues to be debated. Electron micrographs show an electron dense postsynaptic density within OPCs (Bergles et al., 2000; Kukley et al., 2007; Lin et al., 2005), and OPCs express mRNA for classical postsynaptic markers such as PSD-95, scaffolding protein GRIP1, voltage-gated Na^+ channels, AMPA, NMDA, and GABAergic receptors (Biase et al., 2010; Cahoy et al., 2008; Clarke et al., 2012; Kukley et al., 2010; Lin and Bergles, 2003, 2002). Although the current understanding is that this connection in unidirectional, unlike post-synaptic densities in neurons, OPCs express many presynaptic markers such as synaptophysin and bassoon (Cahoy et al., 2008). While the definitive designation as a genuine synapse is debatable, the existence of a structural and physiological connection is well established. For simplicity, this connection will be referred to as a synapse for the remainder of this chapter.

1.6.7.2 Differentiated oligodendrocytes and neurons

It was originally thought that OPCs lose their synaptic connections upon differentiation. Using whole-cell recordings, Kukley and colleagues demonstrated that OPCs show a clear synchronous somatic current that significantly reduces upon differentiation and is undetectable in the mature oligodendrocytes (Kukley et al., 2010), a finding that correlates with the downregulation of many synapse-related mRNAs (Cahoy et al., 2008). In addition, two studies published in 2015 showed that inhibiting vesicular release in neurons decreases the number of sheaths per oligodendrocyte and impacts sheath stability in developing zebrafish (Hines et al., 2015; Mensch et al., 2015). Both studies inhibited axonal exocytosis early in zebrafish development before the

onset of myelination, therefore it is unclear if OPCs received instructional cues about myelination via vesicular release, or if the inhibition of vesicular release directly affected mature oligodendrocytes. Coupled with the loss of somatic current and downregulation of synapse-related mRNA upon differentiation (Cahoy et al., 2008; Kukley et al., 2010), these changes in myelination would seemingly be due to the loss of instructional cues to OPCs; however, more recent publications challenge this idea.

In 2018, Krasnow and colleagues showed that neuronal activity raises intracellular calcium in oligodendrocytes using a zebrafish model (Krasnow et al., 2018). Here, researchers electrically stimulated the zebrafish spinal cord and measured changes in intracellular calcium within oligodendrocyte somas and myelin sheaths using a fluorescent calcium indicator. Despite undetectable calcium transience in the soma of myelinating oligodendrocytes, there is a small but consistent increase in calcium within the myelin sheath after spinal cord stimulation (Krasnow et al., 2018). Importantly, despite the downregulation of mRNA encoding receptors like AMPA and NMDA upon differentiation, mature oligodendrocytes still express these receptors in a seemingly functionally relevant way. The inner tongue of the myelin sheath contains these receptors and activation of these receptors increases intracellular calcium within the sheath under physiological conditions in the optic nerve, and to an even greater extent under pathological conditions of chemical ischemia (Micu et al., 2005, 2016). This finding is intriguing, as Hughes & Appel recently demonstrated that axonal exocytosis sites are positioned under sheaths and post-synaptic assembly proteins, including PSD-95, localizes and accumulates at these sites within the myelin sheath. Additionally, researchers found that perturbation of *Cadm1b*, a synaptic adhesion molecule, reduces sheath length in zebrafish (Hughes and Appel, 2019).

Together, these findings suggest a highly localized synaptic connection within the myelin sheath, leading to the hypothesis of the 'axo-myelinic synapse' originally proposed by Peter K. Stys in 2011 (Stys, 2011). Briefly, the 'axo-myelinic synapse' hypothesis suggests that myelinated axons release neurotransmitters in an activity-dependent manner. As an action potential travels down the length of the axon, low-level glutamate release activates glutamate receptors located on the inner myelin surface, triggering an influx in local calcium within the myelin sheath (Stys, 2011). Although the purpose of local calcium signaling is yet to be determined, it is hypothesized that influxes in intracellular calcium lead to glycolysis and the production of pyruvate, which in turn is transported back to neurons thereby providing a source of local energy for active axons (Micu et al., 2017). Besides metabolic support, myelin contains several calcium sensitive proteins, including calmodulin, phospholipases, and calpains, representing additional targets for local Ca2+ within the sheath (Micu et al., 2017). Despite this elegant putative mechanism of local signaling, the requirement for vesicular release is heterogenous, as inhibition of release is required for myelination in some axons, while others remain unaffected (Koudelka et al., 2016).

1.7 RNA profiling oligodendroglia - technical challenges and promising solutions

1.7.1 Challenges in capturing oligodendroglial RNA

Transcription and translation underscore cellular function, therefore understanding gene expression profiles can provide insight to various physiological and cellular processes. Ideally, profiling the *in vivo* transcriptional and translational state in any cell type helps inform our understanding of cellular processes, however, oligodendroglia present particular challenges for several reasons. Since oligodendroglia move through several developmental stages with distinct functions (see section 1.1 & 1.2 for further discussion), separating the transcriptional and

translational profile at each stage adds an additional layer of complexity. Oligodendroglial morphology represents another technical challenge, as cells within each stage display a highly branched morphology. Most cell isolation techniques typically fracture these cellular processes, resulting in the loss of associated peripheral mRNA. Furthermore, the lipid-rich myelin itself presents a technical challenge for isolating RNA *in vivo*. As myelin becomes established it also becomes more difficult to physically separate, making it a challenge to isolate cell bodies housed within white matter regions. Cell isolation techniques in older animals risk a lower RNA yield and isolate more cortical cells than white matter cells, yet techniques in younger animals are unable to capture transcriptional and translational information past early development. Additionally, when considering the possibility of transcriptional and translational RNA processing, single RNA isolation techniques are unable to both capture and separate the transcriptional and translational state of the cell. Collectively, these limitations present technical barriers in capturing cell/stage specific oligodendroglial transcriptional and translational states.

1.7.2 Cell isolation techniques

Despite the technical challenges in capturing *in vivo* oligodendroglial RNA, many groups have been successful in capturing RNA from different stages of the oligodendrocyte lineage. Early techniques took advantage of antibodies targeted against stage/cell specific antigens expressed at the cell surface. Although aspects of *in vivo* cellular morphology and age limit the type of RNA captured, both immunomagnetic separation and immunopanning led to major discoveries of several important genes. An earlier study used immunopanning to study rat OPCs and assessed their transcriptome via microarray during differentiation *in vitro* (Dugas et al., 2006). This study identified several uncharacterized transmembrane, secreted, and cytoskeletal proteins, as well as

dynamically regulated transcription factors. Following this, Cahoy et. al (Cahoy et al., 2008) established a transcriptome database for all major neural cell types using a combination of immunopanning and FACS to acutely purify different populations of cells from the developing mouse brain, again using a microarray platform to assess gene expression at a genome-wide level. This dataset led to the discovery of the role of the transcription factor, MYRF in CNS myelination (Emery et al., 2009a). Combined with subsequent RNA-Seq databases cataloging splice variation and the human neuro-transcriptome (Zhang et al., 2014a, 2015b), these datasets are used as a springboard and reference throughout the field of neurobiology. From a disease perspective, isolating a pure OPC population from human tissue using immunomagnetic separation allowed for advancements in our understanding of OPC transplants as a treatment for hypomyelinating diseases (Sim et al., 2011). Although many of these studies cannot assess transcription or translation separately, depend exclusively on young animals, and may not capture peripheral mRNA, they significantly impacted our understanding of RNA expression in not only oligodendroglia, but neurobiology as a whole.

1.7.3 Single-cell and single-nuclei techniques

New advancements in cell isolation techniques, such as single-cell and single-nuclei sorting (combined with approaches like fluorescence-activated cell sorting [FACS] or drop-seq) offer attractive options to address many of the previously identified limitations. Although these advancements result in more noise, require more complex bioinformatics, and may still be subject to the loss of peripheral mRNA, they offer the ability to dissect gene expression at single-cell resolution (Chen et al., 2019; Marques et al., 2016, 2019). Perlman et. al used single-cell isolation to evaluate the developmental trajectory of OPCs in the human brain (Perlman et al., 2020). Other

researchers applied these techniques in the context of disease and disorder to evaluate changes in gene expression in oligodendroglia after morphine exposure (Avey et al., 2018), in experimental models of multiple sclerosis (Falcão et al., 2018) and in post-mortem human multiple sclerosis tissue (Jäkel et al., 2019; Schirmer et al., 2019).

A study published by Marques et al. serves as a useful example of how these techniques may provide advancements in our understanding of oligodendroglial heterogeneity (Marques et al., 2016). Although oligodendrocytes move through the three distinct stages of maturation (OPC to newly formed oligodendrocyte to myelinating oligodendrocyte), the level of heterogeneity within each stage remained unclear. Here, researchers sought to assess this by examining the transcriptomes of 5,072 single cells expressing oligodendrocyte lineage makers across 10 brain regions in both juvenile and adult mice. Surprisingly, Marques et al. reported thirteen distinct oligodendroglial populations; twelve of these populations represented a continuum of OPC progression towards mature oligodendrocytes, and one population of *Pdgfra*$^{+}$ cells, distinct from OPCs, were found along blood vessels. Although this study does not assess the functional relevance of the different oligodendroglial populations, it demonstrates how advancements in our understanding of cellular transcriptomic may lead to new insights in cellular function.

1.7.4 Capturing and separating transcription from translation

Single-cell and single-nuclei techniques offer the previously described advantages, however, both techniques are unable to capture and separate transcriptional and translational processes within a given cell. It was once thought that mRNA abundance was a suitable proxy for protein expression, however, several studies demonstrate that mRNA abundance may not accurately predict protein levels due to the translational regulation of mRNA (Kislinger et al., 2006;

Nagaraj et al., 2011; Roch et al., 2004; Tebaldi et al., 2012). Although proteomics may offer the most direct way of measuring protein expression, the current challenges of independently determining protein sequences and measuring low-abundance proteins present major technical limitations (Ingolia et al., 2009). Therefore, capturing the translatome may serve as a useful link between RNA transcription and protein production.

Theoretically, both polysome and ribosome profiling capture actively-translating mRNA. Polysome profiling separates polysomes via sucrose gradient centrifugation and subsequently isolates associated mRNAs (Jin and Xiao, 2017). Ribosome profiling uses the ribosomal footprint of active ribosomes to protect regions of mRNA during the enzymatic digestion required to capture mRNA fragments (Ingolia et al., 2009). The RNA captured from both techniques can be used for RNA-seq to investigate global translation and each technique offers specific advantages and disadvantages. While polysome profiling offers a more direct measurement of translational activity, ribosome profiling captures positional information at the sub-codon level, making it more suitable for revealing alternative translation initiation sites (Jin and Xiao, 2017).

A different approach to polysome purification uses immunopurification, rather than sucrose gradient centrifugation, to isolate tagged-ribosomes and their associated mRNAs. The bac-translating ribosome affinity purification (bac-TRAP) method (Heiman et al., 2008) uses bacterial artificial chromosome (BAC) transgenic mice to express an eGFP-tagged ribosomal transgene in specific cell populations. The RiboTag method (Sanz et al., 2009a) uses a Cre-lox system to express an epitope tagged ribosomal subunit ($RPL22^{HA}$) in cell-specific manner. Both systems use antibody-coated magnetic beads to separate epitope-tagged ribosomes from fresh tissue and predominately capture actively translating mRNA (Doyle et al., 2008; Heiman et al., 2008; Sanz et al., 2009b). The RiboTag method offers two additional advantages over the bac-TRAP

approach. This method drives the expression of the modified *Rpl22* gene from the endogenous locus resulting in efficient expression of the tagged allele at endogenous levels. Additionally, the floxed mice allow researchers to combine the RiboTag system with pre-established Cre-expressing mice, offering broader versatility. Both systems have been used in oligodendroglia (Voskuhl et al., 2019), or specifically from OPCs or mature oligodendrocytes (Avey et al., 2018; Bellesi et al., 2013; Dougherty et al., 2012; Doyle et al., 2008; Forbes et al., 2020; Reddy et al., 2017) to either profile or compare the translatome in different states. A potential caveat to using the RiboTag method is that the captured mRNA may represent actively-translated, stalled, or repressesed RNA, however, studies suggest that the large majority of ribosome-bound mRNA represents translationally active mRNA (Sanz et al., 2009b; Shigeoka et al., 2016).

In an interesting approach, Reddy et al. used the bacTRAP system to capture both ribosome-bound mRNA, via immunopurification, and nuclear RNA, via FACS, from mature oligodendrocytes. Researchers took advantage of ribosomal assembly in the nucleolus, which gave bac-TRAP nuclei the GFP positive signal required for FACS (Reddy et al., 2017). This clever combination of techniques allowed for the capturing and separation of both transcriptional and translational information, but offers less versatility than Cre-lox systems. The isolation of nuclei tagged in specific cell types, or INTACT, method offers an attractive solution to capturing both genomic and transcriptional information in a cell-specific and versatile way (Deal and Henikoff, 2010). Originally used to capture transgenic plant nuclei (Deal and Henikoff, 2010) and eventually applied to transgenic mice (Mo et al., 2015), the INTACT method uses a Cre-lox system to express an eGFP-tagged nuclear envelope protein, SUN-1. Similar to the previous immunopurification methods, INTACT uses antibody-coated magnetic beads to separate eGFP labeled nuclei from freshly harvested tissues. Although INTACT has yet to be used in the oligodendrocyte lineage

cells, it has been successfully used to capture nuclei from different populations of neurons (Mo et al., 2015) and to isolate nuclei from fibrous tissues (Bhattacharyya et al., 2019). To date, no single technique addresses the many challenges that oligodendroglia present in capturing *in vivo* cell and state-specific transcriptional and translational RNA past development, however, different combinations of techniques offer a promising path forward.

1.8 Summary

Chapter one provides an overview of the current understanding of oligodendrocyte function and development, as well as factors that control and influence oligodendroglia. Over the last several decades, oligodendrocytes progressed from static cells, important only for signal propagation, to dynamic cells possibly capable of metabolic support and plasticity. Accordingly, these major and recent advancements in our understanding of oligodendrocyte function leave key mechanisms driving oligodendroglial biology unresolved. Several successful RNA profiling studies led to novel findings that advanced our understanding of oligodendrocyte biology (see section 1.7.1), yet the technical limitations of these studies leave several key areas of investigation unaddressed. To date, no single study has collectively captured, separated, and compared the transcriptional and translational states across the oligodendrocyte lineage.

Advancements in the ability to capture and separate transcriptional and translational states across the oligodendrocyte lineage may be well-suited to answer questions regarding adaptive myelination: How do extrinsic neuronal signals influence oligodendroglia to proliferate, differentiate, and myelinate? Do OPCs and myelinating oligodendrocytes process this signal differently? Given the 'axo-myelinic' hypothesis and the possible importance of local signaling within the myelin sheath (see section 1.6.7), approaches that can capture mRNA in distal processes may be of particular importance.

The overall goal of this thesis is to study oligodendrocyte gene expression. Chapter three describes our efforts comparing the transcriptome and translatome of oligodendrocyte progenitor cells and mature oligodendrocytes in adult mice. Chapter four describes our efforts to study the effect of increased neural activity on the mature oligodendrocyte transcriptome and translatome. By taking advantage of the recent advancements in transcriptional and translational profiling techniques, specifically the RiboTag and INTACT approaches, I hope to both capture and separate the transcriptome and translatome across the oligodendroglial lineage to further understand the oligodendrocyte response to activity and identify novel regulators of CNS myelination.

Chapter 2: Materials and Methods

Mouse husbandry and maintenance. All animal procedures were approved by the Institutional Animal Care and Use Committee of Oregon Health and Science University. Animal experiments were conducted in accordance with NIH Guide for the Care of Use of Laboratory Animals. Animals were housed in a temperature and humidity-controlled facility with a 12-h light/dark cycle. The Cre-inducible Rpl22-HA ("Ribotag") line (Jax line 011029) was crossed with the NG2-CreERT line (Jax line 008538) and the PLP-CreERT line (Jax line 005975) to generate the NG2:RIBO or PLP1:RIBO lines, respectively. The same two CreERT lines were crossed to the Cre-inducible Sun1-eGFP line (Jax 021039) to generate the NG2:NUC and PLP1:NUC lines. All experiments used mice compound heterozygous for both the CreERT and the Rpl22-HA or Sun1-eGFP allele. Tamoxifen (Sigma) was prepared in Corn Oil (Sigma) at 20 mg/ml. Between 18-22 weeks of age, NG2:NUC and NG2:RIBO lines were injected with 100 mg/kg tamoxifen intraperitoneal injection (i.p.), every 24 hrs for 5 days and PLP1:NUC and PLP1:RIBO were injected every 24 hours for 3 days.

Zebrafish husbandry and maintenance. Adult zebrafish were housed and maintained according to institutional animal protocols. All zebrafish experiments were performed in compliance with institutional animal protocols. *Tg(mbp:EGFP-CAAX)* has been previously described (Almeida et al., 2011). Embryos were collected from pair-wise homozygous in-cross matings, injected at the one-cell stage, and raised at 28.5°C in 10 mM HEPES-buffered E3 Embryo medium for all experiments (Westerfield, 2000). All injected embryos were analyzed at 3-5 days post-fertilization (dpf). Staging was performed using standard protocols (Kimmel et al., 1995).

Immunohistochemistry. Mice were deeply anesthetized with 400 mg/kg ketamine (Vetone, Idaho, USA) and 60mg/kg xylazine (Vetone, Idaho, USA) and then perfused transcardially with phosphate buffered saline (PBS), followed by 4% paraformaldehyde/PBS. Brains were removed and postfixed at 4° C for 2 hours, and cryopreserved in 30% sucrose/PBS, followed by embedding in Tissue-Tek OCT compound (Sakura FineTek, Torrance, CA, USA). Brains were stored at -80° C until cryosectioning. 10 μm coronal sections were collected onto Superfrost Plus slides (Menzel Glaser, Braunschweig, Germany). Sections were incubated with a blocking/permeabilization solution (PBS containing 0.3% Triton X-100 and 10% fetal calf serum) for 1 hour at room temperature (RT). Sections were then incubated in the blocking/permeabilization solution with the primary antibody overnight at RT. Sections were washed 3 times in PBS, then incubated in the blocking/permeabilization solution with the secondary antibody (highly cross-absorbed Alexaflour conjugated antibodies, Invitrogen) for one hour at RT. All primary antibodies were used at 1:1000 unless otherwise noted: α-NeuN (Millipore), α-IBA1 (Wako), a-ALDH1L1 (Abcam), CC1 monoclonal (Millipore), α-PDGFRα (1:200; R&D Systems), α-eGFP (Abcam), α-Fos (Phosphosolutions), and α-HA (Cell Signaling).

Cell counting and analysis. To determine the recombination profile of the four mouse lines, immunostained tissue was analyzed by counting the number of cells showing co-localization of the tagged protein (HA for RiboTag or GFP for INTACT) and the cell type-specific marker. Images of stained tissue were acquired using a Zeiss AxioImager. An area of interest was drawn over the image which included dorsal cortex and corpus callosum, corresponding to the area dissected for RNA purifications (depicted in Chapter 3, Fig. 1C). Cell counts were subsequently performed in FIJI/Image J by an investigator blinded to the staining conditions.

RiboTag immunoprecipitation. NG2-RIBO and NG2-NUC mice were used to isolate tagged oligodendroglial ribosome-bound RNA according to previously published protocols (Sanz et al., 2009a, 2019), with minor modifications. Briefly, a ~200 mg region of interest (depicted in Chapter 3, Fig. 1B) was dissected and placed into a dounce homogenizer and lysed in 2 ml lysis buffer (50 mM Tris, pH 7.5, 100 mM KCl, 12 mM MgCl2, 1% Nonidet P-40, 1 mM DTT, 200 U/mL Promega RNasin, 1 mg/mL heparin, 100g /mL cycloheximide, Sigma protease inhibitor mixture). Following lysis, the homogenate was centrifuged at 13,00 RPM at 4°C for 10 minutes. 75µl of the clarified supernatant was reserved as the "input" sample. The remaining sample was incubated for 90 minutes at 4°C with 2 µg 3F10 anti-HA monoclonal (Roche) and then incubated for a further 90 minutes with 40 µl washed Protein G Dynabeads. Beads were washed three times in 50 mM Tris, pH 7.5, 300 mM KCl, 12 mM MgCl2, 1% Nonidet P-40, 1 mM DTT, 100 g/mL cycloheximide. RNA was purified from both the input and the beads using RNeasy Micro kit (Qiagen) according to the manufacturer's protocol.

INTACT immunoprecipitation. NG2:NUC and PLP1:NUC mice were used to isolate Sun1-eGFP tagged oligodendroglial nuclei. A ~200 mg region of interest (depicted in Chapter 3, Fig. 1B) was dissected and placed into a dounce homogenizer with 5 ml of Homogenization Buffer (HB, 0.25 M Sucrose, 25 mM KCl, 5 mM MgCl2, and 20 mM Tricine-KOH) supplemented with EDTA-free Protease Inhibitor and RNAsin Plus. Dounce homogenization was performed (15 strokes pestle A, 10 min on ice, 15 strokes pestle B, 10 min on ice). 320 µl of 5% IPEGAL was added followed by 5 additional strokes with pestle B. 5 ml of working solution was added (5 volumes of Optiprep [60% w/v iodixanol solution, Millipore Sigma]:1 volume of Diluent [Diluent:

150 mM KCl, 30mM MgCl2, 120 mM Tricine-KOH]) and mixed gently. Homogenates were then transferred to 30 ml Corex tubes. A sucrose gradient was formed by underlying the sample with 7.5 ml of 30% iodixanol solution (4.5 ml working solution, 3 ml HB) followed by 4 ml of 40% iodixanol solution (3.2 ml working solution, 0.8 ml HB). Samples were centrifuged at 10,000 g for 18 mins at 4°C. After samples finished spinning, ~1.5 ml of the sample band at 30-40% iodixanol interface was collected. Collected samples were precleared for 15 mins at 4° C using 20 µl of washed Protein G Dynabeads. Samples were then placed on a magnetic separator to remove magnetic beads, and the remaining sample was incubated with 5 µl anti-GFP antibody (Abcam), 60 µl of washed Protein G Dynabeads, 400 µl wash buffer (WB), and 1 µl RNAsin Plus for 20 min at 4° C. Samples were placed back on the magnetic separator, supernatant was removed and reserved for input samples. The magnetic beads with bound nuclei were then passed through a 20 µm filter and washed 3 times with WB. To elute bound RNA, buffer RLT with 1% ßME (Qiagen, cat # 79216) was added to the beads. RNA was purified from both the IP and input sample using a RNeasy Micro kit (Qiagen) according to the manufacturer's protocol.

RNA-sequencing and data analysis. The integrity of purified RNA samples was assessed via Agilent TapeStation, with RIN values falling between 7.9-10. Sequencing libraries were generated using the Clonetech SMARTer stranded RNA-Seq kit. Barcoded libraries were sequenced on the Illumina HiSeq 2500 at the Oregon Health and Science University Massively Parallel Sequencing Shared Resource (100 cycle single end sequencing, 4 samples per lane). Genome alignment, STAR analysis, and DESeq differential expression analysis were performed using workflows on Basepair (https://www.basepairtech.com). One sample (Immunoprecipitant from NG2:NUC) showed high variance compared to the two additional biological replicates and was included in the initial cell-

specificity analysis, but removed from all subsequent analyses. Volcano plots and PCA analysis were generated using START: Shiny Transcriptome Analysis Resource Tool (https://kcvi.shinyapps.io/START/) (Nelson et al., 2016). Heatmaps were generated using GenePattern (https://cloud.genepattern.org/gp/pages/index.jsf). Gene Ontology analysis was performed using Metascape (https://metascape.org/gp/index.html#/main/step1). Gene biotype analysis was performed using ShinyGo v0.51:Gene Ontology Enrichment Analysis + more (http://bioinformatics.sdstate.edu/go51/). Visualizations for the gene biotype analyses and gene expression boxplots were generated using Prism software.

sgRNA Design. gRNA target sequences were chosen from previously published datasets (Wu et al., 2018) or designed using the CHOPCHOP (version 3) web tool (https://chopchop.cbu.uib.no/) (Labun et al., 2016, 2019; Montague et al., 2014) or the CRISPR-Cas9 guide RNA design tool from Integrated DNA Technologies (IDT) (https://www.idtdna.com/site/order/designtool/index/CRISPR_PREDESIGN).

sgRNA *In Vitro* Transcription. Templates for guide RNA production were generated by annealing and elongation (Phusion Flash High-Fidelity Master Mix, Life Technologies) of a forward primer containing a T7 promoter and guide sequence and a reverse primer encoding the standard chimeric sgRNA scaffold (Varshney et al., 2015). Guide-specific primers for each gene were combined for annealing and elongation. Oligonucleotides were obtained from Integrated DNA Technologies (IDT). The DNA template was purified (QIAquick PCR Purification Kit, Qiagen) and *in vitro* transcribed (MEGAshortscript™ T7 Transcription Kit, Invitrogen™). RNA

was purified using RNA Clean and Concentrator-5 (Zymo Research) and stored at -80 °C until use.

Cas9 Ribonucleoprotein (RNP) Preparation and Injection. Standard ribonucleoprotein (RNP) preparation was followed as performed previously (Wu et al., 2018). Briefly, His-tagged Cas9 protein containing a nuclear localization sequence (Alt-R® S.p. Cas9 Nuclease V3) was obtained from Integrated DNA Technologies (IDT). The protein was diluted to yield a 10 µM Cas9 solution in 20 mM Tris-HCl, 600 mM KCl, 20% glycerol and stored at -20 °C. The Cas9 solution was mixed 1:1 with sgRNA (740 ng/µL for *myrf* control and 100-300 ng/µL for other genes) to generate Cas9 RNP complexes. ~0.05% phenol red dye was added for visualization of injections. Microinjection was performed by injecting 0.5-1 nL of the mixture into 1-cell stage embryos in either the yolk or the cell cytoplasm.

Isolation of Genomic DNA and Analysis of Cas9 Editing. Embryos were lysed in 25 mM NaOH, 0.2 mM EDTA for 30 min at 95 °C and neutralized with an equal volume of 50 mM Tris-HCl pH 8.0. Efficient Cas9 editing was determined using a Cleaved Amplified Polymorphic Sequences (CAPS) assay by comparing restriction enzyme fragmentation patterns between uninjected and injected embryos at 3-5 dpf. PCR primers for amplification were selected from CHOPCHOP (https://chopchop.cbu.uib.no) for each target sequence.

Image Acquisition and Analysis. Larvae were visualized at 3-5 dpf using a Vertebrate Automated Sorting Technology (VAST) BioImager (Union Biometrica) coupled to a spinning disc confocal microscope (SDCM) at 16X magnification (Carl Zeiss Microscopy), referred to as VAST-SDCM

(Early et al., 2018). Images were then processed and analyzed as maximum intensity projections (MIPs) using Fiji/ImageJ. Briefly, regions of interest (ROIs) were drawn over the dorsal and ventral spinal cords in between the fourth and sixth body segment. Percent GFP was determined using consistent thresholds and ROI sizes for each dataset to measure percent area of fluorescence. Dorsal brightfield images were used to measure body length. All percent GFP and body length data were visualized using Prism software.

Voluntary wheel running and EdU labeling. Male and female C57Bl/6J mice were used in this investigation. Between the time of weaning and eight weeks of age, male and female animals were housed with sex-paired littermates (3-5 mice per cage). Between eight and ten weeks of age, animals were treated with EdU. EdU (Santa Cruz) was dissolved in the drinking water (0.3 mg/ml) which was available to mice *ad libitum* and replaced every 3 days for 14 days. At day 15, male and female cages were separated in to new cages of 3-4. Groups were kept either in standard housing conditions or in cages with a fixed running wheel for 14 days and animals were sacrificed at the end of the 14-day period.

Detection of EdU. For EdU labeling, fixed, cryosectioned (10 μm) and slide mounted tissue was washed in PBS and incubated in 0.8 % Triton X-100/PBS at 21°C for 20 min. Slides were washed 3X in 1X PBS, then processed following the manufacturer instructions using the Click-iT EdU Alexa Flour-647 Imagining kit (Invitrogen). Slices were then washed and mounted with Prolong Diamond Antifade with DAPI (Invitrogen).

Viral & Clozapine injections. AVV2-hSyn-mCherry (University of North Carolina) or AAV2-hSyn-hM3D-(Gq)-mCherry (Addgene) viruses were used as specified. Both viral titers were $4.8x10^{12}$ GC/ml. Injections were performed on P5 mice pups anesthetized on ice (~3-5 mins or until the absence of a pinch reaction) and maintained under a cold pad throughout the procedure. At the beginning of the procedure, litters were separated for the dams and placed into a separate cage on top of a heated pad with bedding from the original cage. Pups were then individually anesthetized as above and a small incision was made above each injection site (General coordinates). Bilateral injections of 1µl was performed using a Hamilton syringe and needle (syringe-cat. 13205, 30-gauge needle-cat. 7803-07) mounted on a micromanipulator. After the injections, pups were gently placed on a heating pad and monitored during their recovery. Once recovered, pups were placed in a separate cage with home bedding on top a heating pad. All pups were injected and returned back to their home cage. Pups were closely monitored to ensure the mothers acceptance and care of post-operative pups. Mice were allowed to recover for 35 days. A Clozapine/saline solution (0.1 mg/kg) was intraperitoneally injected once into P40 mice expressing AVV2-hSyn-mCherry or AAV2-hSyn-hM3D-(Gq)-mCherry.

Quantitative PCR analysis. All tissue for the qPCR analyses found in Chapter 3 and Chapter 4 were processed using methods described in the "RiboTag immunoprecipitation" and "INTACT immunoprecipitation" method sections. The purified input RNA was used for the *Fos* expression analysis described in Chapter 4, Fig. 2F. Both the purified input and immunoprecipitated RNA was used for the cell-specific purification analysis described in Chapter 3 and 4. First-strand cDNA synthesis was completed according to the manufacture protocols (Invitrogen). Relative expression levels of *Fos, Gapdh, Mog, Pdgfra, Mbp, Aif1, Gja1, Syt1*, and *Enpp6* were determined via

TaqMan Assays and probes (ThermoFisher). Gene expression was first normalized to the *Gapdh* mRNA expression levels within the sample and data were analyzed using the $2^{-\Delta\Delta Ct}$ method.

Sham and iTBS stimulation. Low-intensity repetitive transcranial magnetic stimulation was delivered as described in (Cullen et al., 2019). Briefly, a custom made 120 mT circular coil specifically designed for rodent stimulation was used to deliver 600 pulses of intermittent theta bursts for 192 seconds. The coil was positioned in line with the front ears (~Bregma -3.0) and manually held over midline. Sham mice were treated similarly without the addition of current. Sham and iTBS treatment were repeated daily for 7 days.

Chapter 3: Transcriptional and translational profiling of oligodendrocyte lineage cells

Abstract

Understanding transcriptional and translational regulation provides insight into various cellular processes in many cells, including oligodendrocytes. Here, we compare two separate methods aimed at capturing either the transcriptome or translatome in both oligodendrocyte progenitor cells (OPCs) and mature oligodendrocytes (mOLs). Capturing nuclear RNA using the INTACT method and ribosome-bound RNA using the RiboTag method, we show both purification methods enrich for RNA from the target cell types, but that the INTACT method offers greater cell specificity. Additionally, we show that each method efficiently captures genes with high changes in expression upon differentiation. In a comparison between the nuclear RNA and ribosome-bound RNA within each stage of the lineage (within either OPC or mOL), we show that despite the large overlap in expression profiles, subsets of RNA transcripts are highly overrepresented in either the nuclear or ribosome-bound RNA. Gene ontology enrichment analysis of the preferentially ribosome-bound RNAs reveal enrichment for synapse organization, signaling, and structure in both OPCs and mOLs, suggesting synapse-related protein expression may hold functional relevance throughout oligodendrocyte lineage. We disrupted the expression of a subset of these synapse-related preferentially ribosome-bound genes in zebrafish and identify roles for *camk2a*, *tenm3*, and *sptbn2* in CNS myelination. These data indicate that each method captures either transcriptional or translational information efficiently, and the comparison between the two methods unexpectedly revealed a possible role for synapse-related proteins in myelination.

Introduction

Oligodendrocytes are central nervous system glial cells that ensheath neural axons allowing for rapid and energy-efficient propagation of electrical signals. Oligodendrocytes progress through

different developmental stages: the progenitor population, or oligodendrocyte progenitor cells (OPCs), differentiate to form newly formed oligodendrocytes (NFO) until reaching their final stage of maturity as myelinating oligodendrocytes (mOLs). As in all cell types, transcription and translation underscore cellular function in these cells, therefore understanding gene expression profiles provides insight to various physiological and cellular processes. Great inroads have been made in understanding both the genetic programs and the neuronal/glial communications that underpin this progression. Much of these advancements have been made through the transcriptional profiling of oligodendroglial cells at different stages of differentiation, either through the profiling of the lineage in culture (Dugas et al., 2006; Pol et al., 2017) or direct isolation and profiling of OPCs or OLs from the developing mouse brain (Cahoy et al., 2008; Sohn et al., 2006; Zhang et al., 2014a) via FACS or immunopanning. More recently, single-cell and single-nuclei RNA-Seq studies have been applied to study oligodendroglial heterogeneity and transcriptional changes in both mouse and human development and disease (Falcão et al., 2018; Jäkel et al., 2019; Marques et al., 2016, 2019; Perlman et al., 2020; Schirmer et al., 2019). A key challenge to these approaches is that dissociating viable single cells from neural tissue typically becomes more difficult with age, especially for highly branched cells such as OPCs and OLs. Although some studies have successfully profiled OPCs in the adult CNS (Spitzer et al., 2019), many profiling experiments have been confined to developmental time-points due to this challenge.

Ribosome affinity purification represents a powerful alternative to sorting whole cells from tissue. Several groups have independently generated mouse lines to allow for the expression of genetically tagged ribosomal subunits in specific cell types in the mouse (Doyle et al., 2008; Heiman et al., 2008; Sanz et al., 2009a), allowing for selective immunopurification of ribosome-

bound transcripts from targeted cells. This strategy offers several potential advantages over cell or nuclei sorting techniques. Firstly, capturing ribosome-bound RNAs should provide a snapshot of actively-translating RNAs, or the "translatome" of the cell. Secondly, ribosome affinity purification techniques may have the additional advantage of capturing RNA localized in distal processes that are typically lost in the aforementioned techniques relying on tissue dissociation. This feature is especially beneficially for highly branched oligodendroglia, which are known to traffic and translate transcripts such as *Mbp* within their distal processes (Ainger et al., 1993; Wake et al., 2011). A potential disadvantage of this approach is the underrepresentation of non-coding RNAs, including lncRNA and microRNAs, both of which have been shown to be functionally important to oligodendrocytes (Emery and Lu, 2015; Katsel et al., 2019). Another alternative to sorting whole cells is presented by the INTACT (Isolation of Nuclei Tagged in specific Cell Types) method, pioneered in plants but more recently applied to mice (Deal and Henikoff, 2010; Mo et al., 2015). Knock-in mouse strains have been generated to allow for the Cre-mediated expression of an eGFP tagged nuclear envelope protein (Sun1-eGFP), allowing for immunopurification of genetically labelled nuclei and associated nucleic acids (Tran et al., 2019). This approach bypasses the concern of cellular fragility by directly targeting the relatively robust nuclei.

In this study we compare the use of the RiboTag ribosomal affinity purification and INTACT nuclear purification methods to profile transcriptional and translational changes across the oligodendrocyte lineage *in vivo*. We crossed RiboTag or INTACT floxed mice to either the NG2-CreERT driver to target OPCs and their progeny or the PLP1-CreERT driver to target mOLs. We isolated nuclear and ribosome-bound RNA in 18-22-week-old mice and used bulk RNA-Seq to unbiasedly profile RNA expression at different stages of the oligodendroglial lineage. We found that the genes showing the highest fold changes upon differentiation were similar between the

INTACT and RiboTag profiles, indicating that the majority of differentiation-induced expression changes can be captured by either profiling strategy. Additionally, we compared either nuclear RNA to ribosome-bound RNA within each stage of the lineage. Although most genes show a similar degree of expression using either technique, a subset of RNA transcripts are highly overrepresented in either the nuclear or the ribosome-bound RNA. Gene ontology enrichment analysis of the overrepresented ribosomal-bound RNA (putatively representing highly translated transcripts) revealed enrichment for genes related to synaptic organization, signaling, and structure in both OPCs and mOLs, indicating that many synaptic-related genes may still be translated and functionally important throughout the oligodendrocyte lineage. Using a zebrafish *in vivo* CRISPR/Cas9 approach to disrupt a subset of these preferentially ribosomal-bound synaptic genes, we identify roles for *camk2a*, *tenm3,* and *sptbn2* in CNS myelination. Overall, these results provide transcriptional and translational information on oligodendroglia *in vivo* as well as identifying roles for individual synapse related genes in CNS myelination.

Results

Generation of oligodendroglial-driven INTACT and RiboTag mouse lines for *in vivo* purification of nuclear and ribosomal-bound RNA

To capture both the steady-state RNA (transcriptome) and translational information (translatome) from OPCs and OLs, we used two separate genetic strategies, both of which use affinity purification to isolate RNA from targeted cells *in vivo*. The first genetic strategy, INTACT, uses a floxed mouse line that expresses a nuclear envelope tethered Sun1-eGFP fusion protein upon recombination (Mo et al., 2015). The second strategy, RiboTag, uses a floxed mouse line which expresses a HA-tagged RPL22 ribosomal subunit following recombination (Sanz et al.,

2009a). Both lines allow for affinity purification of the tagged protein to isolate RNA from either the whole intact nuclei (INTACT) or ribosomes in a cell specific manner. We crossed each of these floxed lines to the NG2-CreERT2 (Zhu et al., 2011) mouse line and the PLP-CreERT2 (Doerflinger et al., 2002) mouse line to allow for purification of RNAs from OPCs and their progeny, or mature OLs, respectively. The crossed lines used in this study are hereby referred to as NG2:NUC (NG2-CreERT2^{+}; Sun1-eGFP^{+}), NG2:RIBO (NG2-CreERT2^{+}; Rpl22^{HA+}), PLP1:NUC (PLP1-CreERT^{+}; Sun1-eGFP^{+}), and PLP1:RIBO (PLP1-CreERT^{+}; Rpl22^{HA+}) (Fig. 1A). Young adult mice (18-22 weeks old) were treated with tamoxifen for either 5 days (NG2:NUC and NG2:RIBO lines), or 3 days (PLP1:NUC and PLP:RIBO lines). Tissue was harvested on the third day after the last injection for either immunohistochemistry or RNA purification and subsequent RNA sequencing (RNA-seq) (Fig. 1B).

In order to confirm that the NG2-CreERT2 and PLP1-CreERT2 lines targeted recombination to OPCs and mature oligodendrocytes, respectively, we assessed the recombination pattern of the Sun1-eGFP and RPL22-HA alleles with each line using immunohistochemistry. Immunostaining against either Sun1-eGFP (NUC) or RPL22-HA (RIBO) protein showed expression in cells across both gray and white matter. In order to assess oligodendroglia specificity, we used antibodies against well-known cell-specific targets (PDGFRα for OPCs, CC1 for mOLs, NeuN for neurons, IBA1 for microglia, ALDH1L1 for astrocytes) and quantified the percentage of recombined cells (Sun1-eGFP+ or RPL22-HA+) that were positive for markers of each cell type (Fig. 1C-D, Fig. S3-A). In both the NG2:NUC and the NG2:RIBO lines, the majority of recombined cells expressed PDGFRα (63.5 and 77.0%, respectively) or CC1+ (30.2 and 18.0%, respectively), confirming that the NG2-CreERT driver predominantly drives recombination in OPCs and any newly differentiated oligodendrocytes generated over the experimental time course.

A small number of recombined cells were positive for markers of other lineages (NG2:NUC+ cells being 1.43% NeuN+, 0.11 % IBA1, 1.80% Aldh1l1, 3.0 % undefined, and NUC:RIBO+ cells being 1.31% NeuN+, 0 % IBA1, 2.03% ALDH1L1 and 1.69% undefined). Based on their morphology and localization along blood vessels, these undefined cells were most likely pericytes, which are known to express NG2 and labeled by NG2-Cre drivers (Attwell et al., 2015; Hill et al., 2014). In both the PLP1:NUC and PLP1:RIBO lines, the overwhelming majority of recombined cells were CC1+ (99.4, 98.9%, respectively), with low recombination across all other assessed cell types (PLP1:NUC+ cells being 0.3% PDGFRα+, 1.9% NeuN+, 0% IBA1, 0% ALDH1L1, 0% other; NUC:RIBO+ cells being 0% PDGFRα+, 2.0% NeuN+, 0 % IBA1, 1.9% ALDH1L1, 0% other). Collectively, these data indicate NG2:NUC and NG2:RIBO recombines in mostly OPCs and some (likely) pre-myelinating oligodendrocytes, while the PLP1:NUC and PLP2:RIBO recombines predominately in mOLs.

Purification of nuclear and ribosomal-bound RNA from oligodendroglial cells using INTACT and RiboTag methods

Having established that all four mouse lines label the OL lineage with relatively high specificity, we isolated oligodendroglial RNA by immunopurifying either Sun1-eGFP tagged nuclei (NUC lines) or HA-tagged ribosomes (RIBO lines) from a 5 mm brain section encompassing both cortex and the underlying corpus callosum (Fig. 1B). We used RNA-Seq to profile both the immunopurified (IP) RNA as well as the input, defined here as the flow-through or unbound RNA, for three animals per group. Differential expression analysis comparing the IP to the input for each line identified over-represented genes in the IP relative to the input samples for each line (>2 fold-change with a padj<0.05), with 1,516 and 2,098 enriched genes identified

for the NG2:NUC and NG2:RIBO lines, and 2,246 and 2,171 enriched genes identified for the PLP1:NUC and PLP1:RIBO lines, respectively.

Consistent with successful enrichment of transcripts from OPCs, the genes enriched in the IP from both the NG2:NUC and the NG2:RIBO lines included known OPC genes *Cspg4* and *Pdgfra* as well as markers for newly formed oligodendrocytes such as *Enpp6* and *Epcam*. Enriched genes in the IP of the PLP1:NUC and PLP1:RIBO lines included known markers for mOLs such as *Mbp* and *Plp1*, as well as *Enpp6*, a gene expressed in both newly formed and mOLs (McKenzie et al., 2014). To more thoroughly evaluate the level of enrichment or de-enrichment for transcripts from different cell types, we utilized previous RNA-Seq databases (Cahoy et al., 2008; Zhang et al., 2014b) to curate a list of 10 genes specific to each of the major CNS cell types (see Fig. S2 for full list). For each line, we compared the expression of these markers in the purified RNA relative to the input. Consistent with purification of RNA from OPCs and their recently-differentiated progeny, the NG2:NUC and NG2:RIBO lines show an approximate 3-119 fold enrichment for known markers of both OPCs and NFOs, with de-enrichment for all other cell types (neurons, astrocytes, microglia) (Fig. 2C and S2). No enrichment was seen for more mature OL markers, confirming that the expression of earlier OL markers represented actively differentiating NFOs derived from recombined OPCs rather than recombination within the mature OL population. Both the PLP1:NUC and PLP1:RIBO lines show an approximate 7-37 fold enrichment for known markers of mOLs, with de-enrichment found for markers of other cell types including OPCs and NFOs (Figs. 2D and S2). Interestingly, for both the NG2-CreERT2 and the PLP-CreERT drivers, the NUC lines show increased enrichment for the target cell type compared to RIBO lines (average fold enrichment for the 10 OPC markers being 19-fold for the NG2:NUC and 11-fold for the NG2:RIBO and average fold enrichment for the 10 OL markers being 24-fold for the PLP:NUC

and 10-fold for the PLP:RIBO line, respectively). This suggests that, in our hands at least, the INTACT method offers a more stringent purification procedure than the RiboTag method.

INTACT and RiboTag methods detect major gene changes upon oligodendrocyte differentiation similarly

Cellular differentiation requires the coordinated change in expression profiles of a large number of genes. This is often studied at the transcriptional level and previous studies have characterized the successive waves of transcriptional changes that occur during OPC differentiation and subsequent OL maturation (Cahoy et al., 2008; Dugas et al., 2006; Pol et al., 2017; Sim et al., 2011; Zhang et al., 2014b). Nevertheless, changes in translational levels of individual transcripts in the absence of changes in their steady state RNA levels during differentiation has been shown in other cell types (Baser et al., 2019), suggesting translational control may be an equally important mechanism for regulating gene expression. In order to determine whether oligodendrocyte differentiation associates with similar or disparate changes in steady state RNA and ribosomally-bound (presumably translated) RNAs, we first performed a differential expression analyses on the NG2:NUC and PLP1:NUC IPs to identify genes with dynamic RNA expression levels during OL differentiation and maturation. We set a high cut-off for the p-value to target genes with the highest degree of transcriptional change upon differentiation (FC>4, adj.pval <1.00e-20), resulting in a total of 842 differentially expressed genes (DEGs). We then calculated the corresponding fold change for the same genes with OL differentiation within the translatome by comparing the NG2:RIBO and PLP1:RIBO IPs. Plotting the RNA transcriptional fold-change of these genes against the translatome fold change showed a high degree of concordance. We found that the majority of transcripts (804 genes) showed similar

transcriptional and translational expression changes upon differentiation (Fig. S3A, Pearson correlation=0.84, p=6.31 e-225). A subset of genes showed increased expression with differentiation in the INTACT approach but not the RiboTag approach. Unsurprisingly, these included non-coding RNAs, many of which are known to be enriched in OLs such as *Neat1*, *Mir338,* and *Mir219* (Dugas et al., 2010; Katsel et al., 2019; Marques et al., 2016; Mercer et al., 2010; Zhao et al., 2010) and which would not be expected to be ribosomally-bound or readily detected using the RiboTag method. In addition, a number of protein coding genes including *Enpp2*, *Enpp4*, *Grm3*, *EphB1*, *Adamts2*, *Adamts20, and Sspo,* and *Aplp1* were transcriptionally induced with differentiation in the INTACT analysis but did not show comparable induction in the RiboTag line, suggesting they are transcribed but subject to negative translational regulation during OL differentiation.

We then repeated this process examining the translational changes seen during differentiation (NG2:RPL to PLP1:RPL) and developed a list of the top translational gene changes, resulting in a list of 372 genes (FC>4, adj.pval<1.00e-5). We compared the differentiation-induced fold-changes of this list of transcripts between the RiboTag and the INTACT dataset and found an even higher degree of correlation (Fig. S3B, Pearson correlation=0.94, pval=.05e.132). We found that no genes showed a >4 fold-change increase in ribosomal occupancy upon differentiation that did not also show a corresponding increase in total nuclear RNA levels. Only 3 genes (*Sema3b*, *1700034G24Rik,* and *2810417H13Rik*) showed decreased ribosomal occupancy upon differentiation in the absence of an underlying change in nuclear RNA levels (Table 1). Although these three genes would be candidates for translational silencing during differentiation, manual inspection of the sequence reads aligned to the genome only supported potential translational silencing of *Sema3b* during differentiation; the signal attributed to *1700034G24Rik* and

2810417H13Rik did not clearly align to exons. A list of the genes that showed a difference in either transcriptional (60 genes) or translational changes (3 genes) in gene expression can be found in Table 1. These data indicate that there is an overall high concordance in the transcriptional and translational changes seen with oligodendrocyte differentiation (as measured by the INTACT and RiboTag methods, respectively). This suggests transcriptional changes underlie the bulk of dynamic expression changes during OL differentiation, with only a few minor exceptions. In addition, the INTACT and RiboTag techniques can most likely be used fairly interchangeably to study *in vivo* dynamic gene expression changes during differentiation.

Nuclear and ribosomal-bound RNA shows differential enrichment for a subset of genes

As shown in Fig. S3 A&B, we found an overall high correlation between the transcriptional and translational changes seen during differentiation. Next, we assessed whether interrogation of specific stages of the lineage would enable us to find transcripts that were overrepresented in either the nuclear or ribosome-bound RNA samples. If so, would these transcriptional or translational outliers hold important information regarding OL functions during different stages of the lineage? In order to determine if the nuclear RNA expression was comparable to the ribosomal-bound mRNA expression, we compared the purified NUC RNA to the purified RIBO RNA from either the NG2 (Fig. 3A) or PLP1 (Fig. 3B) drivers.

We first compared the INTACT and RiboTag IPs from the NG2-CreERT line to compare the transcriptome and translatome of OPC/NFOs. Out of the 4,310 DEGs, we found 419 genes were more highly detected in the nuclear RNA (Preferentially Nuclear RNAs, or PN-RNA). The INTACT technique should purify all RNA present in the nucleus, including non-translated RNA such as lncRNA, snoRNA, and microRNAs that would not necessarily be expected to be

ribosomally bound. We therefore expected to find a subset of genes to be more highly detected in the NUC samples relative to the RIBO sample. Consistent with this, examples of non-translated genes such as *Mir3101*, *Mir17hg*, and *Snora68* were strongly overrepresented in the NUC samples (>2 logFC, $p<0.05$). In addition, we that found 615 genes were more highly detected in the RiboTag samples relative to the INTACT samples (Preferentially Ribosomally Bound RNA, or PRB-RNA) (>2 logFC, $p<0.05$). Presumably, these represent transcripts that are more actively translated than would be predicted from their basal RNA expression level.

Next, we compared the INTACT and RiboTag IPs from the PLP1-CreERT line to compare the transcriptome and translatome of mOLs. Out of the 7,895 DEGs, we found 668 PN-RNAs in mOLs (>2 logFC, $p<0.05$). Again, this included non-translated transcripts such as *Mir7052, H2-K2*, *Mir338,* and *Mir219*, the latter two of which have been shown to regulate OPC differentiation (Dugas et al., 2010; Wang et al., 2017; Zhao et al., 2010), and *Neat1*, a lncRNA recently shown be dynamically involved in oligodendrogenesis and myelin gene expression (Katsel et al., 2019; Mercer et al., 2010). Similar to OPCs/NFOs, we found many examples of transcripts overrepresented in the RiboTag compared to the INTACT preparation (545 genes, >2 logFC, $p<0.05$). Several example transcripts with reads aligned to the genome are shown in Fig. 3C. *Neat1*, the lncRNA and PN-RNA gene, shows a higher number of mapped reads in a NUC sample compared to a RIBO sample. *Aspa*, a well-known mOL specific gene, shows an equivalent density of mapped reads in both the NUC and RIBO samples. Note the intronic signal found within the NUC sample, consistent with the presence of unspliced pre-mRNA present in the nucleus. Indeed, the NUC RNA consistently shows a greater percentage of intronic reads compared to the RIBO RNA in both lines (Fig. S3C). *Lrp1*, a low-density lipoprotein receptor and PRB-RNA, shows higher expression in the PLP1:RIBO IP relative to the PLP1:NUC IP. To confirm the NUC and

RIBO IPs were indeed different, we conducted a PCA analysis comparing the NUC and RIBO samples from each driver (Fig. 3D). For both lines, PC1 captured the majority of the variance (NG2-CreERT: 82%, PLP-CreERT: 75%) compared to PC2 (NG2-CreERT: 10%, PLP-CreERT: 8%), suggesting that the majority of the variance is accounted by the difference between samples and confirms the difference between the NUC and RIBO IPs.

Using a gene biotype analysis, we determined the RNA composition of both the PN-RNAs and PRB-RNAs for both driver lines (Fig. 3E). For the NG2-CreERT driver, non-translated RNA (including antisense, lincRNAs, miRNAs, pseudogenes, snoRNAs and other non-coding processed transcripts) represents 19% of the total PN-RNA group, while representing only 3% of the PRB-RNA group. Although it is unsurprising that non-translated RNAs are overrepresented in the PN-RNA group compared to PRB-RNA group, protein coding RNAs represent the majority of the PN-RNA (73%), which presumably represent genes that are translated with relatively low efficiency in OPCs and NFOs. PN-RNA and PRB-RNA from the PLP1-CreERT driver (mOLs) show a similar RNA composition. Although the non-translated RNA represents 28% of the PN-RNA group (compared to 5% in the PRB-RNA group), protein coding genes represent 63% of the RNAs found within the PN-RNA. For both NG2:PRB-RNA and PLP1:PRB-RNA, protein coding genes represent the majority of RNA (94%, 91% respectively). These results indicate that although nuclear RNA is, as expected, enriched for non-coding RNAs relative to the ribosome bound purification, both purification methods additionally enrich for distinct sets of protein coding transcripts.

Gene ontology enrichment analysis shows unexpected enrichment for synapse related genes for PRB-RNA throughout the oligodendrocyte lineage

Based on our finding that a cohort of genes were preferentially ribosome-bound (PRB-RNAs) and over-represented relative to the nuclear pool, we hypothesized that this group of RNAs might represent genes that are translationally abundant and functionally important to the oligodendroglial lineage. To determine whether particular functional pathways were overrepresented in the PRB-RNA groups, we conducted a gene ontology enrichment analysis on the preferentially ribosomally bound genes from OPCs/NFOs (NG2:PRB-RNAs, Fig 4A) and from mOLs (PLP1-PRB-RNAs, Fig. 4B). The top five terms for each group are highlighted in Fig. 4 A-B, and the top 100 GO terms are in Fig. S4. The GO analysis for PRB-RNAs from both OPC/NFOs and mOLs showed many similar terms related to extracellular matrix organization and structure, cell-to-cell adhesion, and morphology. For OPCs/NFOs, the NG2:PRB-RNA group was also highly enriched for mRNAs involved in synapse assembly and organization, such as *Gabara2*, *Nrxn1-2*, *Sema4a*, *Sema4d*, and *Shank1-3*. This is consistent with the fact that OPCs create synapse-like structures with neurons and can directly respond to neuronal stimulation (Bergles et al., 2000; Kukley et al., 2007, 2010; Lin et al., 2005). Both the synaptic input from neurons and the expression of many synapse-related genes is thought to decrease during oligodendrocyte differentiation (Cahoy et al., 2008; Kukley et al., 2010). We were therefore surprised to discover synapse organization, protein localization to synapse, and synapse assembly amongst the top enriched terms for the PLP1:PRB-RNA group (Fig. 4B & S4B), as this would suggest many synapse related transcripts are heavily translated in mOLs in addition to OPCs.

Next, we examined many of the individual genes linked to these synapse related ontology terms, with synapse organization, synaptic signaling, and synaptic structures shown as examples

(Fig. 4C-E). Across most of these genes regardless of the driver, RIBO counts are higher than NUC counts, possibly indicating an increased demand for translation. For the majority of these genes, NG2:NUC and NG2:RIBO counts are higher than the corresponding PLP1:NUC or PLP1:RIBO signal, supporting previously published data indicating that many synapse related genes are downregulated upon differentiation (Biase et al., 2010; Cahoy et al., 2008; Clarke et al., 2012; Kukley et al., 2010; Lin and Bergles, 2003, 2002). However, it is also apparent that many synapse related genes remain associated with ribosomes even in mOLs. The detection of synapse related RNA in the PLP1-PRB-RNA opens up the possibility for individual functional roles for these genes in mOLs, perhaps mediating neuronal-oligodendrocyte communications at the axo-myelinic junction (Micu et al., 2016, 2017; Stys, 2011).

CRISPR targeting of synapse-related genes results in reduction in mbp:eGFP-CAAX expression in zebrafish

Recent work in zebrafish demonstrated that disrupting the expression of synapse-associated genes, such as *Cadm1b* and *Nlgn2* within the oligodendrocyte lineage disrupts the pattern of myelin formation (Hughes and Appel, 2019). To determine if synapse-related genes from the PRB-RNAs list may also impact myelination, we selected four candidates based on their known roles in neuronal synapses: *Camk2a*, *Sptbn2*, *Tenm3*, and *Dbn1*. These transcripts are preferentially ribosome-bound in both OPCs/NFOs and mOLs, with the expectation of *Dbn1*, which is preferentially ribosome-bound in mOLs only (Fig. 5B).

CAMK2 proteins play a role in neuronal functioning, learning, and plasticity (Achterberg et al., 2014; Borgesius et al., 2011; Elgersma et al., 2002; Giese et al., 1998; Kool et al., 2019; Mayford et al., 1995), and human mutations in *CAMK2A* and *CAMK2B* disrupt normal human

development (Akita et al., 2018; Chia et al., 2018; Küry et al., 2017; Stephenson et al., 2017). Interestingly, mutations in *Camk2b* expression disrupts proper morphological maturation and myelin thickness in differentiating oligodendrocytes (Waggener et al., 2013). β-Spectrins are filament actin cross-linking proteins with roles in synaptogenesis and synaptic activity (Efimova et al., 2017; Stankewich et al., 2010). Mutations in *Sptnb2* results in decreased dendritic spine density and impaired synaptogenesis (Efimova et al., 2017; Stankewich et al., 2010), and mutations in human *SPTBN2* have been linked to two separate forms of ataxia (Ikeda et al., 2006; Perkins et al., 2016). Previous studies have shown that axonal expression of both α and β spectrins are important for proper Na^+ and K^+ channel clustering in the node and juxtaparanode (Amor et al., 2017; Brivio et al., 2017; Huang et al., 2017; Zhang et al., 2013), and *Sptbn1* has been shown to play a role in proper paranode formation in Schwann cells (Susuki et al., 2011, 2018; Voas et al., 2007). *Tenm3* encodes a large cell-surface synaptic protein that regulates topographic circuit assembly and connectivity in the retina and hippocampus via homophilic and heterophilic binding with other teneurins (Antinucci et al., 2013; Berns et al., 2018). Notably, mutations in the related *Temn4* gene cause deficits in the myelination of small diameter axons (Hayashi et al., 2020; Suzuki et al., 2012). Drebrin, or *Dbn1*, is also an actin-binding protein with a role in synapse formation and spine morphogenesis (Hayashi et al., 1998; Ishikawa et al., 1994; Mizui et al., 2005; Shirao and Obata, 1986; Takahashi et al., 2003). To date, the roles of *Camk2a*, *Tenm3*, *Sptbn2*, and *Dbn1* in myelination remain unexplored.

We assessed the role of each gene in myelination *in vivo* by utilizing a pooled CRISPR targeting technique in G0 zebrafish developed by Wu et al. (Wu et al., 2018). Briefly, we selected four sgRNAs targeted against each gene and generated guides using *in vitro* transcription (Fig.

5A). Next, we verified that at least one of the four sgRNA for each target gene efficiently caused indels, confirming mutations via restriction enzyme digests of sites overlapping the predicted Cas9 cleavage sites (Fig. S5B). Using the pooled sgRNA and purified Cas9 protein, we formed Cas9-Ribonucleoprotein (RNP) complexes and injected RNP complexes into G0 zebrafish expressing membrane-targeted eGFP under the MBP promoter (mbp:eGFP-CAAX) (Almeida et al., 2011) to label oligodendrocytes and myelin sheaths (Fig. 5A). After 3-5 days, we performed a phenotypic evaluation which assessed gross morphology and the percentage of both the ventral (early myelinating) and dorsal (late myelinating) spinal cord that was eGFP-CAAX positive between body segments 4-6. In the interest of focusing on oligodendrocyte myelination, we excluded analyzing the lateral line, which is myelinated by peripheral Schwann cells (Brösamle and Halpern, 2002).

As a positive control for the assay, we targeted the *myrf* gene, encoding a transcription factor known to be both required for successful CNS myelination in the mouse and expressed in oligodendrocytes in zebrafish (Emery et al., 2009b; Hughes and Appel, 2019). Zebrafish injected with sg*myrf*-RNP showed a significant decrease in eGFP expression compared to uninjected controls in the ventral, but not the dorsal, spinal cord at 3 days post fertilization (dpf) (Fig. 5C). In zebrafish, oligodendrocytes myelinate the ventral spinal cord prior to myelinating the dorsal spinal cord (Brösamle and Halpern, 2002). Reasoning that 3 dpf may be too early to detect changes in eGFP expression in the dorsal spinal cord due to the low baseline mbp:eGFP-CAAX signal in controls, we analyzed additional sg*myrf*-RNP injected zebrafish at 5 dpf, confirming the expected significant reduction in eGFP expression in both the dorsal and ventral spinal cord (Fig. S5D). We analyzed all subsequent experiments at 4 dpf providing a time-point of detectable mbp:eGFP-CAAX expression in both the ventral and dorsal spinal cord.

Zebrafish injected with 100 pg of sg*camk2a*-RNP showed a decrease in the percent eGFP expression in the ventral spinal cord compared to uninjected controls, though no change in the amount of eGFP-CAAX expression was seen in the ventral spinal cord at 50 pg or in the dorsal spinal cord at either concentration (Fig. 5D). Zebrafish injected with sg*tenm3*-RNP showed a dose-dependent decrease in the percent eGFP expression in both the dorsal and ventral spinal cord compared to uninjected controls (Fig. 5E). Zebrafish injected with sg*sptbn2*-RNP showed decreased eGFP expression in the dorsal spinal cord at 50 pg, and in the ventral spinal cord at 100 pg, compared to uninjected controls (Fig. 5F). Zebrafish injected with either 100 or 200 pg of sg*dbn1*-RNP showed no significant difference in percent eGFP expression compared to uninjected controls (Fig. S5E). All experimental conditions showed similar body lengths and gross morphology compared to uninjected controls (Fig. 5C-F & S5C), suggesting any effects on myelination were not secondary to gross developmental delays. Taken together, disruption of the expression of the synaptic genes *camk2a*, *tenm3*, and *sptbn2* resulted in decreased eGFP-CAAX expression, suggesting a possible role in myelination for all three proteins in the developing zebrafish.

Discussion

Given the importance of transcription and translation in cellular function, we sought to further understand both processes across the oligodendrocyte lineage. We used the INTACT (Deal and Henikoff, 2010; Mo et al., 2015) method to purify oligodendroglial nuclear RNA to capture transcriptional information and the RiboTag method to purify oligodendroglial ribosome-bound mRNA to capture translational information. We show that the NG2:NUC and RIBO lines recombine predominately in Pdgfrα^+ cells (approximately 63 and 77%, respectively) and CC1$^+$

cells (approximately 30 and 18%), suggesting that the NG2-CreERT driver predominately recombines in OPCs and newly differentiated oligodendrocytes over the experimental time course. This finding highlights a common challenge to the *in vivo* study of OPCs in CreERT lines, as tamoxifen itself induces OPC differentiation (Barratt et al., 2016; Gonzalez et al., 2016). Additionally, we show that the PLP1:NUC and RIBO lines recombine almost exclusively in $CC1^+$ cells (approximately 99% in each line), indicating that recombination occurs in mOLs.

When comparing the cell-specific purification of both methods, we found that both methods capture cell-specific RNA, with the NG2:NUC and RIBO lines showing an approximate 3 to 119-fold enrichment for known OPC/NFO genes, and the PLP1:NUC and RIBO lines showing an approximate 7 to 37-fold enrichment for known mOL genes (Fig. 2C-D). In addition, we found that the INTACT method shows slightly higher purity that the RiboTag method regardless of driver. NG2:NUC showed a 57% higher fold enrichment of known OPC/NFO genes compared to NG2:RIBO, and PLP1:NUC showed a 42% higher fold enrichment for known mOL genes compared to PLP1:RIBO (Fig. 2C-D). Indeed, one caveat of the RiboTag method is the binding of mRNAs derived from other cells sticking to the magnetic beads, resulting in a low-level background signal (Sanz et al., 2009a; Shigeoka et al., 2016). The INTACT method may offer higher purity as the RNA is safely housed within the nucleus throughout tissue lysing and nuclei separation, remaining unexposed to additional RNAs.

An additional challenge with the RiboTag method is determining the nature of the RNAs. Does the captured RNA represent repressed/stalled RNA or actively-translating RNA? In the original paper describing the floxed RiboTag mouse line, Sanz and colleagues used the expression of the translationally controlled protein, protamine 1 (*Prm1*), to assess the possibility of capturing repressed RNA (Sanz et al., 2009a). In early development, *Prm1* is transcribed but translationally

repressed for several days (Braun et al., 1989). Researchers collected total RNA as well as immunoprecipitated ribosome-bound RNA over three timepoints in early development. They showed that both the amount of total *Prm1* RNA and the ribosome-bound *Prm1* increases over time, however, the *Prm1* ribosome-bound RNA represented only 9% of the total RNA at the first time point, and gradually increased to 30% on the third time point. This suggests that the ribosome-bound mRNA represents translationally active RNA rather than repressed RNA. In a more direct assessment, Shigeoka and colleagues used an in vitro ribosome run-off assay to determine if mRNA represents actively-translating RNA and found that 86% of the ribosome-bound RNA were actively-translated and approximately 15% of RNA may represent stalled RNA (Shigeoka et al., 2016).

By comparing the NUC and RIBO samples from OPCs/NFOs or from mOLs, we found that hundreds of RNAs are overrepresented in either the nuclear or the ribosome-bound IPs (Fig. 3). As expected, many of the overrepresented RNAs found in OPC/NFO or mOL nuclei encode for non-coding RNAs. Many of the PN-RNAs represented non-translated genes such as *Mir17hg*, *Mir3101*, and *Snora68* in the NG2-CreERT line, and *Neat1*, *H2-K2*, and *Mir7052* in the PLP1-CreERT line (Fig. 3A&B). Surprisingly, the majority of the overrepresented RNAs within the nucleus encoded protein coding genes, possibly highlighting transcriptionally repressed genes (Fig. 3E). Likewise, the majority of the overrepresented ribosome-bound RNAs also encode protein coding genes, which may represent genes with a high rate of translation (Fig. 3E). Notably, the nucleus of a cell is surrounded by a ribosome-studded ER, and nuclear isolation techniques may also capture attached mRNA (Reddy et al., 2017). Given that this 'contamination' may dilute the differences between the comparison between the nuclear IP and the ribosome-bound IP, the differences in RNA expression found in this comparison may be an underestimation.

Additionally, we found that many of the overrepresented ribosome-bound RNA from OPCs/NFOs, and surprisingly mOLs, coded for genes related to synapse organization and signaling (Fig 4 A-B). We found that genes related to synapse organization and structure such as *Dag1*, *Ncan*, *Nrxn1*, *Shank1*, and synaptic signaling, such as *Gabrb1* and *Grin2C*, show a higher representation in the RIBO IP compared to the NUC IP in both lines (Fig. 4 C-D). OPCs are known to express proteins related to synaptic signaling, including voltage-gated ion channels (Barres et al., 1990; Sontheimer et al., 1989), and form synapse-like structures with both excitatory and inhibitory neurons (Balia et al., 2013; Bergles et al., 2000; Jabs et al., 2005; Matthias et al., 2003; Orduz et al., 2015; Vélez-Fort et al., 2010). The synaptic connection between OPCs and neurons has been described in several regions of the brain, including the cerebellum, corpus callosum, and the cortex (Lin et al., 2005; Ziskin et al., 2007). OPCs have been shown to maintain this connection through cell division (Ge et al., 2008; Kukley et al., 2008) and previous studies using whole-cell recordings showed a loss of this connection upon differentiation (Kukley et al., 2010). However, more recent studies used zebrafish to evaluate the changes in calcium signals with the cell body and within the myelin sheath in myelinating oligodendrocytes (Krasnow et al., 2018). Despite undetectable changes in calcium signaling within the cell body after stimulation to the spinal cord, researchers found a small and persistent calcium transcients within myelin sheaths. This suggests that the signaling between neurons and oligodendrocytes becomes localized to the myelin sheath upon differentiation.

Indeed, Hughes and Appel recently examined synapse formation between axons and their myelinating oligodendrocytes (Hughes and Appel, 2019). Using a zebrafish model, they demonstrated that presynaptic release machinery, including PSD-95, can accumulate at exocytosis sites within myelin sheaths. Additionally, they showed Cadm1b (SynCAM1), a cell adhesion

molecule, localizes to myelin sheaths. Using a dominant-negative allele that disrupts extracellular adhesion, they demonstrated that oligodendrocytes generate shorter sheaths with no change to the myelinating capacity of the cells, suggesting Cadm1b is involved in tuning the distribution of myelin. Aligned with this finding, we show that the disruption of *Camk2a*, *Sptbn2*, and *Tenm3* results in reduced MBP expression in mbp:eGFP-CAAX expressing zebrafish (Fig. 5 E-F), suggesting a role in oligodendrocyte myelination. Interesting, all three genes show a higher representation in RIBO IP compared to NUC IPs in both OPCs/NFOs and mOLs (Fig. 5B). If each gene's role in myelination is similar to their role in synapses, it is possible that *Camk2a* may regulate local calcium signaling within the sheath, *Sptbn2* may be influence sheath structure or formation, and *Tenm3* may be responsible for the cell-surface interaction between oligodendrocytes and neurons. Although the global disruption of gene expression limits our ability to determine the exact mechanisms underlying these findings, they suggest the translation of synapse-related proteins past differentiation may be important for myelination. Collectively, these findings may provide a possible mechanism to the 'axo-myelinic' synapse (Micu et al., 2016, 2017; Stys, 2011). Alternatively, each genes role in myelination may be completely independent of their role in synapses. Future studies aimed at oligodendrocyte-specific perturbation of synapse-related proteins will help determine the necessity of these proteins for normal myelination.

Figures and Figure Legends

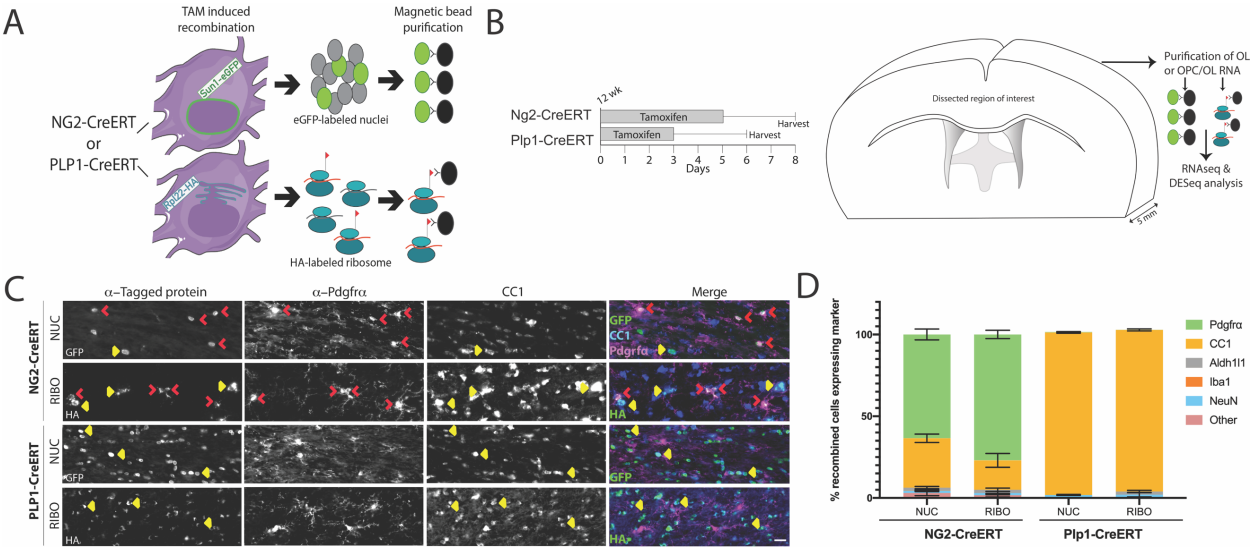

Figure 1: Characterization of INTACT and RiboTag systems to purify RNA from oligodendrocyte lineage cells

(A) Schematic of methods used to immunoprecipitate oligodendroglial nuclear RNA with the INTACT system (Sun1-eGFP) or ribosome-bound RNA with the RiboTag system (RPL22-HA)**.** CreERT expression was driven either by the *Cspg4* (NG2) promoter to target oligodendrocyte progenitor cells (OPCs) or the *Plp1* promoter to target mature oligodendrocytes following tamoxifen administration. (B) Experimental timeline and 5 mm region of interest used for immunohistochemistry and immunoprecipitations. (C) Representative images of nuclear Sun1-eGFP (NUC) or ribosomal Rpl22-HA (RIBO) expression in either oligodendrocyte progenitor cells (Pdgfrα) or mature oligodendrocytes (CC1). Red open arrows indicate PDGFRα$^+$ OPCs, yellow closed arrows indicate postmitotic CC1$^+$ OLs. (D) Quantification of the proportion of Sun1-eGFP$^+$ or Rpl22-HA$^+$ cells expressing selective markers for OPCs (PDGFRα), postmitotic OLs (CC1), astrocytes (ALDH1L1), microglia (IBA1) and neurons (NeuN) in each line. When crossed

to the NG2-CreERT driver, both NUC and RIBO lines show recombination in both OPCs and OLs. When crossed to the PLP1-CreERT driver, recombination in both the NUC and RIBO lines is largely restricted to mature OLs. Results are expressed as mean $\pm$ SEM of 3 animals. Immunostaining for additional cell types shown in Fig. S1.

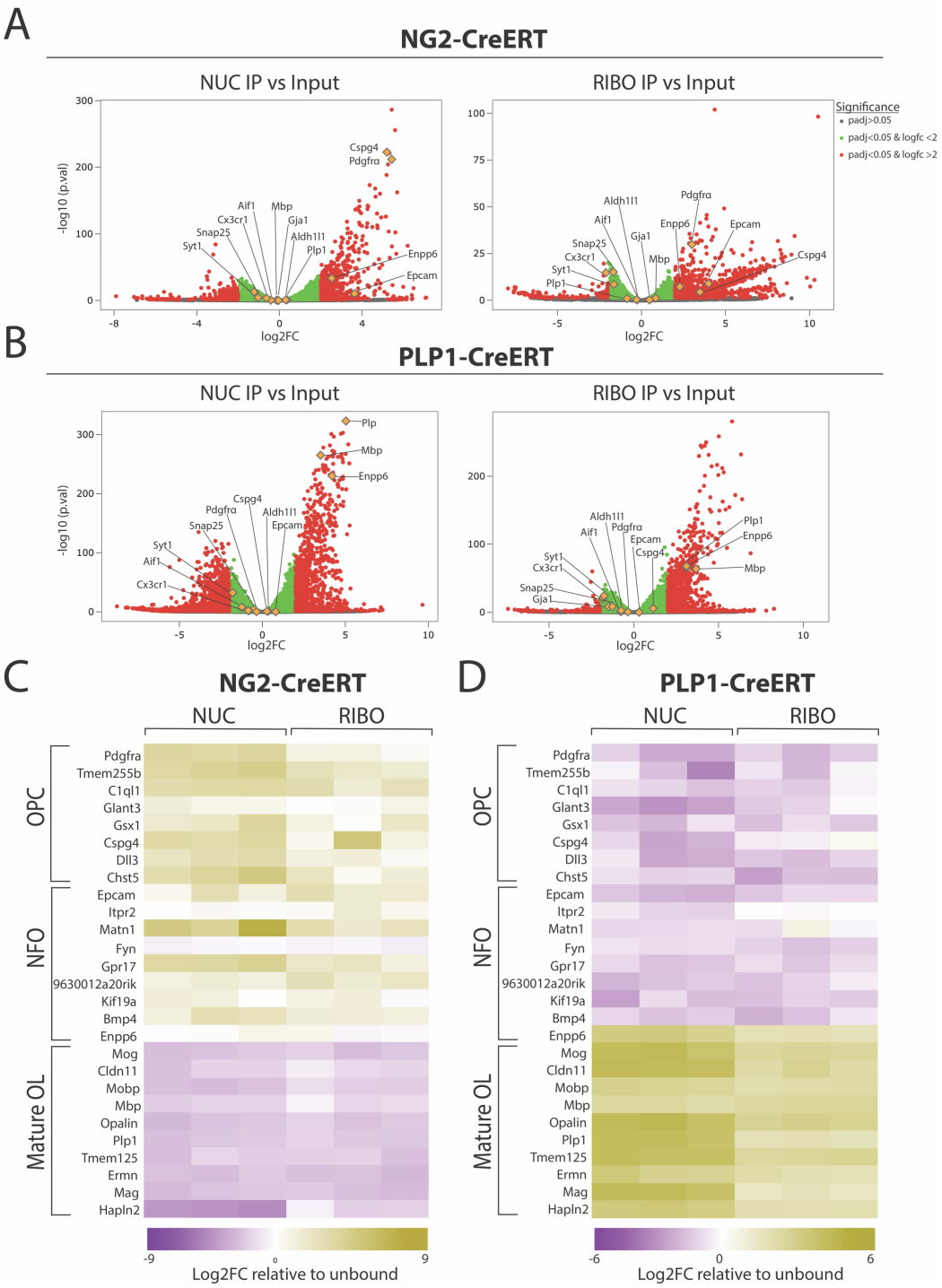

Figure 2: Both NUC and RIBO approaches highly enrich for known oligodendrocyte-lineage specific RNAs from the adult moue brain.

(**A**) Volcano plots showing log2 fold change of transcripts in immunoprecipated RNA samples relative to input (flow-through/unbound RNA) for each line crossed to the NG2-CreERT driver.

Both the NG2:NUC and NG2:RIBO lines show significant enrichment (>2 log2FC, adj. p-val<0.05) for known OPC (*Pdgfrα*, *Cspg4*) and NFO (*Enpp6*, *Epcam*) genes. Transcripts specific to neurons, microglia, astrocytes, and mOLs show either no significant enrichment or significant de-enrichment (n=3 per group). (**B**) Equivalent analysis for the NUC and RIBO crosses using the PLP1-CreERT driver. Volcano plots show significant enrichment for known mature OL transcripts (*Mbp*, *Plp1*) as well as one gene associated with both NFOs and mOLs (*Enpp6*) in both the PLP1:NUC and PLP1:RIBO lines. Genes associated with NFOs, OPCs, and other cell types show no significant enrichment or de-enrichment (n=3 per group). (**C&D**) Heat maps showing enrichment for known oligodendrocyte lineage genes comparing purified RNA to input (flow-through/unbound RNA). Both NG2:NUC and NG2:RIBO lines show significant enrichment for known OPC and newly formed oligodendrocyte (NFO) genes, with no enrichment for more mature markers (**C**). Both PLP1:NUC and PLP1:RIBO lines show significant enrichment for known mature OL genes (**D**). n=3 per group. Heatmap including known markers for additional cell types found in Fig. S2A-B.

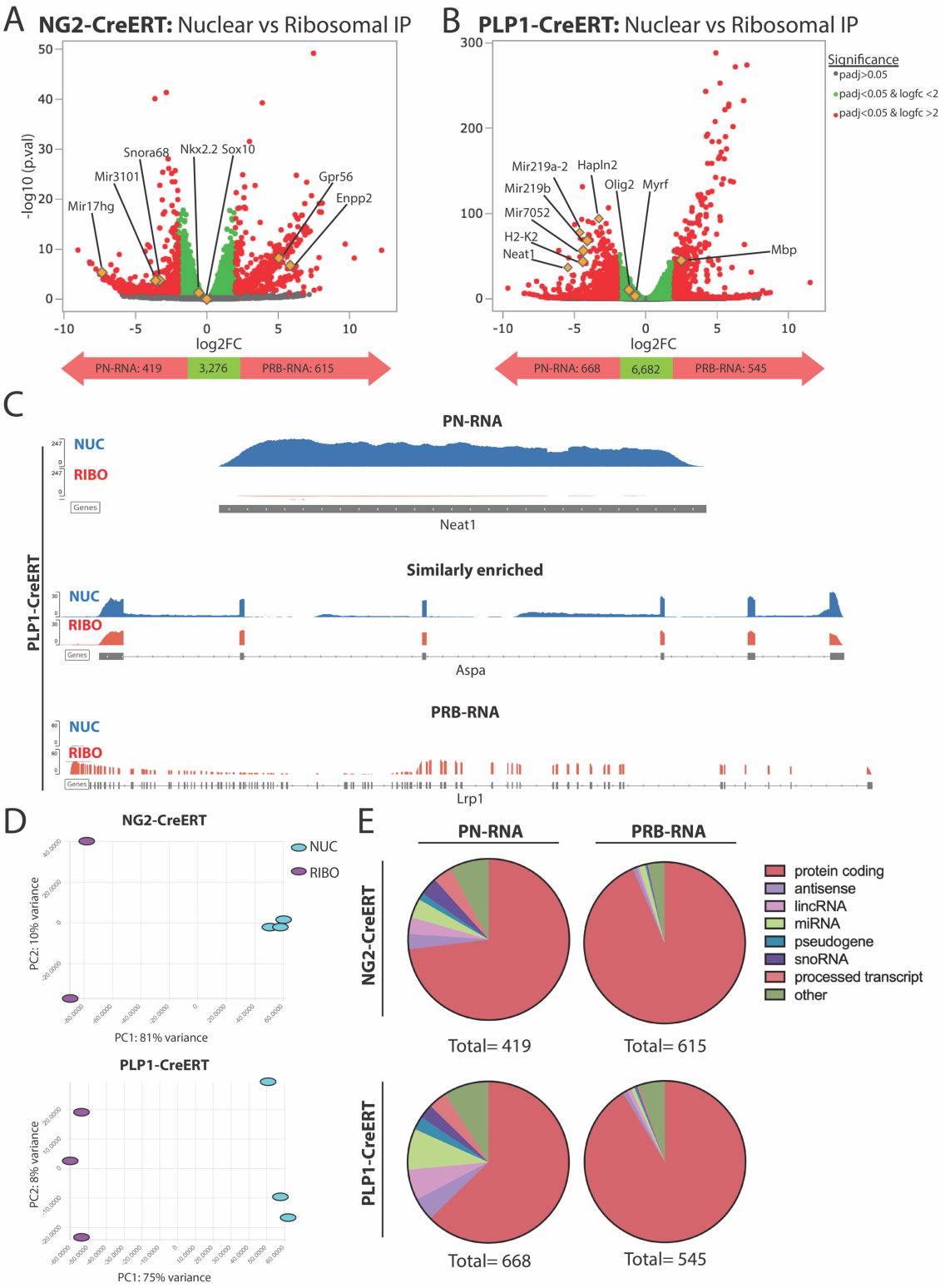
A
NG2-CreERT: Nuclear vs Ribosomal IP
-log10 (p.val)
log2FC
Snora68
Nkx2.2
Sox10
Mir3101
Gpr56
Mir17hg
Enpp2
PN-RNA: 419
3,276
PRB-RNA: 615
B
PLP1-CreERT: Nuclear vs Ribosomal IP
Significance
padj>0.05
padj<0.05 & logfc <2
padj<0.05 & logfc >2
Mir219a-2
Hapln2
Mir219b
Olig2
Myrf
Mir7052
H2-K2
Neat1
Mbp
PN-RNA: 668
6,682
PRB-RNA: 545
C
PLP1-CreERT
PN-RNA
NUC
RIBO
Genes
Neat1
Similarly enriched
Aspa
PRB-RNA
Lrp1
D
NG2-CreERT
NUC
RIBO
PC2: 10% variance
PC1: 81% variance
PLP1-CreERT
PC2: 8% variance
PC1: 75% variance
E
PN-RNA
PRB-RNA
NG2-CreERT
PLP1-CreERT
protein coding
antisense
lincRNA
miRNA
pseudogene
snoRNA
processed transcript
other
Total= 419
Total= 615
Total= 668
Total= 545

Figure 3: Intact (nuclear) and RiboTag (ribosome-bound) purification approaches show differential enrichment for a subset of genes

(A) Volcano plot analysis of differentially detected genes between the NG2:NUC and NG2:RIBO lines. Red dots indicate either preferentially nuclear RNA (PN-RNA; shown on the left of the volcano plot) or preferentially ribosome-bound RNA (PRB-RNA; shown on the right of the volcano plot), adj.pval<0.05 and >2 log2FC. Green dots indicate adj.pval<0.05 with <2 log2FC. Grey dots indicate adj.pval >0.05. Individual example genes in each group are highlighted. The number of genes found within each population is indicated at the bottom of the volcano plot. n=3 (NG2:NUC) n=2 (NG2:RIBO). (**B**) Equivalent analysis for the PLP1:NUC/RIBO lines. n=3 per group. (**C**) Genome browser tracks showing aligned reads from the PLP1-CreERT lines for an example PN-RNA (*Neat1*), an RNA equally represented in each purification technique (*Aspa*) and a PRB-RNA (*Lrp1*). Note strongly enriched signal for *Neat1* from the PLP1:NUC track and of Lrp1in the PLP1:RIBO track. (**D**) Principal Component Analysis (PCA) across all RNA purified samples using either the NG2-CreERT (top) or PLP1-CreERT driver (bottom). For both lines, PC1 captures the majority of the variance (NG2-CreERT: 82%, PLP-CreERT: 75%) compared to PC2 NG2-CreERT: 10%, PLP-CreERT: 8%), suggesting that the majority of the variance is captured by the difference between NUC and RIBO samples. Each dot represents a preparation from an independent animal. (**E**) Transcript biotype distributions for either PN-RNAs or PRB-RNAs using the NG2-CreERT or PLP1-CreERT drivers. Although protein coding mRNAs makes up the majority of preferentially enriched transcripts in each group, the PN groups show greater contributions from non-coding RNAs including antisense, lincRNA, miRNA, pseudogenes

and snoRNAs. RNA categorized as 'other' refers to genes that were unable to be mapped within the gene biotype analysis and TEC-RNA. Genes used as input for each group represent genes with >2 log2FC and adj. p-val<0.05. See Table two for full lists of genes.

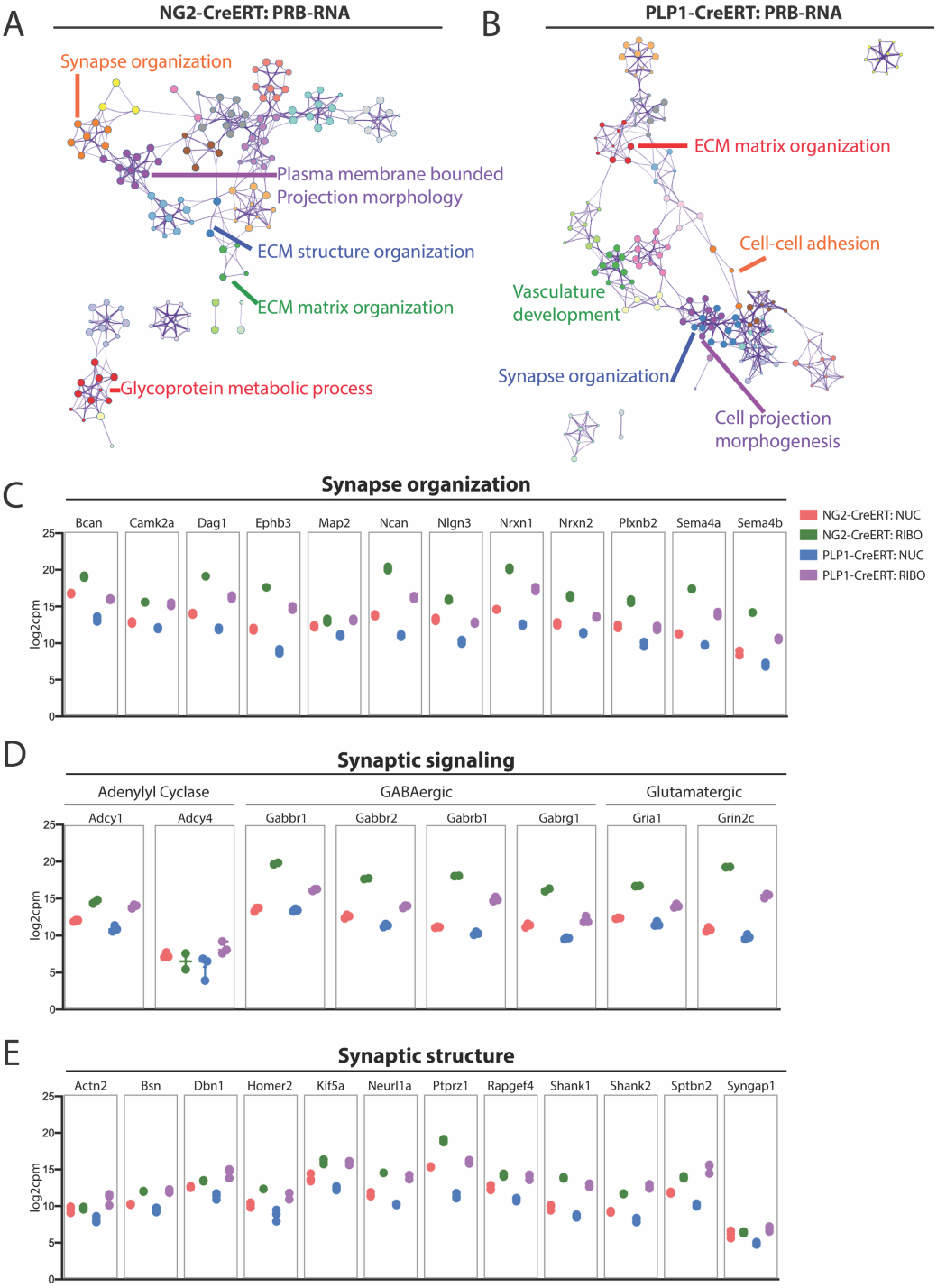

Figure 4: Gene ontology (GO) enrichment analysis provides insight into the biological processes of PRB-RNA and reveals unexpected enrichment for synapse-related genes in both OPC/NFO and mOL ribosome-bound RNAs.

(**A&B)** Network plots of hierarchical clusters using statistically significant gene ontology (GO) terms from PRB-RNAs using either the NG2-CreERT driver (**A**) or the PLP1-CreERT driver **(B**). The top 5 enriched GO terms are labeled for each line. Each term is represented by a circle node and the size of the circle is proportional to the number of genes within each term. The thickness of the line indicates nodal similarity. Input lists for the GO analysis includes the enriched PRB-RNAs (NG2-CreERT: 615 genes, PLP1-CreERT: 545 genes), >2 log2FC and adj. pval<0.05. GO analysis of top 100 terms found in S4. (**C-E**) Boxplots displaying normalized read counts across all four lines. Boxplots highlight expression of example synaptic organization, synaptic signaling, and synapse structure genes identified from the GO enrichment analysis. Although counts for most genes are higher in the NG2-CreERT lines compared to the PLP1-CreERT lines, RiboTag purified samples show higher counts than the INTACT purified samples for both OPC/NFOs and mOLs, suggesting preferential ribosomal occupancy relative to the basal mRNA levels for these synaptic genes even in mature OLs. Each dot represents a separate animal, error bars represent $\pm$ SEM.

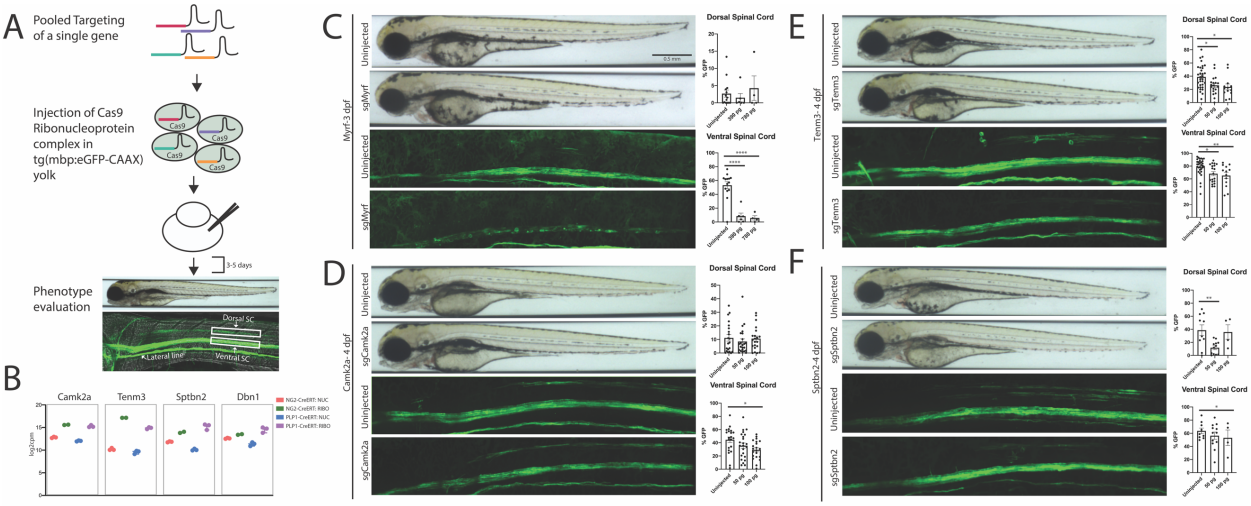

Figure 5: Pooled CRISPR targeting of synapse-related genes reduces mbp:eGFP-CAAX expression in zebrafish

(**A**) Schematic depicting pooled gene editing approach in developing zebrafish. (**B**) Boxplots displaying normalized read counts across all four lines for selected genes of interest. For most genes (excluding *dbn1*), RIBO expression is higher than NUC expression across all lines. *dbn1* shows the highest ribosomal occupancy in mOLs. (**C-F**) Brightfield and fluorescent images of control and RNP injected 3-4 dpf mpb:eGFP-CAAX zebrafish. Quantification of percent GFP expression in dorsal and ventral spinal cord (left). (**C**) Zebrafish injected with sgmyrf-RNP show a significant reduction in ventral, but not dorsal, eGFP expression at 3 dpf compared to uninjected controls (pval<0.0005). (**D**) Zebrafish injected with sgcamk2a-RNP show a significant reduction in ventral eGFP expression at 100 pg, but not 50 pg nor in the dorsal spinal cord at 4 dpf compared to uninjected controls (pval>0.05). (**E**) Zebrafish injected with sgtenm3-RNP show a significant dose-dependent reduction in both the dorsal and ventral spinal cord at 4 dpf compared to uninjected controls (pval<0.05). F) Zebrafish injected with sgsptbn2-RNP show a significant reduction of eGPF expression in the dorsal spinal cord (50 pg, pval<0.050), and the ventral spinal cord (100

pg, pval<0.05) at 4 dpf compared to uninjected controls. Each dot on bar graphs represents a separate animal. All data expressed as mean ± SEM.

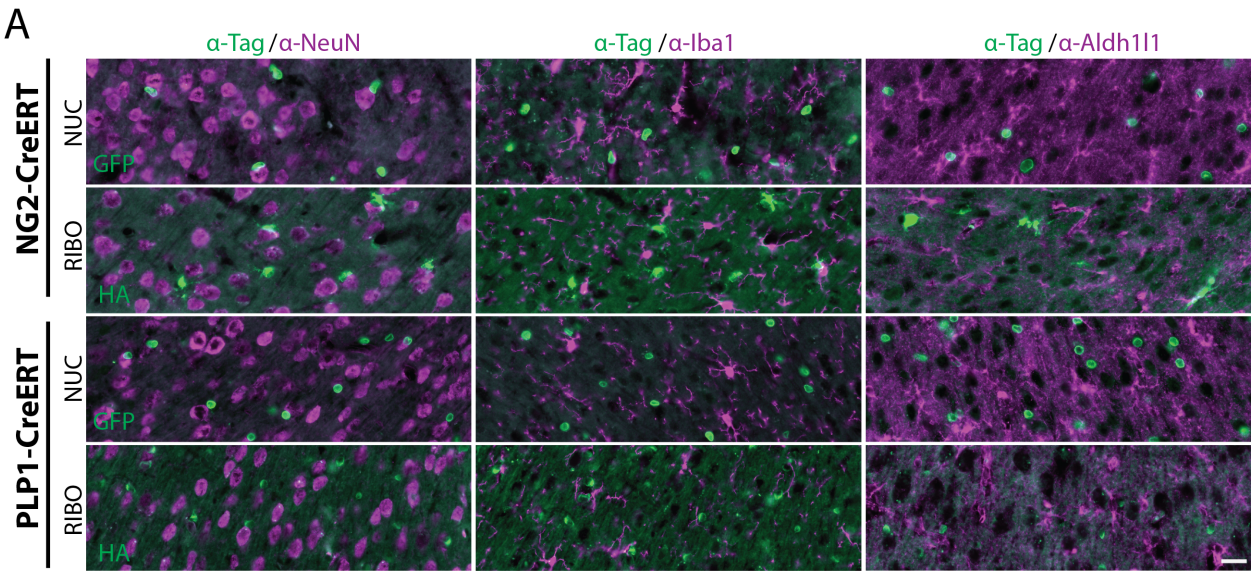

Figure S1: Broad absence of recombination in non-oligodendroglial cells in the INTACT and RiboTag crosses.

(A) IHC on brain sections from the NG2:NUC, NG2:RIBO, PLP1:NUC and PLP1:RIBO lines. Anti-GFP and anti-HA detect the Sun1-eGFP and Rpl22-HA in recombined cells of the INTACT and RiboTag lines, respectively. Anti-NeuN, Iba1, and Aldh1l1 serve as markers for excitatory neurons, microglia and astrocytes, respectively, demonstrating broad lack of recombination in these cell types. Quantification shown in Fig. 1D. n=3 per group.

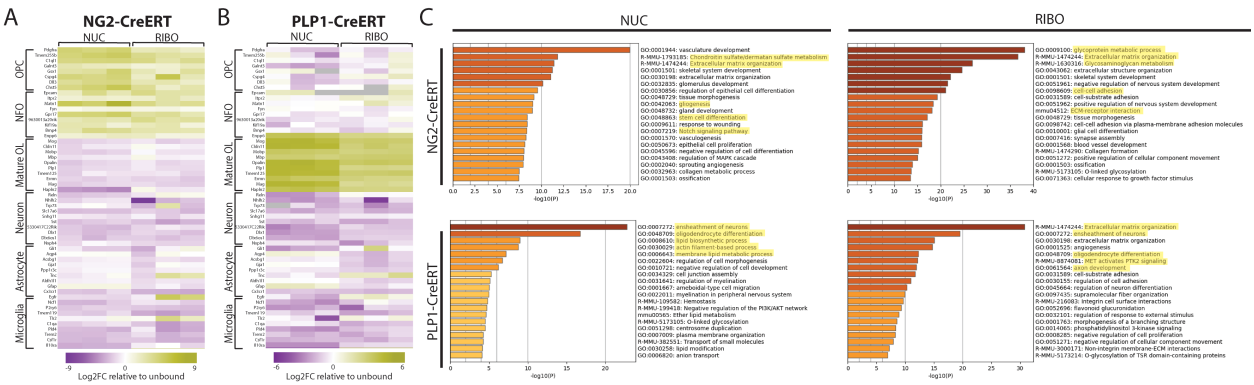

Figure S2: Gene ontology (GO) analysis of purified NUC and RIBO RNA show terms typically associated with OPC or mature OL functions.

(**A&B**) Heat maps showing enrichment for known oligodendrocyte lineage genes and de-enrichment for most neuron, astrocyte, and known microglia markers in RNA purified from NG2:NUC and NG2:RIBO (**A**) and PLP:NUC and PLP:RIBO (**B**). Heat maps show log2 fold change of IPs relative to input (flow-through/unbound RNA). (**C**) GO analysis of genes enriched (>2 log2 fold change, adj. pval<0.001) in IP vs Input for each line. NG2:NUC: 500 genes, NG2:RIBO: 895 genes, PLP1:NUC:851 genes, PLP1:RIBO: 797 genes. Synapse-related terms highlighted in yellow.

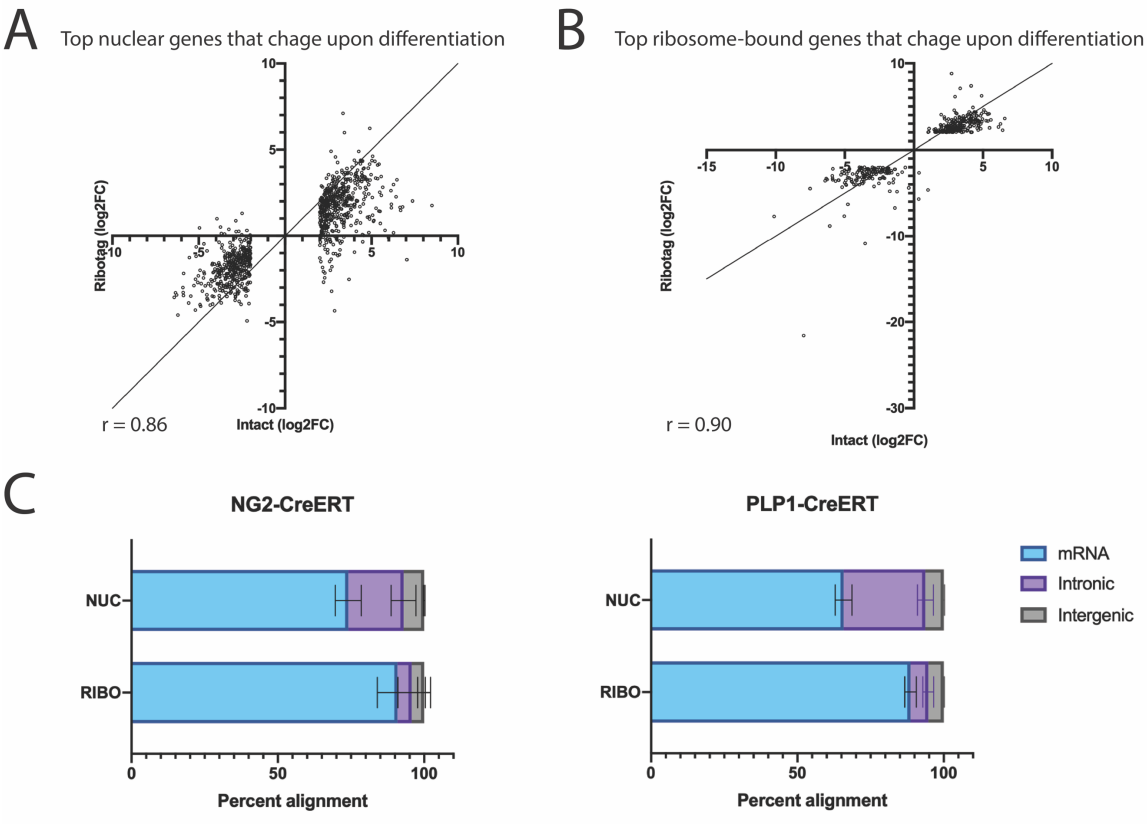

Figure S3: Comparison of RNA captured with INTACT (NUC) and RiboTag (RIBO) techniques.

(**A**&**B**) Scatterplots plotting the log2FC for top nuclear (**A**) and ribosome-bound (**B**) gene changes upon oligodendrocyte differentiation. (**A**) To determine the top differentiation-induced changes in the nuclear samples, NG2:NUC IP was compared to PLP1:NUC IP creating a list of 842 differentially expressed genes upon oligodendrocyte differentiation (476 genes upregulated, 366 genes downregulated, adj.pval<1 e-20). Graphs plot the log2FC (IP/input) in the NG2:NUC and PLP1:NUC lines for each gene; there is an overall high correlation (r=0.86) between the two techniques seen in the fold change with OL differentiation. (**B**) To determine the top ribosome-bound gene changes upon differentiation, the NG2:RIBO IP was compared to the PLP1:RIBO IP, identifying 372 genes that are differentially expressed during OL differentiation (227 genes

upregulated, 145 genes downregulated, adj.pval<1 e-5). Graphs plot the log2FC (IP/input) in the NG2:RIBO and PLP1:RIBO lines for each gene. Again, there is a high concordance (r=0.90) in the degree fold-change during OL differentiation seen with each purification technique within this cohort of genes. **(C)** Quantification of the percentage of reads aligned to exonic, intronic, or intergenic regions of the genome (mean $\pm$ SEM, n=3 in all groups). Both NG2:NUC and PLP1:NUC lines show lower percent alignment to exonic regions (74.1, 65.8%, respectively) compared to NG2:RIBO and PLP1:RIBO lines (91.0, 88.7%, respectively). Both NG2:NUC and PLP1:NUC lines show greater percent alignment for intronic regions within the NUC samples (18.8, 28.0 %, respectively) compared to the RIBO samples (4.8, 6.1% respectively).

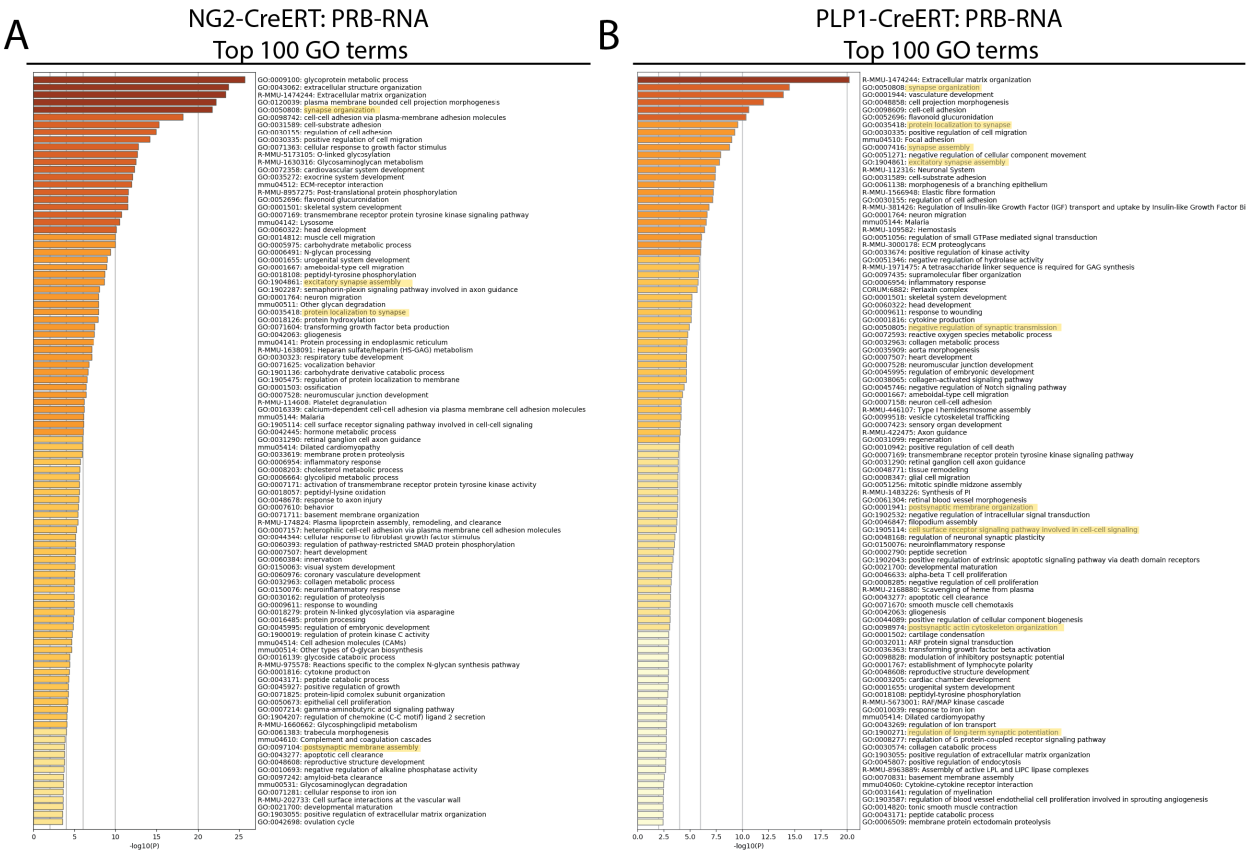

Figure S4: Gene ontology (GO) analysis of genes identified as enriched in the ribosomal vs. nuclear preparations (PRB-RNAs) using either the NG2-CreERT (A) or PLP1-CreERT (B) driver. Top 100 terms shown. Synapse terms highlighted in yellow.

A

Gene	Target Sequence
myrf	CATTGACACCAGTATCCTGG, CGGATGGACGGGCATCCCAC, TGCCACGGCTGAGACGGGTA, GCAGGTTACTAAAGTCACGG
camk2a	CACAAAGAAGCTGTCTACTC, GCTGTCTGGTGCAGAGTAAC, GAGAGTTACACGTGAGTTTT, ACTGTGTCCCACTCGGGTGA
tenm3	GGCGGTGCAGGACTCTGATT, AAAGCAGACGTGAGGAGTCG, GGTCTGGACACATAGTCTTC, GGGTGCATCTAATCCGACTG
sptbn2	GAATAAGCATGCGTCCATCG, TATCCAAGCCTCCATGTCAT, TCTGTTTGACGCTAACCGAG, TGACTGCACGCTCATGTCGA
dbn1	CAGTGACCTTTGATAACACC, GGAGAACACGTGGTAGGTGA, CCAGAGGCCCAGTAACCCAC, AGCCACGTCCACAAGGCTGG

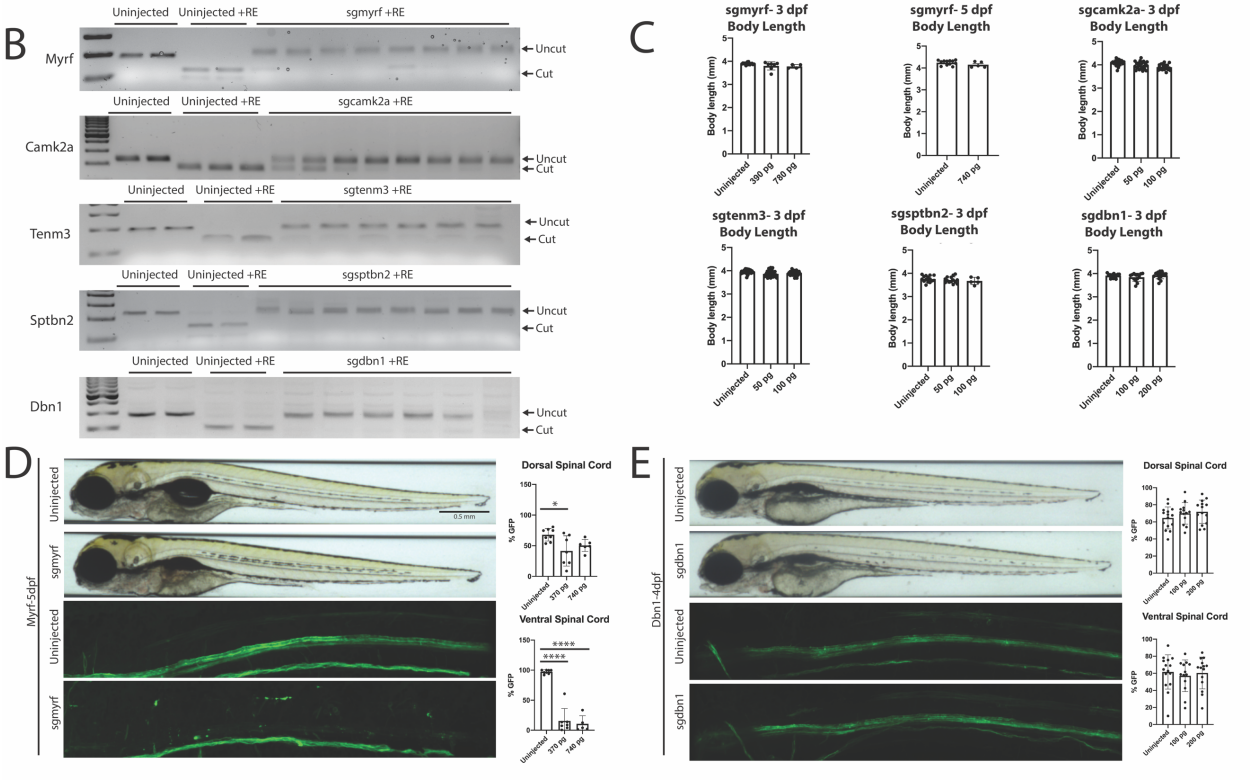

Figure S5: Targeting synapse-related genes of interest in developing zebrafish

(**A**) Table displaying the four sequences for each gene of interest targeted with sgRNAs. (**B**) Cleaved Amplified Polymorphic Sequences (CAPS) assay showing DNA edits for each gene of interest. (**C**) Bar graphs showing body lengths for uninjected control and sg-RNA-RNP groups. No significant changes in body lengths were detected across in any sg-RNA-RNP injected groups. (**D**) Zebrafish injected with sgnyrf-RNP show a significant reduction of eGPF expression in both the dorsal (370 pg, pval<0.05), and the ventral spinal cord (pval<0.00005) at 5 dpf compared to uninjected controls. (**E**) Zebrafish injected with sgdbn1-RNP show no significant change in eGFP

expression in the dorsal or ventral spinal cord at 4 dpf compared to controls. Each dot on bar graphs represents a separate animal. All data expressed as mean ± SEM.

Table one: RNAseq normalized read counts in IP samples and log2FC relative to inputs for all lines.

Table two: List of all enriched preferentially nuclear (PN-RNAs) or preferentially ribosome-bound (PRB-RNAs) for the NG2-CreERT and PLP1-CreERT drivers.

Chapter 4: Investigating oligodendroglial transcriptional and translational responses to neuronal activity

Abstract

Changes to neural activity influence oligodendrocyte dynamics and can influence the cellular decisions to proliferate, differentiate, and myelinate. The genetic mechanisms controlling these response remain unknown, however, determining the possible changes in gene expression that occur within oligodendrocytes in response to activity may help further elucidate mechanisms influencing these decisions. Here, we attempt to establish three separate methods to increase activity in order to assess transcriptional and translational responses in mature oligodendrocytes using the INTACT and RiboTag approaches. We tested whether exercise via voluntary running, pharmacogenetic stimulation via DREADD activation, and repetitive transcranial magnetic stimulation in mice could result in a robust increases in neural activity. In addition, we profiled the oligodendrocyte transcriptional and translational responses to repetitive transcranial stimulation. The following chapter will discuss these efforts.

Introduction

Over the last several decades, a collection of evidence positions neuronal activity as a potent regulator of oligodendrocyte biology. The relationship between activity and its effects on oligodendroglial cells appears important, as studies demonstrating the impact of this relationship span several different models; from *in vitro* studies, to zebrafish and rodent, to human. In humans, juggling, working memory tasks, and piano practicing result in structural changes to white matter tracts which may indicate a relationship between neuronal activity and myelination (Bengtsson et al., 2005; Scholz et al., 2009; Takeuchi et al., 2010). Many more studies demonstrate that modulating activity influences oligodendrocyte progenitor cell proliferation, differentiation, maturation, and even de-novo myelination (see section 1.6 for a detailed discussion). Although

several lines of evidence support the notion that activity impacts oligodendrocyte dynamics, the functional relevance for this relationship remains open to speculation. Do oligodendrocytes respond to activity in order to fine-tune circuitry, similar to the plasticity seen in neurons? Do oligodendrocytes provide metabolic support essential for the proper neuronal functioning? Does the purpose of this response change over time, with activity playing a different role in development compared to adulthood? Which mechanisms control oligodendroglial proliferation, differentiation, and myelination in response to activity? Transcriptional and translational regulation underlie all biology, therefore, understanding how activity effects oligodendroglial gene expression may help uncover relevant mechanisms and address the unanswered questions of functional importance.

Here, we sought to transcriptionally and translationally profile the oligodendroglial responses to increases in neural activity. To increase neuronal activity, we selected three methods previously shown to impact oligodendroglial dynamics: exercise using a voluntary running wheel, pharmacogenetic stimulation via designer receptors exclusively activated by designer drugs (DREADDs), and transcranial magnetic stimulation. Previous studies show that voluntary running can lead to increases in proliferation and differentiation (Alvarez-Saavedra et al., 2016; Keiner et al., 2017; McKenzie et al., 2014; Xiao et al., 2016; Zheng et al., 2019), with acute responses in OPC proliferations and differentiation in as little as 2-3 hours after wheel exposure (Xiao et al., 2016). Additionally, voluntary running induces myelination in mice with impaired motor function (Alvarez-Saavedra et al., 2016). In a more targeted approach, previous studies from the Emery lab showed that pharmacogenetic stimulation of cortical neurons via DREADDs also results in increased OPC proliferation and differentiation (Mitew et al., 2018). Similar to optogenetic stimulation (Gibson et al., 2014), DREADD stimulated axons showed thicker myelin compared to non-stimulated axons. In recent publications, Cullen et al. demonstrate that repetitive

transcranial magnetic stimulation in adult mice leads to increased survival of newborn oligodendrocytes and enhanced myelination (Cullen et al., 2019, 2020). This chapter will discuss our efforts to 1) Establish a robust method to increase neuronal activity in order to 2) capture the oligodendrocyte transcriptional and translational response by using the previously discussed INTACT and RiboTag approaches.

Results

14-day voluntary running wheel access does not significantly promote neurogenesis within the adult hippocampus.

The objective of this experiment was to determine if voluntary exercise could provide a robust response in activity in order to assess the effect of increased neuronal activity on the oligodendroglial gene expression. Voluntary exercise in rats and mice leads to exercised-induced neuronal activity in the dentate gyrus (Oladehin and Waters, 2001), increased hippocampal neurogenesis (Lee et al., 2000; Pencea et al., 2001; Praag et al., 1999; Rhodes et al., 2003), and increased oligodendrocyte progenitor cell proliferation and differentiation (Alvarez-Saavedra et al., 2016; McKenzie et al., 2014; Xiao et al., 2016). Here, we used neurogenesis a proxy to determine if voluntary running wheel access results in a robust activity response. Both male and female mice (8-weeks-old) were exposed to 5-ethynyl-2'-deoxyuridine (EdU) for 14-days (Fig. 1A) prior to access to a voluntary running wheel. EdU is a thymidine analog that incorporates into the DNA of cells during replication to label actively-dividing cells and labels the progenitor population within the dentate gyrus. Pre-labeling diving cells before exposure to voluntary wheel-running captures the cellular proliferation that occurs during voluntary running (Praag et al., 2005).

After the 14-day EdU exposure, mice were then transferred into new cages and separated into two conditions: a sedentary group with no access to voluntary running, and a group with access to voluntary running via a fixed running wheel for 14-days. Tissue was harvested on the subsequent day for immunohistochemistry analysis (Fig. 1A).

Both experimental groups showed EdU nuclear incorporation dentate gyrus cells after a 14-day exposure to EdU, showing successful labeling of the active-proliferating cell population (Fig. 1B-E). Although mice with voluntary running wheel access showed an approximate 42% increase in $EdU^+/DAPI^+$ nuclei relative to non-running controls, this increase failed to reach statistical significance. Considering that it is well-established that voluntary exercises increases hippocampal neurogenesis in mice, we tried to determine why running-wheel access failed to promote neurogenesis in our hands. Previously published work indicates that adult male mice show increased BDNF protein expression (Venezia et al., 2016) and an enhanced hippocampal LTP response (Titterness et al., 2011) compared to female mice after voluntary running wheel exposure, suggesting a possible sex difference in the hippocampal response to exercise. To determine if there may be an underlying sex difference in the hippocampal response to voluntary exercise with our dataset, we separated the groups by sex and found a greater percent increase between male wheel exposure groups (~57%) compared to female wheel exposure groups (~28%). The number of mice per group was too low to run a meaningful statistical analysis, however, these data indicate a trend towards a more sensitive male response to voluntary exercise. Regardless of sex-differences, voluntary running-wheel access failed to significantly induce an increase in neurogenesis in our hands. This suggests that any increase in activity provided through exercise may be modest at best, making this method insufficient for exploring the effect of increased activity on oligodendroglial gene expression.

Bilateral pharmacogenetic stimulation does not promote robust c-Fos expression

Pharmacogenetics such as designer receptors exclusively activated by designer drugs, otherwise known as DREADDs, provide a tool to modulate and study neuronal activity (Armbruster et al., 2007). Previous studies report that increases in activity via DREADDs leads to increases in OPC proliferation and differentiation (Mitew et al., 2018) and similar approaches using optogenetic approaches to increase activity report similar findings (Gibson et al., 2014; Ortiz et al., 2019). Here, we sought to determine if the activation of the excitatory DREADD, hM3Dq, provided a robust response in neuronal activity in order to assess the effects of increased activity on the oligodendroglial gene expression. Using a neuron-specific promoter to virally target cortical neurons, we injected either hSyn-mCherry or hSyn-hM3D-(Gq)-mCherry (hM3Dq-mCherry) into the motor and somatosensory cortex in P5 mice (Fig. 2A). By using a bi-lateral injection approach, we increased the area of viral spread, therefore increasing areas of possible activation (Fig. 2A&B). Juvenile mice were allowed to recover for 35 days before each group received a single injection of the hM3D receptor agonist clozapine (Gomez et al., 2017a). Tissue was harvested 90 minutes after the clozapine injection for immunohistochemical and quantitative PCR analysis.

Both hSyn-mCherry or hSyn-hM3Dq-mCherry injected mice showed robust mCherry expression through the motor and somatosensory cortex in each hemisphere (Fig 2 B&C). At the center of the viral injection, named the viral zone in Fig. 2B, the mCherry expression extended across several layers of the cortex in each hemisphere for both viruses. cFos is an immediate early gene commonly used as a proxy for neuronal activity, as both c-Fos protein and *Fos* mRNA expression increase after neuronal activation (Bisler et al., 2002; Mello and Ribeiro, 1998; Zangenehpour and Chaudhuri, 2002), therefore we quantified the number of c-Fos expressing cells

across the upper cortex (Fig. 2D) or within the viral zone (Fig. 2E). Although the number of mice per group was too low to run a meaningful statistical analysis, the number of c-Fos^{+} cells/mm^{2} was far below the number of c-Fos+ cells found in previous studies conducted by the Emery lab (Mitew et al., 2018). For example, compared to the number of cFos+ cells found after hM3Dq stimulation reported by Mitew et al., the average number of cFos+ cells found in this study is approximately 7-fold lower in controls, and 50-fold lower in hM3D expressing mice. To determine if the number of c-Fos+ cells was diluted across the large area of the upper cortex, we quantified the number of c-Fos+ cells within the viral region (Fig. 2E). Again, the total number of c-Fos+ cells within both groups was significantly lower than expected, indicating a possible problem with the c-Fos antibody itself, tissue preparation, or experimental design. We attempted to rectify possible technical issues by testing a different c-Fos antibody, using antigen retrieval and microwave fixation, and by testing more acute time-points after clozapine injection, however, none of the procedural changes resulted in clearer or more robust c-Fos expression in hM3D stimulated brains (data not shown). It is possible that a robust activity response could be detected using *Fos* mRNA expression rather than protein expression (Bisler et al., 2002). To determine if hM3D-mCherry stimulation results in increased *Fos* mRNA expression, I used harvested cortical tissue from the previously described experimental paradigm (Fig. 2A) and performed a qPCR analysis Both hSyn-mCherry and hSyn-hM3Dq-mCherry expressing groups showed similar relative *Fos* expression 90 minutes after Clozapine injection (Fig. 2F). Together, these results indicate that the use of the pharmacogenetic tool, DREADDs, does not produce a robust or detectable response in our hands and is insufficient for modulating activity to determine its effects on oligodendroglial gene expression.

Both INTACT and RiboTag methods enrich for myelinating oligodendrocyte RNA after sham or iTBS treatment

Repetitive transcranial magnetic stimulation is a non-invasive form of neural stimulation that uses a magnetic field to apply a focal region of electric current to the brain (Barker et al., 1987), which can modulate neuronal firing depending on the intensity, frequency, and pattern of stimulation (Hoppenrath et al., 2016; Müller-Dahlhaus and Vlachos, 2013; Tang et al., 2017). Specifically, low intensity transcranial magnetic stimulation delivered in intermittent theta-bursts (iTBS) has been shown to increase the number of newborn or newly-differentiated cortical oligodendrocytes, increase myelin internode extension, decrease nodal length, and influences the axo-myelinic ultrastructure in adult mice (Cullen et al., 2019, 2020). In collaboration with Dr. Kaylene Young's lab, we sought to determine if iTBS resulted in changes to the transcriptome and translatome of mature oligodendrocytes using the previously described INTACT (Sun1-eGFP) and RiboTag (RPL22-HA) immunopurification techniques. Previously, Dr. Kaylene Young's lab demonstrated that pre-existing oligodendrocytes, rather than newly generated oligodendrocytes, facilitate the nodal shorting response to iTBS (Cullen et al., 2020). Therefore, we decided to determine if iTBS treatment promoted gene expression changes within mature oligodendrocytes by using the PLP1-CreERT driver.

We first sought to determine the cell-specificity that each immunopurification method offered using RNA derived from the INTACT (PLP1-CreERT:NUC) and RiboTag (PLP1-CreERT:RIBO) lines (Fig. S1A-B). Using quantitative PCR analysis, we found that each method showed an enrichment for a gene expressed both in newly-formed and mOLs, *Enpp6,* and known mOL genes *Mog* (A) or *Mbp* (B). As *Mbp* transcripts are known to be trafficked outside of the nucleus (Ainger et al., 1993; Wake et al., 2011), we expected lower enrichment for *Mbp* within the

nuclear IP and therefore chose to use *Mog* to detect mOL enrichment in the INTACT line and *Mbp* to detect mOL enrichment in the RiboTag line. Interestingly, the INTACT method shows a significantly greater enrichment for the known NFO/mOL genes (~40-fold and 70-fold enrichment, respectively) compared to the RiboTag enrichment NFO/mOL genes (~13-fold and 11-fold enrichment, respectively). In addition, we assessed the relative enrichment for genes that serve as specific markers for other cell types: *Aif1* (microglia), *Gja1* (astrocytes), *Syt1* (neurons), and *Pdgfra* (oligodendrocyte progenitor cells). While no enrichment was detected for this set of genes in the INTACT IPs, the RiboTag IPs detected low-levels of enrichment for known genes of other cell types (<2-fold enrichment). This indicates that the INTACT method offers a cleaner purification method compared to the RiboTag method; a result that agrees with conclusions drawn in Chapter 3. Despite this difference, both methods significantly enrich the purified NFO/mOL transcripts with relatively high specificity.

Next, PLP1-CreERT:NUC and PLP1-CreERT:RIBO 17-22 week old mice were separated into sham or iTBS treatment groups (Fig. 3A). Both groups were manually handled to position the stimulation coil positioned in line with their ears. For 7 days, iTBS mice received daily stimulation of 600 pulses of intermitted theta burst while shams received identical treatment with no current passed through the coil. On day 4, mice received daily Tamoxifen injections for 3 days to promote recombination. On the 7th day, mice received a final sham or iTBS treatment and tissue was harvested immediately following treatment to perform immunoprecipitation. To ensure that purified RNA from each line and condition properly captured mOL RNA before RNA sequencing, IP samples were tested for the enrichment of the known mOL gene, *Mog* (Fig. 3B) via qPCR. Both PLP1-CreERT:NUC and PLP1-CreERT:RIBO sham and iTBS conditions show ~20-30 fold enrichment for *Mog*, with no significant difference in enrichment between sham and iTBS treated

conditions. Next, we used RNA-seq to profile the RNA derived from the input, defined as the flow-through/unbound RNA, and the IP across all conditions. Using a differential expression analysis comparing the IP to the input, we identified several hundred genes over-represented in the IP relative to the input for each line (>4 fold-change with a padj<0.05), with 939 genes enriched from the INTACT samples, and 964 genes enriched genes from the RiboTag samples (Fig. 3C). Consistent with the results in Supp. 1A-B, the IPs from both sham and iTBS treated samples from both lines show enrichment for *Enpp6*, *Mog*, and *Mbp* relative to their inputs. To ensure each sample showed greater enrichment for mOL transcripts compared to other cell types, we used the same curated list of 10 genes specific to each major CNS cell type found in Chapter 3 and compared the expression of each marker in the purified RNA relative to the input (Fig. 3C). Consistent with the purification of RNA from mOLs, both lines showed consistent and relatively even enrichment for known mOL genes across samples (INTACT: ~10.6-39.4 fold enrichment, RiboTag: ~8.5-18 fold enrichment), with de-enrichment for other cell types (neurons, astrocytes, microglia, and OPCs). Across all samples, the INTACT samples showed an approximate 26-fold average enrichment for mOL maker compared to the ~12-fold average enrichment found in the RiboTag samples, again supporting the previous finding that the INTACT method consistently show increased enrichment for the target cell type compared to the RiboTag method. Together, these data demonstrate that both PLP1-CreERT:NUC and PLP1-CreERT:RIBO IPs enrich for RNA derived from mOLs across all samples.

iTBS treatment does not promote significant changes in gene expression within mature oligodendrocytes using INTACT and RiboTag immunopurification

To determine whether iTBS treatment modulates the mOL transcriptional (PLP1-CreERT:NUC) or translational (PLP1-CreERT:RIBO) profiles, we conducted a differential expression analysis comparing the sham and iTBS treated IP samples (Fig. 4A). Surprisingly, we found few differentially expressed genes (DEGs) in either the PLP1-CreERT:NUC and PLP1-CreERT:RIBO lines. We did not find any genes to be significantly upregulated by iTBS in either line. iTBS treatment significantly downregulated *Tph2* in the PLP1-CreERT:NUC line, and a number of genes from the PLP1-CreERT:RIBO line, including *Ccdc81, Tc2n, Il20ra, and Fgf3*. Upon further analysis, all these DEGs showed FKPMs under 0.5, suggesting that these genes represent false-positives (the high variability of lowly expressed genes giving them a higher false discovery rate).

This result may indicate that 1) mOLs do not transcriptionally or translationally respond to iTBS treatment, which is would be surprising given the previously reported morphological changes within mOL after iTBS (Cullen et al., 2019, 2020) or 2) iTBS treatment did not result in a sufficient perturbation in neural activity to elicit a detectable response. If iTBS treatment resulted in a substantial increase in neural activity, we would also expect to find DEGs within the input/unbound samples. In order to assess the differential expression of genes within the input, we conducted a differential expression analysis between the sham and iTBS treated conditions and found only one DEG within the PLP1-CreERT:NUC lines, *Pdcd1,* and two DEGs in the PLP1-CreERT:RIBO lines, *Tdrd1* and *Stra6l* (Fig. 4B). However, similar to the DEGs within the IPs, all three of the DEGs found within the input samples showed FKPMs <0.2. In agreement with this data, the expression of both *Fos* and *Bdnf*, show a similar number of counts between sham and

iTBS treated groups (Fig. 4C). As previously mentioned, *Fos* expression is known to increase upon neuronal activation, and *Bdnf* has specifically been shown to increase after repetitive transcranial magnetic stimulation (Castillo-Padilla and Funke, 2016; Makowiecki et al., 2014; Müller et al., 2000; Zhang et al., 2015a). Although it is possible that both transcripts returned back to normal levels within the two days after iTBS treatment, taken together with the previous data, we conclude that in our hands, iTBS treatment does not result in significant mOL gene expression changes detectable by the INTACT and RiboTag approaches.

Discussion

The goal of the experiments in this chapter was to evaluate the oligodendrocyte transcriptional and translational responses to increased neuronal activity *in vivo*. Understanding how oligodendrocytes transcriptionally and translationally respond to activity could provide a pathway to unraveling relevant mechanisms and establishing the functional relevance of this relationship. We first sought to determine a method that could robustly increase activity in our hands, reasoning that a robust response would be necessary in order to detect changes at a transcriptional and translational level. Towards this goal, we attempted to establish three methods known to cause an increase in activity: exercise via voluntary running, pharmacogenetic stimulation via DREADD activation, and transcranial magnetic stimulation.

Providing rodents with running wheel access allows researchers to study the effects of voluntary exercise within various contexts. Voluntary exercise results in both increased activity within the dentate gyrus (Oladehin and Waters, 2001) and increased hippocampal neurogenesis (Lee et al., 2000; Pencea et al., 2001; Praag et al., 1999; Rhodes et al., 2003). Additionally, various exercise regiments result in improved motor and cognitive function across a variety of disease

models, including stroke, Parkinson's and Alzheimer's disease, and most notably within the context of the oligodendrocytes, ataxia and multiple sclerosis (Abbott et al., 2004; Colcombe et al., 2004; Cruise et al., 2011; Fryer et al., 2011; Heyn et al., 2004; Khalil et al., 2012; Vinkers et al., 2003). Previously published studies indicate that voluntary exercise via running wheel access also affect oligodendroglia. Alvarez-Saavedra et al. reported that mice with conditional deletion of the helicase-coding gene, *Snf2h,* display cerebellar hypoplasia, impaired motor function, and do not survive past early development (Alvarez-Saavedra et al., 2014). In a follow-up study, researchers showed that voluntary running increased the survival in *Snf2h* knockout mice, accompanied by an increase in hindbrain myelination (Alvarez-Saavedra et al., 2016). Both McKenzie et al. and Xiao et al. showed that access to a voluntary exercise leads to increases in OPC proliferation and differentiation (McKenzie et al., 2014; Xiao et al., 2016). Here, researchers introduced an interesting running wheel modification by removing rungs within the wheel creating uneven gaps. This "complex running wheel" still allowed for voluntary exercise in mice, however, the modification also required mice to learn a novel motor task, presumably activating associated regions responsible for motor control and learning. Notably, the use of a "complex running wheel" is not necessary to influence oligodendroglial dynamics, as voluntary exercise via "normal running wheel" exposure also increases OPC proliferation and myelination (Alvarez-Saavedra et al., 2016; McKenzie et al., 2014; Xiao et al., 2016; Zheng et al., 2019).

Given the evidence that voluntary running affects oligodendroglial dynamics, we tested if voluntary exercise could increase neural activity in our hands. After pre-labeling the dividing stem cell population with EdU and providing access to a voluntary running wheel, we found that mice with voluntary running access did not show a significant increase in newborn neurons (Fig. 1B-E). Particular aspects of the experimental design may account for the lack of a robust increase in

neurogenesis. First, it is possible that mice with access to the running wheel simply did not run. Our data may point to this difference, as males showed a trend towards an increase in neurogenesis compared to females (Fig. 1D-E). Additionally, male mice have been shown engage in voluntary running more frequently compared to females (Titterness et al., 2011; Venezia et al., 2016). Given these possible sex-differences, increasing the number of total mice may help account for this variability. In addition, mice in our study were housed with 3-4 mice per cage to avoid the known effects of social isolation on the oligodendrocytes (Liu et al., 2012; Makinodan et al., 2012). Unfortunately, this may have resulted in variable access to the wheel, as some mice may run more frequently thereby limiting the running access for others. Future improvements to the experimental design, including directly measuring wheel use, increasing the number of animals, and singly housing animals, may help researchers use this method to study the oligodendroglial response to exercise and increased activity.

Additionally, we sought to establish the use of the pharmacogenetic tool, DREADDs, as a potent activator of neural activity. DREADD are a class of genetically modified GPCRs that were designed to response exclusively to the activating ligand, clozapine N-oxide (CNO) (Armbruster et al., 2007), though subsequent studies indicated that the CNO metabolite clozapine was the more active ligand *in vivo* (Gomez et al., 2017a). Within this study, we virally expressed the excitatory DREADDs, hM3D-Gq, which releases intracellular CA^{2+} and enhances neuronal excitation (Armbruster et al., 2007). A previous study published by the Emery lab also used the excitatory hM3d-Gq to increase activity (Mitew et al., 2018). Here, researchers showed a significant increase in the number of cFos+ cells following the administration of CNO, indicating enhanced activity. This increase in activity lead to increased OPC proliferation and differentiation, as well as thicker myelin surrounding active axons (Mitew et al., 2018). Using a similar approach, we virally

expressed hM3d-Gq within the motor and somatosensory cortex and assessed activation by quantifying the number of cFos+ cells across the cortex and within the area of high viral expression (Fig. 2B-E). Although we did not see a difference in cFos+ cells between control and hM3D-Gq expressing mice (Fig. 3D-F), one major difference between the previously published results and the current study is the chemical used to activate the hM3d-Gq receptor itself.

DREADD receptors were originally modified to selectively bind the inert compound, clozapine-N-oxide (CNO), rather than the native activating ligand, acetylcholine (Armbruster et al., 2007). However, more recent work tested this mechanism *in vivo* and demonstrated that CNO fails to enter the brain after systemic injection and shows a low affinity for the DREADD receptor (Gomez et al., 2017b). Instead, CNO is rapidly converted in to the atypical antipsychotic drug, clozapine, and shows a significantly higher affinity to the DREADDs at a lower concentration. Using the inhibitory hM4d-Gi DREADD, researchers showed a DREADD specific behavioral response after clozapine injection using a specific concentration (0.1 mg/kg) (Gomez et al., 2017b). Based off of these findings, we reasoned that using clozapine instead of CNO would avoid any metabolic processing of the ligand and deliver a more accurate ligand concentration to the brain. At the time of this experimental design, few studies were published applying the excitatory DREADD receptor and clozapine to *in vivo* studies, therefore we used the provided concentration based off the aforementioned study. To our knowledge, no current study investigates the clozapine concentration required for the *in vivo* activation of the excitatory receptor hM3Dq, therefore, it is possible that this concentration may sufficiently activate hM3Di but not hM3Dq. In addition, clozapine has various dose-dependent effects, including antagonizing effects on histamine, noradrenaline, serotonin, dopamine and acetylcholine receptors (Ashby and Wang, 1996; Schotte et al., 1993), and studies show that concentrations as low as 0.05 mg/kg result in detectable

behavioral changes in wild-type mice (Ilg et al., 2018). A more careful investigation of the necessary concentration of clozapine required to activate hM3Dq *in vivo* may be required before using this tool to investigate the effects of activity on oligodendroglial gene expression.

Finally, we tested whether repetitive transcranial magnetic stimulation resulted in changes in the transcriptome and translatome in myelinating oligodendrocytes using the INTACT and RiboTag methods. Transcranial magnetic stimulation is a non-invasive procedure which uses magnetic fields to generate electrical currents in the brain (Barker et al., 1987). The beneficial effects of repetitive transcranial magnetic stimulation have been tested within a variety of clinical contexts, including multiple sclerosis (Gaede et al., 2018; Hulst et al., 2017; Mori et al., 2011; Nielsen et al., 1996). Previous studies adapted this technique for rodent use and showed that low-intensity intermittent theta-bursts (iTBS) treatment results in an increase in the survival of newborn or newly-differentiated cortical oligodendrocytes, as well as longer internodes and shorted nodal lengths changes in the myelin ultrastructure (Cullen et al., 2019, 2020). To determine if newly-generated oligodendrocytes or pre-existing oligodendrocytes were responsible for the changes in nodal length, researchers selectively measured nodal lengths in Plp-CreERT:Tau-mGFP transgenic mice (Cullen et al., 2020). Here, researchers measured Nav1.6+ nodes of Ranvier flanked by pre-existing myelin segments labeled with a membrane-targeted eGFP and found that iTBS treatment tended to decrease the length of nodes surrounded by pre-existing myelin. These results suggest that mature oligodendrocytes, rather than newly-generated oligodendrocytes, may facilitate in nodal shortening in response to iTBS.

In collaboration with Dr. Kaylene Young's lab, we sought to determine if iTBS treatment would result in detectable changes in mature oligodendrocyte RNA expression. Here, INTACT (PLP1-CreERT:NUC) or RiboTag (PLP1-CreERT:RIBO) positive mice received sham or iTBS

treatment for 7 days before tissue was harvested and immunopurification was performed (Fig. 3A). Both sham and iTBS treated mice from both lines showed an increased enrichment for known mature oligodendrocyte genes (Fig. 3B-C) indicating a successful purification of nuclear and ribosome-bound RNA from the target cell-type. Surprisingly, iTBS treatment did not cause a significant change in gene expression within the extracted nuclear or ribosome-bound RNA profiles, or within the input (Fig. 4A-B).

It is possible that the 5 mm region of interest shown in Fig. 3A could account for the lack of a detectable transcriptional and translational changes from all cells (Fig. 4B) or mature oligodendrocytes (Fig. 4A) following sham or iTBS treatment. In a previous study published by the Young lab, researchers show that iTBS treatment only increases new oligodendrocyte numbers within layer VI of the cortex after 7 days (Cullen et al., 2019). In addition, researchers showed that regions directly underneath the coil contained more new oligodendrocytes compared to the center of the coil, suggesting that only brain regions found directly underneath the circumference of the coil were affected. Although the 5 mm section of tissue used for this study included the area directly underneath the coil, it is possible that any changes in gene expression occurring within a small population of cells were below the threshold of detection. Future experiments could micro dissect a smaller region directly underneath the coil to determine if a more targeted approach results in increased detection of gene expression changes following iTBS treatment.

Despite the challenges in establishing each method as a robust tool to increase neural activity, these methods still offer attractive advantages to test their effect on oligodendroglial gene expression. Voluntary exercise provides a more natural way of increasing activity and allows researchers the ability to investigate regional differences important for exercise with the use of a standard running wheel, or exercise and novel-learning with the use of a modified running wheel.

DREADD technology offers a more direct stimulation and by expressing DREADDs in neurons with contralateral projections that pass through the white matter regions, like those found in the motor cortex, researcher could investigate the effect of activity within cortical and white matter oligodendrocytes. Lastly, iTBS treatment offers a powerful non-invasive strategy to modulate activity and also offers high translational value in the treatment of diseases such as multiple sclerosis. Future experiments could aim towards addressing the aforementioned improvements to establish a robust method to increase activity. Applying these strategies with *in vivo* immunopurification methods, such as INTACT or RiboTag, offers a combination of techniques suitable to study the effects of activity on oligodendroglia.

Figures and legends

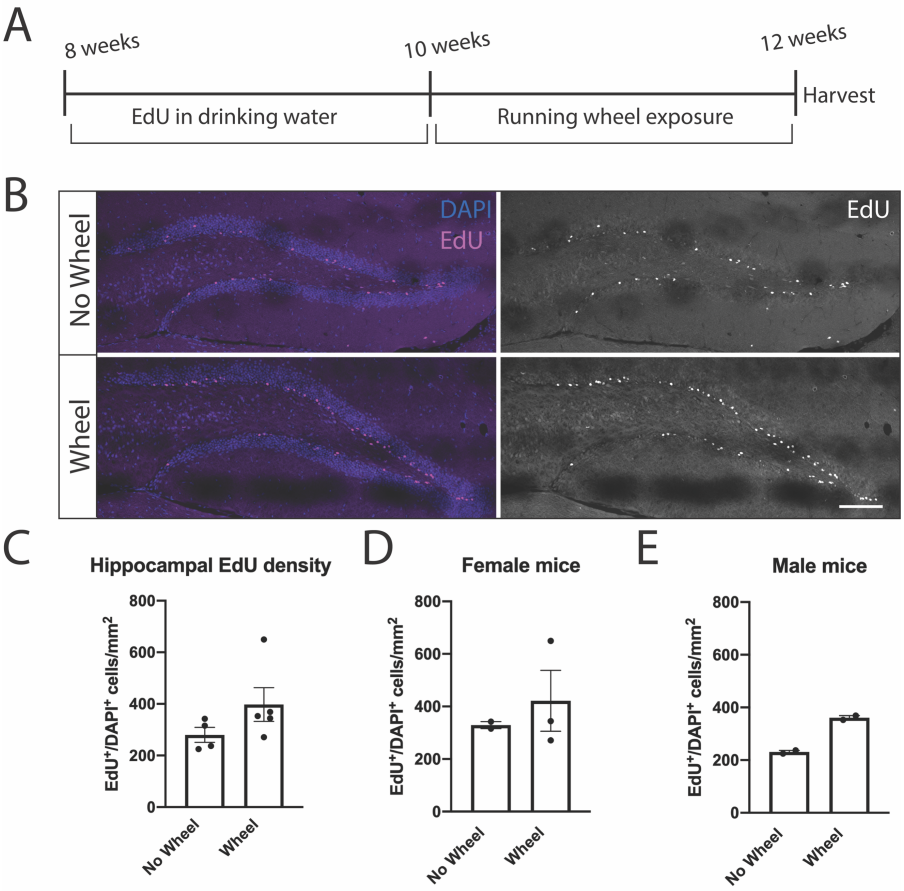

Figure 1: Voluntary wheel-running access does not significantly promote neurogenesis in the dentate gyrus

A) Schematic of experimental design. EdU was administered via the drinking water in 8-week-old wild-type mice for two weeks. Animals were assigned to one of two groups: either housed under standard housing conditions with no running wheel access or housed with voluntary access to a fixed running wheel.

B) Representative images of EdU-labeled cells within the dentate gyrus in animals with or without exposure to a voluntary running wheel.

C-E) Quantitative analysis of newly-born hippocampal cells ($EdU^+/DAPI^+$) in animals with or without voluntary running wheel access. C) Quantification of $EdU^+/DAPI^+$ hippocampal cells across all groups with or without voluntary running wheel access (n=5 and 4, respectively. $p>0.05$). D) Quantification of $EdU^+/DAPI^+$ hippocampal cells across all groups with or without access to a running wheel in female mice (n=3 and 2, respectively). E) Quantification of $EdU^+/DAPI^+$ hippocampal cells across all groups with or without access to a running wheel in male mice (n=2 per group). Each dot represents a separate animal, error bars represent $\pm$ SEM. Scale bar 200 μm.

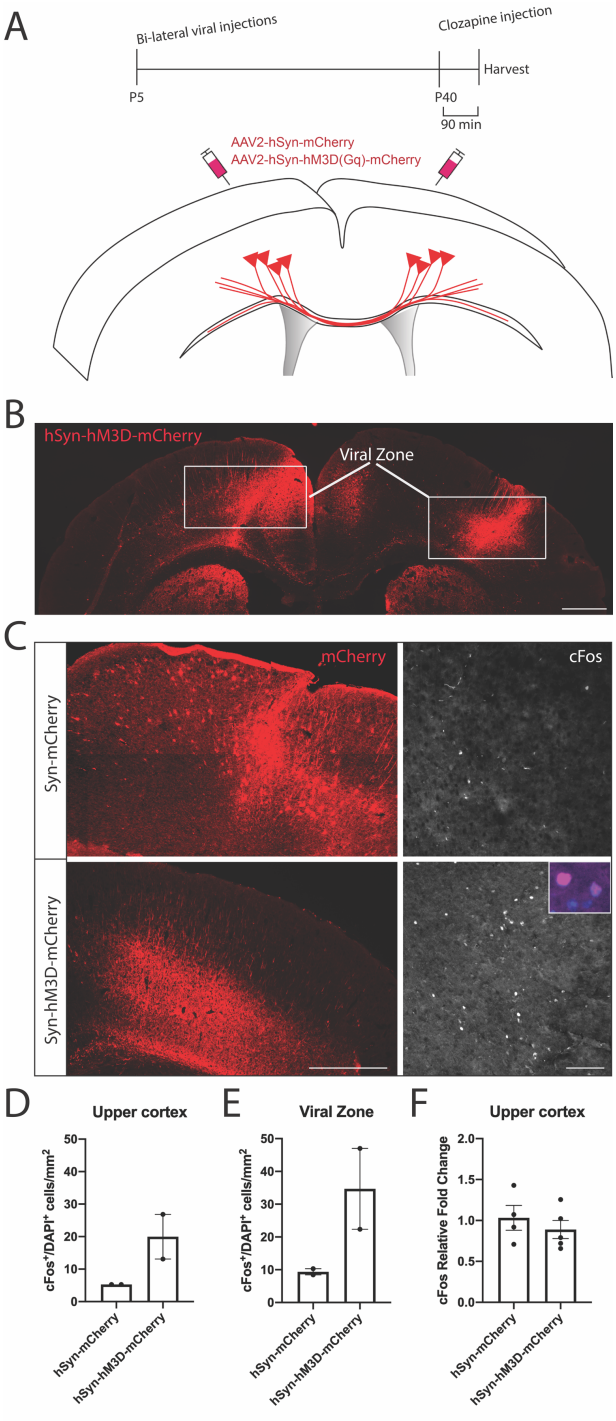

Figure 2: Pharmacogenetic stimulation of neuronal activity does not robustly increase c-Fos expression

A) Schematic of experimental paradigm illustrating bi-lateral viral injection of hSyn-mCherry control or hSyn-hM3D(Gq)-mCherry in P5 juvenile mice. After a recovery period, P40 mice were injected with Clozapine. Tissue was collected 90 mins after Clozapine injection for immunohistochemical quantitative PCR analysis.

B) P40 coronal slice of hSyn-hM3D(Gq)-mCherry bi-lateral expression. White boxes indicate the regions of the high mCherry expression.

C) Representative images of mCherry cortical expression from hSyn-mCherry controls, or hSyn-hM3D-mCherry injected mice (Left). Right panel shows cortical cFos expression. Inset shows nuclear localization of cFos expression (Blue-DAPI, Red-cFos).

D-F) Quantification cFos protein expression (D-E) or mRNA expression (F). Quantification of cortical $cFos^{+}/DAPI^{+}$ cells across the entire upper cortex (D) or within the viral zone (E) depicted in panel B. (n=2 per group)

F) Quantitative PCR analysis to determine the relative cFos mRNA expression 90 mins after Clozapine injection in mCherry control or hM3Dq-mCherry injected mice (n=4, 5 respectively). $p>0.05$. Each dot represents a separate animal, error bars represent $\pm$ SEM. Scale bar 500 μm (B& C, right), 100 μm (C, left).

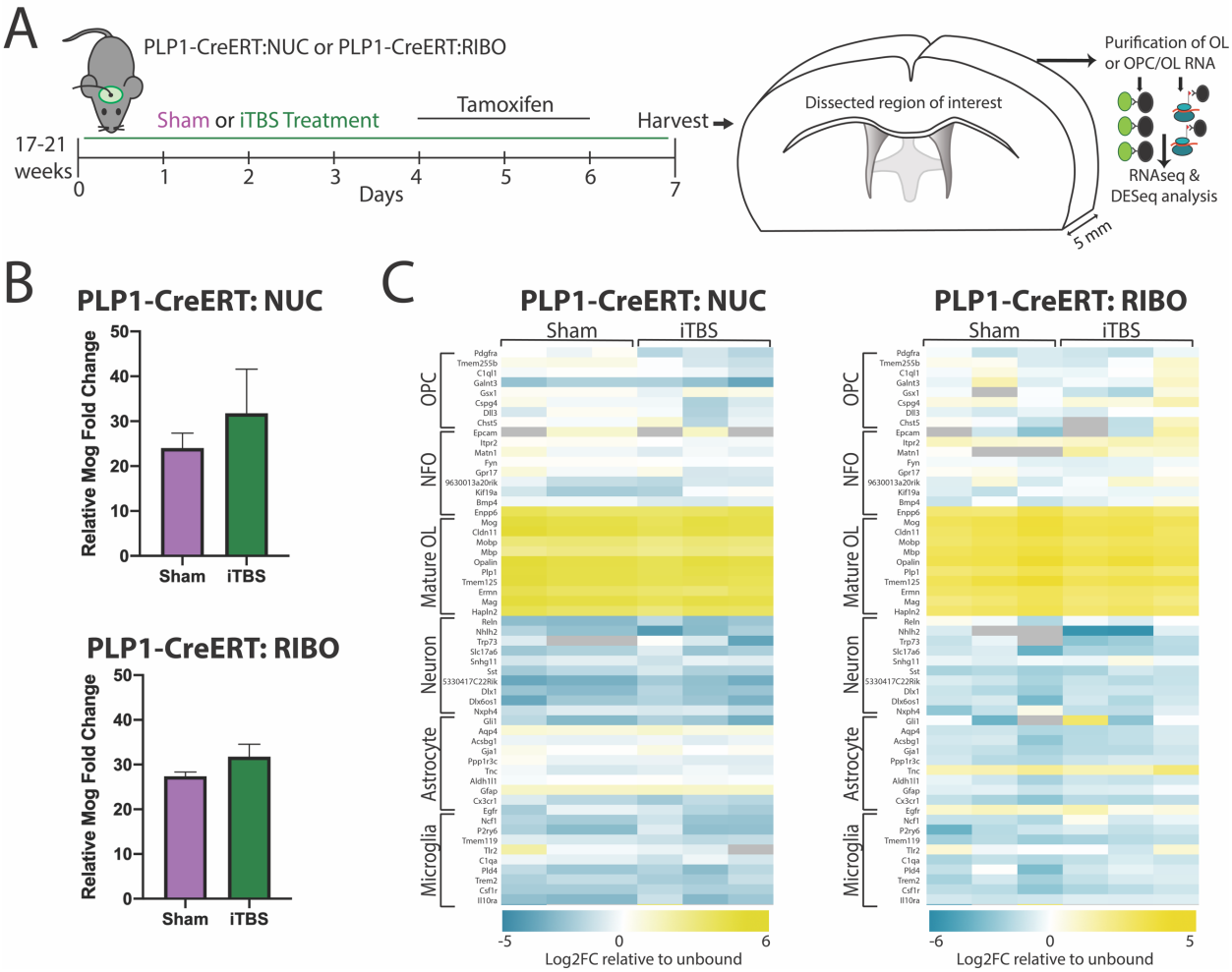

Figure 3: Both INTACT and RiboTag approaches enrich for known mature oligodendrocyte specific RNAs after iTBS

A) Schematic depicting the experimental approach to immunoprecipitate mature oligodendrocyte nuclear RNA with the INTACT/Sun1-eGFP (NUC) method or ribosome-bound RNA/Rpl22-HA (RIBO) method after sham or iTBS treatment. PLP1-CreERT:NUC and PLP1-CreERT:RIBO mice received sham or iTBS treatment for seven days. At day five of treatment, mice received daily Tamoxifen injections for three days. On the seventh day following

treatment, tissue was harvested and a five mm region of tissue was collected, immunopurified, and RNA was prepared for sequencing.

B) Verification of the enrichment for the known mature oligodendrocyte gene, *Mog.* Graphs show enrichment for both sham and iTBS immunoprecipitated samples in PLP1-CreERT:NUC and PLP1-CreERT:RIBO lines. Both PLP1-CreERT:NUC and PLP1-CreERT:RIBO sham and iTBS conditions show ~20-30 fold enrichment for *Mog*, with no significant difference in enrichment between the two conditions. (n=3 per group, $p>0.05$). Graph shows relative gene enrichment compared to *Gapdh*. Error bars represent $\pm$ SEM.

C) Heat maps showing enrichment for known cell-specific genes comparing purified RNA to input (flow-through/unbound RNA). Both PLP1-CreERT:NUC and PLP1-CreERT:RIBO sham and iTBS conditions show significant and predominate enrichment for known mature oligodendrocyte markers and de-enrichment for most oligodendrocyte progenitor cells (OPC), newly-formed oligodendrocytes (NFO), neurons, astrocytes, and microglia markers in purified RNA. Heatmaps show log2 fold change of IPs relative to input. (n=3 per group).

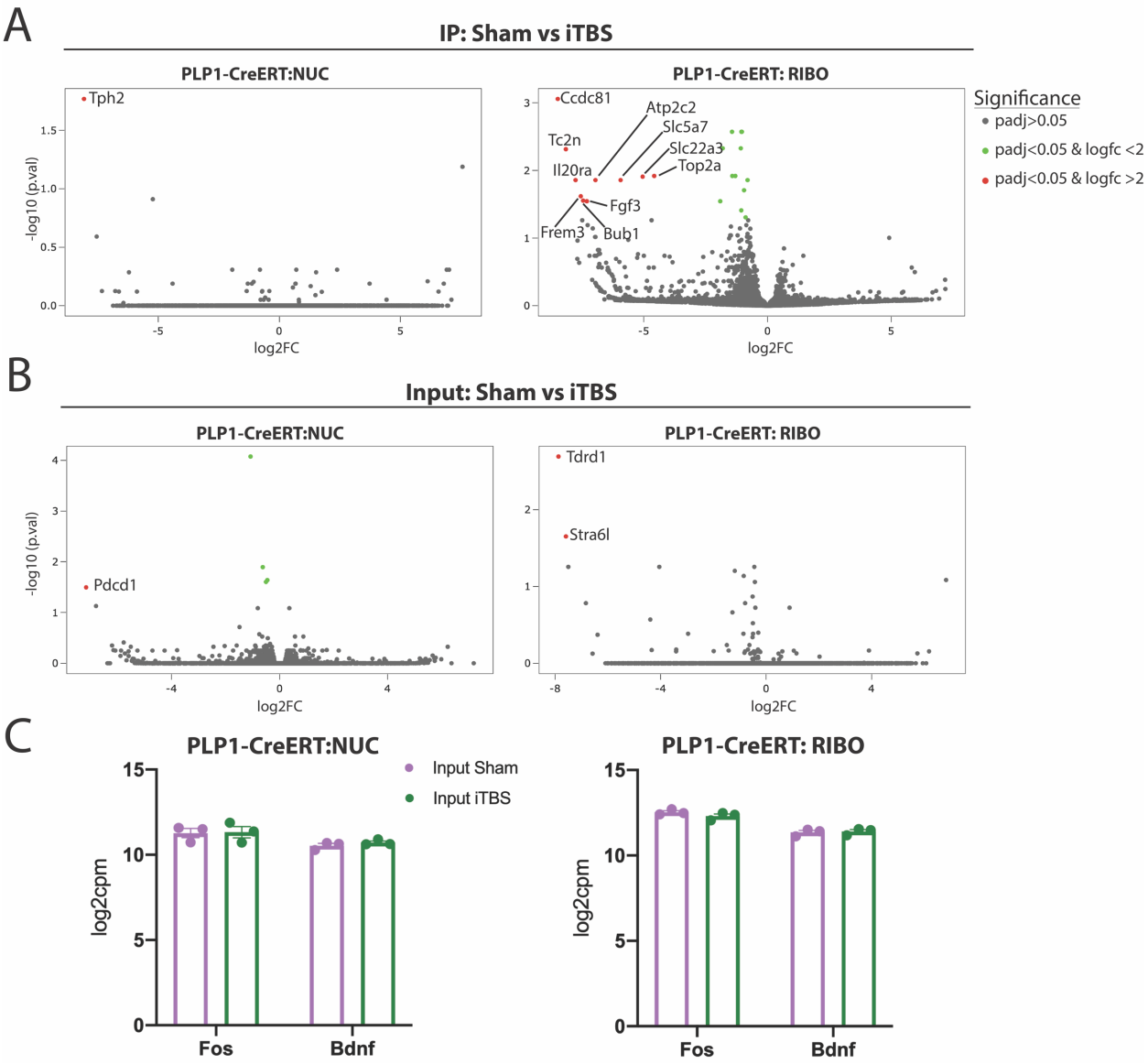

Figure 4: iTBS treatment shows no clear changes in gene expression compared to sham treated animals

A&B) Volcano plot analysis of differentially expressed genes found within the IP (A) or input (B) in sham and iTBS treated animals from both lines. Sham IP shown on the left of the volcano plot, iTBS IP shown on the right of the volcano plot. Red dots indicate enriched genes found in the shams (left of the volcano plot), adj.pval<0.05 and >2 log2FC. Green dots indicate

adj.pval<0.05 with <2 log2FC. Grey dots indicate adj.pval >0.05. Individual example genes in each group are highlighted (n=3 per group).

A) Differentially enriched genes found within the IP samples between sham and iTBS treated animals from PLP1-CreERT:NUC (left) or PLP1-CreERT:RIBO (right) lines.

B) Equivalent analysis for the input samples.

C) Boxplots displaying normalized read counts for genes typically enriched upon increased neuronal activity, *Fos* and *Bdnf,* in PLP1-CreERT:NUC (left) or PLP1-CreERT:RIBO (right) lines. For both lines, input samples from sham or iTBS treated groups show no significant difference in *Fos* or *Bdnf* normalized read counts (n=3 per group). Each dot represents a separate animal, error bars represent ± SEM.

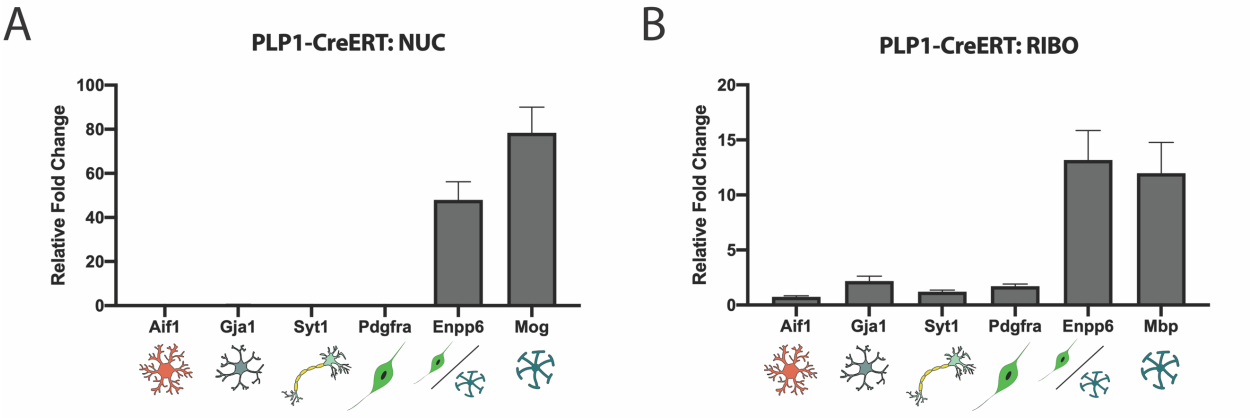

Figure S1: Both INTACT and RiboTag methods show enrichment for known newly-formed and mature oligodendrocyte genes via qPCR

A) Immunoprecipitated RNA from PLP1-CreERT:NUC mice showed an approximate 40-fold enrichment for the known newly-formed oligodendrocyte gene, *Enpp6*, and an approximate 70-fold enrichment for known mature oligodendrocyte gene, *Mog*. Immunoprecipitated RNA showed no enrichment for known genes of other cell types, including microglia (*Aif1),* astrocytes (*Gja1),* neurons (*Syt1)*, and oligodendrocyte progenitor cells (*Pdgfra)*. (n=3 per group).

B) Immunoprecipitated RNA from PLP1-CreERT:RIBO mice showed an approximate 13-fold enrichment for *Enpp6*, and an approximate 11-fold enrichment for known mature oligodendrocyte gene, *Mbp*. In addition, there is low enrichment for known genes of other cell types, *Aif1, Gja1, Syt1, and Pdgfra,* (>2-fold enrichment). (n=3 per group) Graphs show relative gene enrichment compared to *Gapdh.* Error bars represent ± SEM.

Chapter 5: Concluding remarks

Final summary and future directions

The understanding of oligodendrocyte biology and function has shifted considerably over the last several decades. In chapter one, we discuss the evolutionary importance of how these specialized cells helped solve the paradoxical issue of ensuring efficient conduction speed over long distances without relying on axonal giantism. By tightly wrapping axons in segments of a non-conducting sheath, oligodendrocytes increase membrane resistance, decrease capacitance, and provide the one of the structures essential for saltatory conduction. However, decades of research suggest that oligodendrocytes may serve more diverse functions as well. These dynamic cells move through different stages of development, from progenitors to myelinating cells, and each cell stages possess distinct characteristics and function in itself. OPCs represent the proliferative population that maintains a homeostatic number of oligodendrocytes and are capable of responding to a variety of context including health and disease (see (Dimou and Gallo, 2015) for a detailed review). Outside of the function of saltatory conduction, mature oligodendrocytes may also be involved in metabolic support and capable of plasticity.

Each discovery that advances our understanding of oligodendrocyte biology demonstrates how their function depends on the interactions between extrinsic and intrinsic regulation, and one aim of the cellular biologist is to fully understand and integrate how extrinsic and intrinsic signals integrate to shape function. A previously discussed mechanism describes integration: the well-known neurotrophic factor BDNF is released from active neurons and shows diverse roles in regulating neuronal morphology and synaptic plasticity through binding the receptor tyrosine kinase, TrkB) (see (Leal et al., 2015) for a detailed review). Interestingly, the activity-induced release of BDNF may also act on OPCs, as OPCs also express TrkB receptors and BDNF activation of TrkB receptors promotes OPC proliferation and myelination (Peckham et al., 2015; Wong et

al., 2013; Xiao et al., 2011). One study demonstrated that contrary to controls, mice lacking the activity-dependent expression of *Bdnf* fail to show an increase in OPC proliferation and myelin thickness (Geraghty et al., 2019). Together, this suggests that the activity-dependent release of BDNF from neurons may regulate OPC proliferation and myelination through TrkB, and demonstrates how extrinsic signaling effects and impacts the intrinsic proliferation and myelination programming of OPCs.

Chapter one also discusses how advancements in our understanding of oligodendroglial transcription and translation may expand our ability to integrate extrinsic signaling, intrinsic signaling, and determine functional consequences. Recent technological advancements in cell-specific single-cell and single nuclei sorting, as well as progresses in transcriptional and translational profiling techniques, addresses many of the previous challenges in assessing transcriptional and translational states in oligodendroglia. These advancements provide methods to evaluate changes to transcriptional and translational states in the context of health, aging, and disorder and disease and provides an exciting future direction in our understanding of oligodendrocyte lineage cells.

Chapter 3 discusses our work capturing and comparing the transcriptional and translational profiles of OPCs and myelinating oligodendrocytes. Here, we used the INTACT (Deal and Henikoff, 2010; Mo et al., 2015) approach to isolate oligodendroglial nuclear RNA and the RiboTag (Sanz et al., 2009b) approach to isolate ribosome-bound RNA in across the oligodendrocyte lineage. We show that both techniques successfully enrich transcripts from the target cell types and both techniques detect major gene changes induced during oligodendrocyte differentiation. Although each method is suitable for capturing the RNA profiles in oligodendroglia, we show that the INTACT approach offers a cleaner cell-specific purification

compared to the RiboTag approach, making this technique attractive to researchers interested in high cell-specific enrichment with low contamination.

Interestingly, we uncovered two sets of differently enriched genes by comparing compared the nuclear and ribosome-bound immunopurification to each other. In both OPCs and mature oligodendrocytes, we found that a subset of RNAs were enriched in the nuclear IP compared to the ribosome-bound IP and a different subset of genes were enriched in the ribosome-bound IP compared to the nuclear IP. Although many genes that were preferentially enriched in the nuclear samples encoded non-translated RNAs, such as lnc-RNAs and miRNAs, a substantial proportion of these RNAs code for protein-coding genes, possibly representing transcriptionally silenced genes. Conversely, most of the preferentially ribosome-bound RNAs were protein coding mRNAs, which may represent possible transcriptionally active or locally trafficked genes. Through a further analysis of the preferentially ribosome-bound genes, we were surprised to find that many of these genes were related to synapse organization and function. We chose to disrupt the expression of four candidate genes (*Camk2a, Sptbn2, Tenm3, Dbn1*) that were preferentially ribosome-bound RNAs to examine the possible importance of each gene in developmental myelination within the zebrafish. By globally disrupting the expression of *Camk2a, Sptbn2, and Temn3,* we demonstrated that the loss of each gene could reduce the spinal cord myelination. These findings may suggest a role for each gene in regulating oligodendrocyte differentiation or myelin formation, perhaps by regulating calcium signaling (*Camk2a*), establishing sheath structure (*Sptbn2*), or regulating neuroglial interactions (*Tenm3*). All three genes have known roles outside of myelination, therefore, it is possible that the disruption of their expression in non-oligodendroglial cell types may indirectly lead to reduced myelination. In addition, although these candidate genes were selected based off of their known role in synapses, their potential role in oligodendrocytes may be

unrelated to synapses. A global disruption of gene expression makes determining the exact mechanism governing this reduction in spinal cord myelination difficult to pin-point, therefore, determining the cell type and mechanism by which these genes impact myelination will require additional study.

In chapter four, we discuss our efforts to determine how increases in neural activity may modify the oligodendrocyte transcriptome and translatome. Here, we determine whether three separate methods previously shown to impact oligodendroglial dynamics could robustly increase activity in our hands: exercise via voluntary running, pharmacogenetic stimulation via DREADDs activation, and transcranial magnetic stimulation. We show that 14-day access to voluntary running does not robustly increase hippocampal neurogenesis, indicating that this method does not robustly increase activity in our hands. We discuss the possibility of sex-differences within our data and suggest that increasing the number of mice, singly-housing animals, and monitoring the use of the running wheel could improve the experimental design, possibly rendering this method as a useful tool to perturb activity.

In addition, we demonstrate that pharmacogenetic stimulation via excitatory DREADDs expression and activation does not increase the number of $cFos^{+}$ cells or *Fos* mRNA expression, suggesting that this method does not robustly increase activity in our hands. We note that a major difference between ours and previously published work using DREADDs was the chemical activator we chose. Previously published findings demonstrating that it is the metabolically processed drug clozapine, rather than the originally proposed clozapine-N-oxide (CNO), that enters the brain to activate DREADDs (Gomez et al., 2017a). We reasoned that we could avoid metabolic processing and deliver a more accurate concentration of the activating ligand by using clozapine. However, it is possible that the concentration of injected clozapine may not sufficiently

activate the excitatory hM3D-Gq receptor *in vivo*, therefore, we discuss how a more careful investigation determining the optimal concentration required for *in vivo* hM3D-Gq activation may help establish this tool as a robust way to increase neural activity.

Lastly, we demonstrate that low-intensity transcranial magnetic stimulation delivered in intermittent theta-bursts (iTBS) does not detectably alter gene expression in mature oligodendrocytes. Here, mice expressing either Sun1-eGFP (INTACT) or RPL22-HA (RiboTag) under a mature oligodendrocyte promoter (PLP1-CreERT)] mice received sham or iTBS treatment for 7 days before the a 5mm region of brain tissue was harvested for immunopurification and RNA sequencing. We confirm our previous findings that each immunopurification method enriches for mature oligodendrocyte RNA and that the INTACT system offers a cleaner method of purification. By comparing the immunoprecipitated RNA from sham and iTBS mice, we show that iTBS treatment does not promote detectable changes to the transcriptional or translational profiles of mature oligodendrocytes. By comparing the input/un-bound RNA between sham and iTBS treated mice, we show that iTBS treatment did not result detectable global differences in gene expression. Given that the previously published work demonstrating that iTBS treatment enhances newborn oligodendrocyte survival and enhances myelination in a restricted region directly underneath the stimulation coil (Cullen et al., 2019, 2020), we suspect that iTBS-dependent gene expression changes may have been underneath the limit of detection. We postulate the using a more restricted area may be necessary to investigate how iTBS alters the transcriptional and translational profile of oligodendrocytes.

Despite our challenges in establishing tools that robustly increase activity and our challenges in determining the effects of iTBS on oligodendrocyte gene expression, the successful application of each strategy could greatly enhance our understanding of adaptive myelination.

Investigating the transcriptional and translational profiles of oligodendrocytes from active environments could provide a foundation to answer several outstanding questions, including determining the related changes in gene expression that underlie the cellular changes in differentiation and myelination, to higher level questions regarding the functional relevance of adaptive myelination.

In addition, our efforts to transcriptionally and translationally profile cells across the oligodendrocyte lineage could be applied to inform several branches of oligodendrocyte biology. First, researchers could further explore the refined list of preferentially ribosome-bound synapse-related proteins to further understand synaptic structure and function in oligodendrocytes. Although previously published RNA-seq databases could be mined for oligodendrocyte expressed synapse-related genes, our dataset further refines candidate genes that may represent transcriptionally active or locally translated genes in both OPCs and mature oligodendrocytes. By examining preferentially nuclear RNA, we provide a list of non-coding and potentially transcriptionally silenced genes in OPCs and oligodendrocytes. Mounting evidence casts doubts on a 1:1 relationship between transcription and translation (Kislinger et al., 2006; Nagaraj et al., 2011; Roch et al., 2004), therefore, it is becoming increasingly important to understand the regulation that occurs at each step of RNA processing. Our efforts provide a foundation to understand the transcriptional and translational differences between OPCs and mature oligodendrocytes, as well as a foundation to understand how transcription and translation is regulated within each stage of the oligodendroglial lineage.

References

Abbott, R.D., White, L.R., Ross, G.W., Masaki, K.H., Curb, J.D., and Petrovitch, H. (2004). Walking and Dementia in Physically Capable Elderly Men. Jama *292*, 1447–1453.

Abney, E.R., Bartlett, P.P., and Raff, M.C. (1981). Astrocytes, ependymal cells, and oligodendrocytes develop on schedule in dissociated cell cultures of embryonic rat brain. Dev Biol *83*, 301–310.

Achterberg, K.G., Buitendijk, G.H.S., Kool, M.J., Goorden, S.M.I., Post, L., Slump, D.E., Silva, A.J., Woerden, G.M. van, Kushner, S.A., and Elgersma, Y. (2014). Temporal and Region-Specific Requirements of αCaMKII in Spatial and Contextual Learning. J Neurosci *34*, 11180–11187.

Aggarwal, S., Yurlova, L., Snaidero, N., Reetz, C., Frey, S., Zimmermann, J., Pähler, G., Janshoff, A., Friedrichs, J., Müller, D.J., et al. (2011). A Size Barrier Limits Protein Diffusion at the Cell Surface to Generate Lipid-Rich Myelin-Membrane Sheets. Developmental Cell *21*, 445–456.

Aggarwal, S., Snaidero, N., Pähler, G., Frey, S., Sánchez, P., Zweckstetter, M., Janshoff, A., Schneider, A., Weil, M.-T., Schaap, I.A.T., et al. (2013). Myelin Membrane Assembly Is Driven by a Phase Transition of Myelin Basic Proteins Into a Cohesive Protein Meshwork. PLoS Biology *11*, e1001577.

Ainger, K., Avossa, D., Morgan, F., Hill, S.J., Barry, C., Barbarese, E., and Carson, J.H. (1993). Transport and localization of exogenous myelin basic protein mRNA microinjected into oligodendrocytes. J Cell Biology *123*, 431–441.

Ainsley, J.A., Drane, L., Jacobs, J., Kittelberger, K.A., and Reijmers, L.G. (2014). Functionally diverse dendritic mRNAs rapidly associate with ribosomes following a novel experience. Nat Commun *5*, 4510.

Akita, T., Aoto, K., Kato, M., Shiina, M., Mutoh, H., Nakashima, M., Kuki, I., Okazaki, S., Magara, S., Shiihara, T., et al. (2018). De novo variants in CAMK2A and CAMK2B cause neurodevelopmental disorders. Ann Clin Transl Neur *5*, 280–296.

Alcover-Sanchez, B., Garcia-Martin, G., Wandosell, F., and Cubelos, B. (2020). R-Ras GTPases Signaling Role in Myelin Neurodegenerative Diseases. Int J Mol Sci *21*, 5911.

Alder, J., Thakker-Varia, S., Bangasser, D.A., Kuroiwa, M., Plummer, M.R., Shors, T.J., and Black, I.B. (2003). Brain-Derived Neurotrophic Factor-Induced Gene Expression Reveals Novel Actions of VGF in Hippocampal Synaptic Plasticity. J Neurosci *23*, 10800–10808.

Almeida, R.G., and Lyons, D.A. (2017). On Myelinated Axon Plasticity and Neuronal Circuit Formation and Function. J Neurosci Official J Soc Neurosci *37*, 10023–10034.

Almeida, R.G., Czopka, T., ffrench-Constant, C., and Lyons, D.A. (2011). Individual axons regulate the myelinating potential of single oligodendrocytes in vivo. Development *138*, 4443–4450.

Althaus, H.H., Hempel, R., Kl□ppner, S., Engel, J., Schmidt-Schultz, T., Kruska, L., and Heumann, R. (1997). Nerve growth factor signal transduction in mature pig oligodendrocytes. J Neurosci Res *50*, 729–742.

Alvarez-Saavedra, M., Repentigny, Y.D., Lagali, P.S., Ram, E.V.S.R., Yan, K., Hashem, E., Ivanochko, D., Huh, M.S., Yang, D., Mears, A.J., et al. (2014). Snf2h-mediated chromatin organization and histone H1 dynamics govern cerebellar morphogenesis and neural maturation. Nat Commun *5*, 4181.

Alvarez-Saavedra, M., De Repentigny, Y., Yang, D., O'Meara, R.W., Yan, K., Hashem, L.E., Racacho, L., Ioshikhes, I., Bulman, D.E., Parks, R.J., et al. (2016). Voluntary Running Triggers VGF-Mediated Oligodendrogenesis to Prolong the Lifespan of Snf2h-Null Ataxic Mice. Cell Reports *17*, 862–875.

Amerongen, R. van, and Nusse, R. (2009). Towards an integrated view of Wnt signaling in development. Dev Camb Engl *136*, 3205–3214.

Amor, V., Zhang, C., Vainshtein, A., Zhang, A., Zollinger, D.R., Eshed-Eisenbach, Y., Brophy, P.J., Rasband, M.N., and Peles, E. (2017). The paranodal cytoskeleton clusters Na+ channels at nodes of Ranvier. Elife *6*, e21392.

Antinucci, P., Nikolaou, N., Meyer, M.P., and Hindges, R. (2013). Teneurin-3 Specifies Morphological and Functional Connectivity of Retinal Ganglion Cells in the Vertebrate Visual System. Cell Reports *5*, 582–592.

Armbruster, B.N., Li, X., Pausch, M.H., Herlitze, S., and Roth, B.L. (2007). Evolving the lock to fit the key to create a family of G protein-coupled receptors potently activated by an inert ligand. Proc National Acad Sci *104*, 5163–5168.

Armstrong, R.C., Harvath, L., and Dubois-Dalcq, M.E. (1990). Type 1 astrocytes and oligodendrocyte-type 2 astrocyte glial progenitors migrate toward distinct molecules. J Neurosci Res *27*, 400–407.

Ashby, C.R., and Wang, R.Y. (1996). Pharmacological actions of the atypical antipsychotic drug clozapine: A review. Synapse *24*, 349–394.

Attwell, D., Mishra, A., Hall, C.N., O'Farrell, F.M., and Dalkara, T. (2015). What is a pericyte? J Cereb Blood Flow Metabolism Official J Int Soc Cereb Blood Flow Metabolism *36*, 451–455.

Avey, D., Sankararaman, S., Yim, A.K.Y., Barve, R., Milbrandt, J., and Mitra, R.D. (2018). Single-Cell RNA-Seq Uncovers a Robust Transcriptional Response to Morphine by Glia. Cell Reports *24*, 3619-3629.e4.

Azim, K., and Butt, A.M. (2011). GSK3β negatively regulates oligodendrocyte differentiation and myelination in vivo. Glia *59*, 540–553.

Back, S.A., Luo, N.L., Borenstein, N.S., Levine, J.M., Volpe, J.J., and Kinney, H.C. (2001). Late Oligodendrocyte Progenitors Coincide with the Developmental Window of Vulnerability for Human Perinatal White Matter Injury. J Neurosci *21*, 1302–1312.

Bakhti, M., Aggarwal, S., and Simons, M. (2014). Myelin architecture: zippering membranes tightly together. Cellular and Molecular Life Sciences *71*, 1265–1277.

Balia, M., Vélez-Fort, M., Passlick, S., Schäfer, C., Audinat, E., Steinhäuser, C., Seifert, G., and Angulo, M.C. (2013). Postnatal Down-Regulation of the GABAA Receptor γ2 Subunit in Neocortical NG2 Cells Accompanies Synaptic-to-Extrasynaptic Switch in the GABAergic Transmission Mode. Cereb Cortex *25*, 1114–1123.

Bansal, R., Magge, S., and Winkler, S. (2003). Specific inhibitor of FGF receptor signaling: FGF-2-mediated effects on proliferation, differentiation, and MAPK activation are inhibited by PD173074 in oligodendrocyte-lineage cells. J Neurosci Res *74*, 486–493.

Barker, A.T., Freeston, I.L., Jalinous, R., and Jarratt, J.A. (1987). Proceedings of the First International Symposium on Motor System Evoked Potential Monitoring, Purdue University, West Lafayette, Indiana, June 16 and 17, 1986. Neurosurgery *20*, 67.

Baron, W., and Hoekstra, D. (2010). On the biogenesis of myelin membranes: Sorting, trafficking and cell polarity. FEBS Letters *584*, 1760–1770.

Baron, W., Metz, B., Bansal, R., Hoekstra, D., and Vries, H. de (2000). PDGF and FGF-2 Signaling in Oligodendrocyte Progenitor Cells: Regulation of Proliferation and Differentiation by Multiple Intracellular Signaling Pathways. Mol Cell Neurosci *15*, 314–329.

Barratt, H.E., Budnick, H.C., Parra, R., Lolley, R.J., Perry, C.N., and Nesic, O. (2016). Tamoxifen promotes differentiation of oligodendrocyte progenitors in vitro. Neuroscience *319*, 146–154.

Barres, B., and Raff, M. (1993). Proliferation of oligodendrocyte precursor cells depends on electrical activity in axons. Nature *361*, 361258a0.

Barres, B.A., and Raff, M.C. (1994). Control of oligodendrocyte number in the developing rat optic nerve. Neuron *12*, 935–942.

Barres, B.A., Koroshetz, W.J., Swartz, K.J., Chun, L.L.Y., and Corey, D.P. (1990). Ion channel expression by white matter glia: The O-2A glial progenitor cell. Neuron *4*, 507–524.

Barres, B.A., Hart, I.K., Coles, H.S.R., Burne, J.F., Voyvodic, J.T., Richardson, W.D., and Raff, M.C. (1992). Cell death and control of cell survival in the oligodendrocyte lineage. Cell *70*, 31–46.

Baser, A., Skabkin, M., Kleber, S., Dang, Y., Balta, G.S.G., Kalamakis, G., Göpferich, M., Ibañez, D.C., Schefzik, R., Lopez, A.S., et al. (2019). Onset of differentiation is post-transcriptionally controlled in adult neural stem cells. Nature *566*, 100–104.

Baumann, N., and Pham-Dinh, D. (2001). Biology of Oligodendrocyte and Myelin in the Mammalian Central Nervous System. Physiological Reviews *81*, 871–927.

Baydyuk, M., Morrison, V.E., Gross, P.S., and Huang, J.K. (2020). Extrinsic Factors Driving Oligodendrocyte Lineage Cell Progression in CNS Development and Injury. Neurochem Res *45*, 630–642.

Behrens, J., Kries, J.P. von, Kühl, M., Bruhn, L., Wedlich, D., Grosschedl, R., and Birchmeier, W. (1996). Functional interaction of β-catenin with the transcription factor LEF-1. Nature *382*, 638–642.

Bellesi, M., Pfister-Genskow, M., Maret, S., Keles, S., Tononi, G., and Cirelli, C. (2013). Effects of Sleep and Wake on Oligodendrocytes and Their Precursors. J Neurosci *33*, 14288–14300.

Bengtsson, S.L., Nagy, Z., Skare, S., Forsman, L., Forssberg, H., and Ullén, F. (2005). Extensive piano practicing has regionally specific effects on white matter development. Nat Neurosci *8*, 1148–1150.

Bercury, K., Dai, J., and of …, S.-H. (2014). Conditional ablation of raptor or rictor has differential impact on oligodendrocyte differentiation and CNS myelination.

Bergles, D.E., Roberts, J., Somogyi, P., and Jahr, C.E. (2000). Glutamatergic synapses on oligodendrocyte precursor cells in the hippocampus. *405*.

Berns, D.S., DeNardo, L.A., Pederick, D.T., and Luo, L. (2018). Teneurin-3 controls topographic circuit assembly in the hippocampus. Nature *554*, 328–333.

Bhat, N.R., and Zhang, P. (2002). Activation of Mitogen-Activated Protein Kinases in Oligodendrocytes. J Neurochem *66*, 1986–1994.

Bhattacharyya, S., Sathe, A.A., Bhakta, M., Xing, C., and Munshi, N.V. (2019). PAN-INTACT enables direct isolation of lineage-specific nuclei from fibrous tissues. Plos One *14*, e0214677.

Biase, L.M.D., Nishiyama, A., and Bergles, D.E. (2010). Excitability and synaptic communication within the oligodendrocyte lineage. J Neurosci Official J Soc Neurosci *30*, 3600–3611.

Bisler, S., Schleicher, A., Gass, P., Stehle, J.H., Zilles, K., and Staiger, J.F. (2002). Expression of c-Fos, ICER, Krox-24 and JunB in the whisker-to-barrel pathway of rats: time course of induction upon whisker stimulation by tactile exploration of an enriched environment. J Chem Neuroanat *23*, 187–198.

Borgesius, N.Z., Woerden, G.M. van, Buitendijk, G.H.S., Keijzer, N., Jaarsma, D., Hoogenraad, C.C., and Elgersma, Y. (2011). βCaMKII Plays a Nonenzymatic Role in Hippocampal Synaptic Plasticity and Learning by Targeting αCaMKII to Synapses. J Neurosci *31*, 10141–10148.

Boulton, T.G., Nye, S.H., Robbins, D.J., Ip, N.Y., Radzlejewska, E., Morgenbesser, S.D., DePinho, R.A., Panayotatos, N., Cobb, M.H., and Yancopoulos, G.D. (1991). ERKs: A family of protein-serine/threonine kinases that are activated and tyrosine phosphorylated in response to insulin and NGF. Cell *65*, 663–675.

Bozdagi, O., Rich, E., Tronel, S., Sadahiro, M., Patterson, K., Shapiro, M.L., Alberini, C.M., Huntley, G.W., and Salton, S.R.J. (2008). The neurotrophin-inducible gene Vgf regulates hippocampal function and behavior through a brain-derived neurotrophic factor-dependent mechanism. J Neurosci Official J Soc Neurosci *28*, 9857–9869.

Braun, R.E., Peschon, J.J., Behringer, R.R., Brinster, R.L., and Palmiter, R.D. (1989). Protamine 3'-untranslated sequences regulate temporal translational control and subcellular localization of growth hormone in spermatids of transgenic mice. Gene Dev *3*, 793–802.

Bräunig, P., and Burrows, M. (2004). Projection patterns of posterior dorsal unpaired median neurons of the locust subesophageal ganglion. Journal of Comparative Neurology *478*, 164–175.

Brinkmann, B.G., Agarwal, A., Sereda, M.W., Garratt, A.N., Müller, T., Wende, H., Stassart, R.M., Nawaz, S., Humml, C., Velanac, V., et al. (2008). Neuregulin-1/ErbB Signaling Serves Distinct Functions in Myelination of the Peripheral and Central Nervous System. Neuron *59*, 581–595.

Brivio, V., Faivre-Sarrailh, C., Peles, E., Sherman, D.L., and Brophy, P.J. (2017). Assembly of CNS Nodes of Ranvier in Myelinated Nerves Is Promoted by the Axon Cytoskeleton. Curr Biol *27*, 1068–1073.

Brösamle, C., and Halpern, M.E. (2002). Characterization of myelination in the developing zebrafish. Glia *39*, 47–57.

Bujalka, H., Koenning, M., Jackson, S., Perreau, V.M., Pope, B., Hay, C.M., Mitew, S., Hill, A.F., Lu, R.Q., Wegner, M., et al. (2013). MYRF Is a Membrane-Associated Transcription Factor That Autoproteolytically Cleaves to Directly Activate Myelin Genes. *11*.

Buller, B., Chopp, M., Ueno, Y., Zhang, L., Zhang, R., Morris, D., Zhang, Y., and Zhang, Z. (2012). Regulation of serum response factor by miRNA-200 and miRNA-9 modulates oligodendrocyte progenitor cell differentiation. Glia *60*, 1906–1914.

Byravan, S., Foster, L.M., Phan, T., Verity, A.N., and Campagnoni, A.T. (1994). Murine oligodendroglial cells express nerve growth factor. Proc National Acad Sci *91*, 8812–8816.

Cahoy, J.D., Emery, B., Kaushal, A., Foo, L.C., Zamanian, J.L., Christopherson, K.S., Xing, Y., Lubischer, J.L., Krieg, P.A., Krupenko, S.A., et al. (2008). A Transcriptome Database for Astrocytes, Neurons, and Oligodendrocytes: A New Resource for Understanding Brain Development and Function. J Neurosci *28*, 264–278.

Cai, J., Qi, Y., Hu, X., Tan, M., Liu, Z., Zhang, J., Li, Q., Sander, M., and Qiu, M. (2005). Generation of Oligodendrocyte Precursor Cells from Mouse Dorsal Spinal Cord Independent of Nkx6 Regulation and Shh Signaling. Neuron *45*, 41–53.

Cai, J., Chen, Y., Cai, W.-H., Hurlock, E.C., Wu, H., Kernie, S.G., Parada, L.F., and Lu, Q.R. (2007). A crucial role for Olig2 in white matter astrocyte development. Development *134*, 1887–1899.

Caldwell, J.H. (2009). Encyclopedia of Neuroscience. Subject Classification: Molecular and Cell Biology of Nervous SystemsCellular Excitability: Axon, Dendrite, Soma: Molecular and Cell Biology of Nervous Systems: Cellular Excitability: Axon, Dendrite, Soma: Article Titles: A 23–29.

Calver, A.R., Hall, A.C., Yu, W.-P., Walsh, F.S., Heath, J.K., Betsholtz, C., and Richardson, W.D. (1998). Oligodendrocyte Population Dynamics and the Role of PDGF In Vivo. Neuron *20*, 869–882.

Castillo-Padilla, D.V., and Funke, K. (2016). Effects of chronic iTBS-rTMS and enriched environment on visual cortex early critical period and visual pattern discrimination in dark-reared rats. Dev Neurobiol *76*, 19–33.

Castro, F. de, and Bribián, A. (2005). The molecular orchestra of the migration of oligodendrocyte precursors during development. Brain Research Reviews *49*, 227–241.

Chen, G., Ning, B., and Shi, T. (2019). Single-Cell RNA-Seq Technologies and Related Computational Data Analysis. Frontiers Genetics *10*, 317.

Chen, M., Xu, Y., Huang, R., Huang, Y., Ge, S., and Hu, B. (2016). N-Cadherin is Involved in Neuronal Activity-Dependent Regulation of Myelinating Capacity of Zebrafish Individual Oligodendrocytes In Vivo. Mol Neurobiol *54*, 6917–6930.

Chéreau, R., Saraceno, E.G., Angibaud, J., Cattaert, D., and Nägerl, V.U. (2017). Superresolution imaging reveals activity-dependent plasticity of axon morphology linked to changes in action potential conduction velocity. Proceedings of the National Academy of Sciences *114*, 1401–1406.

Chia, P.H., Zhong, F.L., Niwa, S., Bonnard, C., Utami, K.H., Zeng, R., Lee, H., Eskin, A., Nelson, S.F., Xie, W.H., et al. (2018). A homozygous loss-of-function CAMK2A mutation causes growth delay, frequent seizures and severe intellectual disability. Elife *7*, e32451.

Clarke, L.E., Young, K.M., Hamilton, N.B., Li, H., Richardson, W.D., and Attwell, D. (2012). Properties and Fate of Oligodendrocyte Progenitor Cells in the Corpus Callosum, Motor Cortex, and Piriform Cortex of the Mouse. J Neurosci *32*, 8173–8185.

Clevers, H., and Nusse, R. (2012). Wnt/β-catenin signaling and disease. Cell *149*, 1192–1205.

Colcombe, S.J., Kramer, A.F., McAuley, E., Erickson, K.I., and Scalf, P. (2004). Neurocognitive aging and cardiovascular fitness. J Mol Neurosci *24*, 9–14.

Colello, R., Pott, U., and Schwab, M. (1994). The role of oligodendrocytes and myelin on axon maturation in the developing rat retinofugal pathway. J Neurosci *14*, 2594–2605.

Conway, G.D., O'Bara, M.A., Vedia, B.H., Pol, S.U., and Sim, F.J. (2012). Histone deacetylase activity is required for human oligodendrocyte progenitor differentiation. Glia *60*, 1944–1953.

Cruise, K.E., Bucks, R.S., Loftus, A.M., Newton, R.U., Pegoraro, R., and Thomas, M.G. (2011). Exercise and Parkinson's: benefits for cognition and quality of life. Acta Neurol Scand *123*, 13–19.

Cullen, C.L., Senesi, M., Tang, A.D., Clutterbuck, M.T., Auderset, L., O'Rourke, M.E., Rodger, J., and Young, K.M. (2019). Low-intensity transcranial magnetic stimulation promotes the survival and maturation of newborn oligodendrocytes in the adult mouse brain. Glia *67*, 1462–1477.

Cullen, C.L., Pepper, R.E., Clutterbuck, M.T., Pitman, K.A., Oorschot, V., Auderset, L., Tang, A.D., Ramm, G., Emery, B., Rodger, J., et al. (2020). Periaxonal and nodal plasticity modulate action potential conduction in the adult mouse brain. Biorxiv 726760.

Czopka, T., ffrench-Constant, C., and Lyons, D.A. (2013). Individual Oligodendrocytes Have Only a Few Hours in which to Generate New Myelin Sheaths In Vivo. Developmental Cell *25*, 599–609.

Dai, J., Bercury, K.K., and Macklin, W.B. (2014). Interaction of mTOR and Erk1/2 signaling to regulate oligodendrocyte differentiation. Glia *62*, 2096–2109.

Dai, X., Lercher, L.D., Clinton, P.M., Du, Y., Livingston, D.L., Vieira, C., Yang, L., Shen, M.M., and Dreyfus, C.F. (2003). The Trophic Role of Oligodendrocytes in the Basal Forebrain. Journal of Neuroscience *23*, 5846–5853.

Dawson, M.R.L., Polito, A., Levine, J.M., and Reynolds, R. (2003). NG2-expressing glial progenitor cells: an abundant and widespread population of cycling cells in the adult rat CNS. Mol Cell Neurosci *24*, 476–488.

Deal, R.B., and Henikoff, S. (2010). The INTACT method for cell type–specific gene expression and chromatin profiling in Arabidopsis thaliana. Nat Protoc *6*, 56–68.

Deiner, M.S., and Sretavan, D.W. (1999). Altered Midline Axon Pathways and Ectopic Neurons in the Developing Hypothalamus of Netrin-1- and DCC-Deficient Mice. J Neurosci *19*, 9900–9912.

Demerens, C., Stankoff, B., Logak, M., Anglade, P., Allinquant, B., Couraud, F., Zalc, B., and Lubetzki, C. (1996). Induction of myelination in the central nervous system by electrical activity. *93*.

Dhaunchak, A.S., Huang, J.K., Faria, O., Roth, A.D., Pedraza, L., Antel, J.P., Bar-Or, A., and Colman, D.R. (2010). A proteome map of axoglial specializations isolated and purified from human central nervous system. Glia *58*, 1949–1960.

Dimou, L., and Gallo, V. (2015). NG2-glia and their functions in the central nervous system. *63*.

Doerflinger, N.H., Macklin, W.B., and Popko, B. (2002). Inducible site-specific recombination in myelinating cells. Genesis *35*, 63–72.

Dong, X., Chen, K., Duran, R., You, Y., Sloan, S.A., Zhang, Y., Zong, S., Cao, Q., Barres, B.A., and Wu, J. (2015). Comprehensive Identification of Long Non-coding RNAs in Purified Cell Types from the Brain Reveals Functional LncRNA in OPC Fate Determination. PLoS Genetics *11*, e1005669.

Dougherty, J.D., Fomchenko, E.I., Akuffo, A.A., Schmidt, E., Helmy, K.Y., Bazzoli, E., Brennan, C.W., Holland, E.C., and Milosevic, A. (2012). Candidate pathways for promoting differentiation or quiescence of oligodendrocyte progenitor-like cells in glioma. Cancer Res *72*, 4856–4868.

Doyle, J.P., Dougherty, J.D., Heiman, M., Schmidt, E.F., Stevens, T.R., Ma, G., Bupp, S., Shrestha, P., Shah, R.D., Doughty, M.L., et al. (2008). Application of a translational profiling approach for the comparative analysis of CNS cell types. Cell *135*, 749–762.

Du, Y., Lercher, L.D., Zhou, R., and Dreyfus, C.F. (2006). Mitogen-activated protein kinase pathway mediates effects of brain-derived neurotrophic factor on differentiation of basal forebrain oligodendrocytes. J Neurosci Res *84*, 1692–1702.

Dugas, J.C., and Notterpek, L. (2011). MicroRNAs in Oligodendrocyte and Schwann Cell Differentiation. Dev Neurosci-Basel *33*, 14–20.

Dugas, J.C., Tai, Y.C., Speed, T.P., Ngai, J., and Barres, B.A. (2006). Functional Genomic Analysis of Oligodendrocyte Differentiation. J Neurosci *26*, 10967–10983.

Dugas, J.C., Cuellar, T.L., Scholze, A., Ason, B., Ibrahim, A., Emery, B., Zamanian, J.L., Foo, L.C., McManus, M.T., and Barres, B.A. (2010). Dicer1 and miR-219 Are Required for Normal Oligodendrocyte Differentiation and Myelination. Neuron *65*, 597–611.

Dupree, J.L., Suzuki, K., and Popko, B. (1998a). Galactolipids in the formation and function of the myelin sheath. Microscopy Research and Technique *41*, 431–440.

Dupree, J.L., Coetzee, T., Blight, A., Suzuki, K., and Popko, B. (1998b). Myelin Galactolipids Are Essential for Proper Node of Ranvier Formation in the CNS. Journal of Neuroscience *18*, 1642–1649.

Durand, B., and Raff, M. (2000). A cell-intrinsic timer that operates during oligodendrocyte development. Bioessays *22*, 64–71.

Early, J.J., Cole, K.L., Williamson, J.M., Swire, M., Kamadurai, H., Muskavitch, M., and Lyons, D.A. (2018). An automated high-resolution in vivo screen in zebrafish to identify chemical regulators of myelination. Elife *7*, e35136.

Efimova, N., Korobova, F., Stankewich, M.C., Moberly, A.H., Stolz, D.B., Wang, J., Kashina, A., Ma, M., and Svitkina, T. (2017). βIII Spectrin Is Necessary for Formation of the Constricted Neck of Dendritic Spines and Regulation of Synaptic Activity in Neurons. J Neurosci Official J Soc Neurosci *37*, 6442–6459.

Elbaz, B., Aaker, J.D., Isaac, S., Kolarzyk, A., Brugarolas, P., Eden, A., and Popko, B. (2018). Phosphorylation State of ZFP24 Controls Oligodendrocyte Differentiation. Cell Reports *23*, 2254–2263.

Elgersma, Y., Fedorov, N.B., Ikonen, S., Choi, E.S., Elgersma, M., Carvalho, O.M., Giese, K.P., and Silva, A.J. (2002). Inhibitory Autophosphorylation of CaMKII Controls PSD Association, Plasticity, and Learning. Neuron *36*, 493–505.

Emery, B. (2010). Regulation of Oligodendrocyte Differentiation and Myelination. Science *330*, 779–782.

Emery, B., and Lu, R.Q. (2015). Transcriptional and Epigenetic Regulation of Oligodendrocyte Development and Myelination in the Central Nervous System. Cold Spring Harbor Perspectives in Biology *7*, a020461.

Emery, B., Agalliu, D., Cahoy, J.D., Watkins, T.A., Dugas, J.C., Mulinyawe, S.B., Ibrahim, A., Ligon, K.L., Rowitch, D.H., and Barres, B.A. (2009a). Myelin Gene Regulatory Factor Is a Critical Transcriptional Regulator Required for CNS Myelination. *138*.

Emery, B., Agalliu, D., Cahoy, J., Watkins, T., and Cell, D.-J. (2009b). Myelin gene regulatory factor is a critical transcriptional regulator required for CNS myelination.

Etxeberria, A., Hokanson, K.C., Dao, D.Q., Mayoral, S.R., Mei, F., Redmond, S.A., Ullian, E.M., and Chan, J.R. (2016). Dynamic Modulation of Myelination in Response to Visual Stimuli Alters Optic Nerve Conduction Velocity. J Neurosci Official J Soc Neurosci *36*, 6937–6948.

Evercooren, A.B.-V., Olichon-Berthe, C., Kowalski, A., Visciano, G., and Obberghen, E.V. (1991). Expression of IGF-I and insulin receptor genes in the rat central nervous system: A developmental, regional, and cellular analysis. J Neurosci Res *28*, 244–253.

Falcão, A.M., Bruggen, D. van, Marques, S., Meijer, M., Jäkel, S., Agirre, E., Samudyata, Floriddia, E.M., Vanichkina, D.P., Ffrench-Constant, C., et al. (2018). Disease-specific oligodendrocyte lineage cells arise in multiple sclerosis. Nat Med *24*, 1837–1844.

Fancy, S.P., Baranzini, S.E., Zhao, C., Yuk, D.-I., Irvine, K.-A., Kaing, S., Sanai, N., Franklin, R.J., and Rowitch, D.H. (2009). Dysregulation of the Wnt pathway inhibits timely myelination and remyelination in the mammalian CNS. Genes & Development *23*, 1571–1585.

Fang, N., Cheng, J., Zhang, C., Chen, K., Zhang, C., Hu, Z., Bi, R., Furber, K.L., Thangaraj, M., Nazarali, A.J., et al. (2019). Sirt2 epigenetically down-regulates PDGFRα expression and promotes CG4 cell differentiation. Cell Cycle *18*, 1095–1109.

Feigenson, K., Reid, M., See, J., Crenshaw, E.B., and Grinspan, J.B. (2009). Wnt signaling is sufficient to perturb oligodendrocyte maturation. Mol Cell Neurosci *42*, 255–265.

Feigenson, K., Reid, M., See, J., III, E.B.C., and Grinspan, J.B. (2011). Canonical Wnt signalling requires the BMP pathway to inhibit oligodendrocyte maturation. Asn Neuro *3*, e00061.

Fields, R.D. (2005). Myelination: An Overlooked Mechanism of Synaptic Plasticity? Neurosci *11*, 528–531.

Fields, R.D. (2008). White matter in learning, cognition and psychiatric disorders. Trends Neurosci *31*, 361–370.

Fields, D.R., Woo, D., and Basser, P.J. (2015). Glial Regulation of the Neuronal Connectome through Local and Long-Distant Communication. Elsevier Inc. *86*.

Finzsch, M., Stolt, C.C., Lommes, P., and Wegner, M. (2008). Sox9 and Sox10 influence survival and migration of oligodendrocyte precursors in the spinal cord by regulating PDGF receptor α expression. Development *135*, 637–646.

Flores, A., Narayanan, S., and of …, M.-E. (2008). Constitutively active Akt induces enhanced myelination in the CNS.

Forbes, T.A., Goldstein, E.Z., Dupree, J.L., Jablonska, B., Scafidi, J., Adams, K.L., Imamura, Y., Hashimoto-Torii, K., and Gallo, V. (2020). Environmental enrichment ameliorates perinatal brain injury and promotes functional white matter recovery. Nat Commun *11*, 964.

Ford, M., Alexandrova, O., Cossell, L., Stange-Marten, A., Sinclair, J., Kopp-Scheinpflug, C., Pecka, M., Attwell, D., and Grothe, B. (2015). Tuning of Ranvier node and internode properties in myelinated axons to adjust action potential timing. *6*.

Foster, A.Y., Bujalka, H., and Emery, B. (2019). Axoglial interactions in myelin plasticity: Evaluating the relationship between neuronal activity and oligodendrocyte dynamics. Glia.

Frost, E., Kiernan, B.W., Faissner, A., and ffrench-Constant, C. (1996). Regulation of Oligodendrocyte Precursor Migration by Extracellular Matrix: Evidence for Substrate-Specific Inhibition of Migration by Tenascin-C. Dev Neurosci-Basel *18*, 266–273.

Fruttiger, M., Karlsson, L., Hall, A.C., Abramsson, A., Calver, A.R., Boström, H., Willetts, K., Bertold, C.H., Heath, J.K., Betsholtz, C., et al. (1999). Defective oligodendrocyte development and severe hypomyelination in PDGF-A knockout mice. Dev Camb Engl *126*, 457–467.

Fryer, J.D., Yu, P., Kang, H., Mandel-Brehm, C., Carter, A.N., Crespo-Barreto, J., Gao, Y., Flora, A., Shaw, C., Orr, H.T., et al. (2011). Exercise and Genetic Rescue of SCA1 via the Transcriptional Repressor Capicua. Science *334*, 690–693.

Fu, H., Qi, Y., Tan, M., Cai, J., Takebayashi, H., Nakafuku, M., Richardson, W., and Qiu, M. (2002). Dual origin of spinal oligodendrocyte progenitors and evidence for the cooperative role of Olig2 and Nkx2.2 in the control of oligodendrocyte differentiation. Development (Cambridge, England) *129*, 681–693.

FÜLLEKRUG, J., and SIMONS, K. (2004). Lipid Rafts and Apical Membrane Traffic. Annals of the New York Academy of Sciences *1014*, 164–169.

Fünfschilling, U., Supplie, L.M., Mahad, D., Boretius, S., Saab, A.S., Edgar, J., Brinkmann, B.G., Kassmann, C.M., Tzvetanova, I.D., Möbius, W., et al. (2012). Glycolytic oligodendrocytes maintain myelin and long-term axonal integrity. Nature *485*, 517.

Furusho, M., Dupree, J.L., Nave, K.-A., and Bansal, R. (2012). Fibroblast growth factor receptor signaling in oligodendrocytes regulates myelin sheath thickness. J Neurosci Official J Soc Neurosci *32*, 6631–6641.

Furusho, M., Ishii, A., and Bansal, R. (2017). Signaling by FGF Receptor 2, Not FGF Receptor 1, Regulates Myelin Thickness through Activation of ERK1/2–MAPK, Which Promotes mTORC1 Activity in an Akt-Independent Manner. The Journal of Neuroscience *37*, 2931–2946.

Fyffe-Maricich, S.L., Karlo, J.C., Landreth, G.E., and Miller, R.H. (2011). The ERK2 mitogen-activated protein kinase regulates the timing of oligodendrocyte differentiation. J Neurosci Official J Soc Neurosci *31*, 843–850.

Fyffe-Maricich, S.L., Schott, A., Karl, M., Krasno, J., and Miller, R.H. (2013). Signaling through ERK1/2 controls myelin thickness during myelin repair in the adult central nervous system. J Neurosci Official J Soc Neurosci *33*, 18402–18408.

Gaede, G., Tiede, M., Lorenz, I., Brandt, A.U., Pfueller, C., Dörr, J., Bellmann-Strobl, J., Piper, S.K., Roth, Y., Zangen, A., et al. (2018). Safety and preliminary efficacy of deep transcranial magnetic stimulation in MS-related fatigue. Neurology - Neuroimmunol Neuroinflammation *5*, e423.

Gaesser, J.M., and Fyffe-Maricich, S.L. (2016). Intracellular signaling pathway regulation of myelination and remyelination in the CNS. Experimental Neurology *283*, 501–511.

Garratt, A.N., Voiculescu, O., Topilko, P., Charnay, P., and Birchmeier, C. (2000). A Dual Role of erbB2 in Myelination and in Expansion of the Schwann Cell Precursor Pool. J Cell Biology *148*, 1035–1046.

Ge, W.-P., Zhou, W., Luo, Q., Jan, L.Y., and Jan, Y.N. (2008). Dividing glial cells maintain differentiated properties including complex morphology and functional synapses. Proc National Acad Sci *106*, 328–333.

Geraghty, A.C., Gibson, E.M., Ghanem, R.A., Greene, J.J., Ocampo, A., Goldstein, A.K., Ni, L., Yang, T., Marton, R.M., Paşca, S.P., et al. (2019). Loss of Adaptive Myelination Contributes to Methotrexate Chemotherapy-Related Cognitive Impairment. Neuron *103*, 250-265.e8.

Gibson, E.M., Purger, D., Mount, C.W., Goldstein, A.K., Lin, G.L., Wood, L.S., Inema, I., Miller, S.E., Bieri, G., Zuchero, B.J., et al. (2014). Neuronal Activity Promotes Oligodendrogenesis and Adaptive Myelination in the Mammalian Brain. Science *344*, 1252304.

Gielen, E., Baron, W., Vandeven, M., Steels, P., Hoekstra, D., and Ameloot, M. (2006). Rafts in oligodendrocytes: Evidence and structure–function relationship. Glia *54*, 499–512.

Giese, K.P., Fedorov, N.B., Filipkowski, R.K., and Silva, A.J. (1998). Autophosphorylation at Thr286 of the α Calcium-Calmodulin Kinase II in LTP and Learning. Science *279*, 870–873.

Goebbels, S., Oltrogge, J.H., Kemper, R., Heilmann, I., Bormuth, I., Wolfer, S., Wichert, S.P., Möbius, W., Liu, X., Lappe-Siefke, C., et al. (2010). Elevated Phosphatidylinositol 3,4,5-Trisphosphate in Glia Triggers Cell-Autonomous Membrane Wrapping and Myelination. J Neurosci *30*, 8953–8964.

Goebbels, S., Wieser, G.L., Pieper, A., Spitzer, S., Weege, B., Yan, K., Edgar, J.M., Yagensky, O., Wichert, S.P., Agarwal, A., et al. (2016). A neuronal PI(3,4,5)P3-dependent program of oligodendrocyte precursor recruitment and myelination. Nat Neurosci *20*, 10–15.

Gokhan, S., Marin-Husstege, M., Yung, S.Y., Fontanez, D., Casaccia-Bonnefil, P., and Mehler, M.F. (2005). Combinatorial Profiles of Oligodendrocyte-Selective Classes of Transcriptional Regulators Differentially Modulate Myelin Basic Protein Gene Expression. J Neurosci *25*, 8311–8321.

Gomez, J.L., Bonaventura, J., Lesniak, W., Mathews, W.B., Sysa-Shah, P., Rodriguez, L.A., Ellis, R.J., Richie, C.T., Harvey, B.K., Dannals, R.F., et al. (2017a). Chemogenetics revealed: DREADD occupancy and activation via converted clozapine. Science *357*, 503–507.

Gomez, J.L., Bonaventura, J., Lesniak, W., Mathews, W.B., Sysa-Shah, P., Rodriguez, L.A., Ellis, R.J., Richie, C.T., Harvey, B.K., Dannals, R.F., et al. (2017b). Chemogenetics revealed: DREADD occupancy and activation via converted clozapine. *357*.

Gonsalvez, D., Ferner, A.H., Peckham, H., Murray, S.S., and Xiao, J. (2016). The roles of extracellular related-kinases 1 and 2 signaling in CNS myelination. Neuropharmacology *110*, 586–593.

Gonzalez, G.A., Hofer, M.P., Syed, Y.A., Amaral, A.I., Rundle, J., Rahman, S., Zhao, C., and Kotter, M.R.N. (2016). Tamoxifen accelerates the repair of demyelinated lesions in the central nervous system. Sci Rep-Uk *6*, 31599.

Gow, A., Southwood, C.M., Li, J., Pariali, M., Riordan, G.P., Brodie, S.E., Danias, J., Bronstein, J.M., Kachar, B., and Lazzarini, R.A. (1999). CNS Myelin and Sertoli Cell Tight Junction Strands Are Absent in Osp/Claudin-11 Null Mice. Cell *99*, 649–659.

Griffiths, I., Klugmann, M., Anderson, T., Yool, D., Thomson, C., Schwab, M.H., Schneider, A., Zimmermann, F., McCulloch, M., Nadon, N., et al. (1998). Axonal Swellings and Degeneration in Mice Lacking the Major Proteolipid of Myelin. Science *280*, 1610–1613.

Guardiola-Diaz, H.M., Ishii, A., and Bansal, R. (2012). Erk1/2 MAPK and mTOR signaling sequentially regulates progression through distinct stages of oligodendrocyte differentiation. Glia *60*, 476–486.

Gyllensten, L., and Malmfors, T. (1963). Myelinization of the optic nerve and its dependence on visual function--a quantitative investigation in mice. J Embryol Exp Morph *11*, 255–266.

Hamilton, N.B., Clarke, L.E., Arancibia-Carcamo, L.I., Kougioumtzidou, E., Matthey, M., Káradóttir, R., Whiteley, L., Bergersen, L.H., Richardson, W.D., and Attwell, D. (2017). Endogenous GABA controls oligodendrocyte lineage cell number, myelination, and CNS internode length. Glia *65*, 309–321.

Harrington, E.P., Zhao, C., Fancy, S.P.J., Kaing, S., Franklin, R.J.M., and Rowitch, D.H. (2010). Oligodendrocyte PTEN is required for myelin and axonal integrity, not remyelination. Ann Neurol *68*, 703–716.

Harris, J.J., and Attwell, D. (2012). The energetics of CNS white matter. J Neurosci Official J Soc Neurosci *32*, 356–371.

Hartline, D.K., and Colman, D.R. (2007). Rapid Conduction and the Evolution of Giant Axons and Myelinated Fibers. Current Biology *17*, R29–R35.

Hayashi, C., Suzuki, N., Takahashi, R., and Akazawa, C. (2020). Development of type I/II oligodendrocytes regulated by teneurin-4 in the murine spinal cord. Sci Rep-Uk *10*, 8611.

Hayashi, K., Suzuki, K., and Shirao, T. (1998). Rapid conversion of drebrin isoforms during synapse formation in primary culture of cortical neurons. Dev Brain Res *111*, 137–141.

He, L., Vanlandewijck, M., Raschperger, E., Mäe, M.A., Jung, B., Lebouvier, T., Ando, K., Hofmann, J., Keller, A., and Betsholtz, C. (2016). Analysis of the brain mural cell transcriptome. Sci Rep-Uk *6*, 35108.

Heiman, M., Schaefer, A., Gong, S., Peterson, J.D., Day, M., Ramsey, K.E., Suárez-Fariñas, M., Schwarz, C., Stephan, D.A., Surmeier, D.J., et al. (2008). A translational profiling approach for the molecular characterization of CNS cell types. Cell *135*, 738–748.

Heyn, P., Abreu, B.C., and Ottenbacher, K.J. (2004). The effects of exercise training on elderly persons with cognitive impairment and dementia: A meta-analysis1 1No commercial party having a direct financial interest in the results of the research supporting this article has or will confer a benefit upon the author(s) or upon any organization with which the author(s) is/are associated. Arch Phys Med Rehab *85*, 1694–1704.

Hill, R.A., Patel, K.D., Goncalves, C.M., Grutzendler, J., and Nishiyama, A. (2014). Modulation of oligodendrocyte generation during a critical temporal window after NG2 cell division. Nature Neuroscience *17*, nn.3815.

Hill, R.A., Li, A.M., and Grutzendler, J. (2018). Lifelong cortical myelin plasticity and age-related degeneration in the live mammalian brain. Nat Neurosci *21*, 683–695.

Hines, J., Ravanelli, A., Schwindt, R., Scott, E., and Appel, B. (2015). Neuronal activity biases axon selection for myelination in vivo. *18*.

Hirahara, Y., Bansal, R., Honke, K., Ikenaka, K., and Wada, Y. (2004). Sulfatide is a negative regulator of oligodendrocyte differentiation: Development in sulfatide-null mice. Glia *45*, 269–277.

Hodgkin, A.L. (1954). A note on conduction velocity. J Physiology *125*, 221–224.

Hoppenrath, K., Härtig, W., and Funke, K. (2016). Intermittent Theta-Burst Transcranial Magnetic Stimulation Alters Electrical Properties of Fast-Spiking Neocortical Interneurons in an Age-Dependent Fashion. Front Neural Circuit *10*, 22.

Hornig, J., Fröb, F., Vogl, M.R., Hermans-Borgmeyer, I., Tamm, E.R., and Wegner, M. (2013). The transcription factors Sox10 and Myrf define an essential regulatory network module in differentiating oligodendrocytes. Plos Genet *9*, e1003907.

Howng, S.B., Avila, R.L., Emery, B., Traka, M., Lin, W., Watkins, T., Cook, S., Bronson, R., Davisson, M., Barres, B.A., et al. (2010). ZFP191 is required by oligodendrocytes for CNS myelination. Genes & Development *24*, 301–311.

Hoz, L. de, and Simons, M. (2015). The emerging functions of oligodendrocytes in regulating neuronal network behaviour. Bioessays *37*, 60–69.

Huang, C.Y.-M., Zhang, C., Zollinger, D.R., Leterrier, C., and Rasband, M.N. (2017). An αII Spectrin-Based Cytoskeleton Protects Large-Diameter Myelinated Axons from Degeneration. J Neurosci *37*, 11323–11334.

Huang, J., Vogel, G., Yu, Z., Almazan, G., and Richard, S. (2011). Type II arginine methyltransferase PRMT5 regulates gene expression of inhibitors of differentiation/DNA binding Id2 and Id4 during glial cell differentiation. J Biological Chem *286*, 44424–44432.

Hughes, A.N., and Appel, B. (2019). Oligodendrocytes express synaptic proteins that modulate myelin sheath formation. Nat Commun *10*, 4125.

Hughes, E., Kang, S., Fukaya, M., and neuroscience, B.-D. (2013). Oligodendrocyte progenitors balance growth with self-repulsion to achieve homeostasis in the adult brain.

Hughes, E.G., Orthmann-Murphy, J.L., Langseth, A.J., and Bergles, D.E. (2018). Myelin remodeling through experience-dependent oligodendrogenesis in the adult somatosensory cortex. Nature Neuroscience *21*, 696–706.

Hulst, H.E., Goldschmidt, T., Nitsche, M.A., Wit, S.J. de, Heuvel, O.A. van den, Barkhof, F., Paulus, W., Werf, Y.D. van der, and Geurts, J.J.G. (2017). rTMS affects working memory performance, brain activation and functional connectivity in patients with multiple sclerosis. J Neurology Neurosurg Psychiatry *88*, 386.

Ikeda, Y., Dick, K.A., Weatherspoon, M.R., Gincel, D., Armbrust, K.R., Dalton, J.C., Stevanin, G., Dürr, A., Zühlke, C., Bürk, K., et al. (2006). Spectrin mutations cause spinocerebellar ataxia type 5. Nat Genet *38*, 184–190.

Ilg, A.-K., Enkel, T., Bartsch, D., and Bähner, F. (2018). Behavioral Effects of Acute Systemic Low-Dose Clozapine in Wild-Type Rats: Implications for the Use of DREADDs in Behavioral Neuroscience. Front Behav Neurosci *12*, 173.

Ingolia, N.T., Ghaemmaghami, S., Newman, J.R.S., and Weissman, J.S. (2009). Genome-Wide Analysis in Vivo of Translation with Nucleotide Resolution Using Ribosome Profiling. Science *324*, 218–223.

Ishii, A., Dutta, R., Wark, G.M., Hwang, S.-I., Han, D.K., Trapp, B.D., Pfeiffer, S.E., and Bansal, R. (2009). Human myelin proteome and comparative analysis with mouse myelin. Proceedings of the National Academy of Sciences *106*, 14605–14610.

Ishii, A., Fyffe-Maricich, S.L., Furusho, M., Miller, R.H., and Bansal, R. (2012). ERK1/ERK2 MAPK signaling is required to increase myelin thickness independent of oligodendrocyte differentiation and initiation of myelination. J Neurosci Official J Soc Neurosci *32*, 8855–8864.

Ishii, A., Furusho, M., and Bansal, R. (2013). Sustained activation of ERK1/2 MAPK in oligodendrocytes and schwann cells enhances myelin growth and stimulates oligodendrocyte progenitor expansion. J Neurosci Official J Soc Neurosci *33*, 175–186.

Ishikawa, R., Hayashi, K., Shirao, T., Xue, Y., Takagi, T., Sasaki, Y., and Kohama, K. (1994). Drebrin, a development-associated brain protein from rat embryo, causes the dissociation of tropomyosin from actin filaments. J Biological Chem *269*, 29928–29933.

Jabs, R., Pivneva, T., Hüttmann, K., Wyczynski, A., Nolte, C., Kettenmann, H., and Steinhäuser, C. (2005). Synaptic transmission onto hippocampal glial cells with hGFAP promoter activity. J Cell Sci *118*, 3791–3803.

Jäkel, S., Agirre, E., Falcão, A.M., Bruggen, D. van, Lee, K.W., Knuesel, I., Malhotra, D., Ffrench-Constant, C., Williams, A., and Castelo-Branco, G. (2019). Altered human oligodendrocyte heterogeneity in multiple sclerosis. Nature *566*, 543–547.

Jarjour, A.A., Manitt, C., Moore, S.W., Thompson, K.M., Yuh, S.-J., and Kennedy, T.E. (2003). Netrin-1 Is a Chemorepellent for Oligodendrocyte Precursor Cells in the Embryonic Spinal Cord. J Neurosci *23*, 3735–3744.

Jin, H.Y., and Xiao, C. (2017). Next Generation Sequencing, Methods and Protocols. Methods Mol Biology Clifton N J *1712*, 1–18.

Kalani, M.Y.S., Cheshier, S.H., Cord, B.J., Bababeygy, S.R., Vogel, H., Weissman, I.L., Palmer, T.D., and Nusse, R. (2008). Wnt-mediated self-renewal of neural stem/progenitor cells. P Natl Acad Sci Usa *105*, 16970–16975.

Kassmann, C.M., Lappe-Siefke, C., Baes, M., Brügger, B., Mildner, A., Werner, H.B., Natt, O., Michaelis, T., Prinz, M., Frahm, J., et al. (2007). Axonal loss and neuroinflammation caused by peroxisome-deficient oligodendrocytes. Nat Genet *39*, 969–976.

Katsel, P., Roussos, P., Fam, P., Khan, S., Tan, W., Hirose, T., Nakagawa, S., Pletnikov, M.V., and Haroutunian, V. (2019). The expression of long noncoding RNA NEAT1 is reduced in schizophrenia and modulates oligodendrocytes transcription. Npj Schizophrenia *5*, 3.

Keiner, S., Niv, F., Neumann, S., Steinbach, T., Schmeer, C., Hornung, K., Schlenker, Y., Förster, M., Witte, O.W., and Redecker, C. (2017). Effect of skilled reaching training and enriched environment on generation of oligodendrocytes in the adult sensorimotor cortex and corpus callosum. BMC Neuroscience *18*, 31.

Kessaris, N., Fogarty, M., Iannarelli, P., Grist, M., Wegner, M., and Richardson, W.D. (2005). Competing waves of oligodendrocytes in the forebrain and postnatal elimination of an embryonic lineage. Nat Neurosci *9*, 173–179.

Khalil, H., Quinn, L., Deursen, R. van, Dawes, H., Playle, R., Rosser, A., and Busse, M. (2012). What effect does a structured home-based exercise programme have on people with Huntington's disease? A randomized, controlled pilot study. Clin Rehabil *27*, 646–658.

Kimmel, C.B., Ballard, W.W., Kimmel, S.R., Ullmann, B., and Schilling, T.F. (1995). Stages of embryonic development of the zebrafish. Dev Dynam *203*, 253–310.

Kirby, B.B., Takada, N., Latimer, A.J., Shin, J., Carney, T.J., Kelsh, R.N., and Appel, B. (2006). In vivo time-lapse imaging shows dynamic oligodendrocyte progenitor behavior during zebrafish development. Nature Neuroscience *9*, 1506–1511.

Kislinger, T., Cox, B., Kannan, A., Chung, C., Hu, P., Ignatchenko, A., Scott, M.S., Gramolini, A.O., Morris, Q., Hallett, M.T., et al. (2006). Global Survey of Organ and Organelle Protein Expression in Mouse: Combined Proteomic and Transcriptomic Profiling. Cell *125*, 173–186.

Klugmann, M., Schwab, M.H., Pühlhofer, A., Schneider, A., Zimmermann, F., Griffiths, I.R., and Nave, K.-A. (1997). Assembly of CNS Myelin in the Absence of Proteolipid Protein. Neuron *18*, 59–70.

Knapp, P.E., Bartlett, W.P., and Skoff, R.P. (1987). Cultured oligodendrocytes mimic in vivo phenotypic characteristics: Cell shape, expression of myelin-specific antigens, and membrane production. Dev Biol *120*, 356–365.

Koenning, M., Jackson, S., Hay, C.M., Faux, C., Kilpatrick, T.J., Willingham, M., and Emery, B. (2012). Myelin gene regulatory factor is required for maintenance of myelin and mature oligodendrocyte identity in the adult CNS. J Neurosci Official J Soc Neurosci *32*, 12528–12542.

Kool, M.J., Onori, M.P., Borgesius, N.Z., Bree, J.E. van de, Elgersma-Hooisma, M., Nio, E., Bezstarosti, K., Buitendijk, G.H.S., Jolfaei, M.A., Demmers, J.A.A., et al. (2019). CAMK2-dependent signaling in neurons is essential for survival. J Neurosci Official J Soc Neurosci *39*, 5424–5439.

Kornfeld, S.F., Cummings, S.E., Fathi, S., Bonin, S.R., and Kothary, R. (2020). MiRNA-145-5p prevents differentiation of oligodendrocyte progenitor cells by regulating expression of myelin gene regulatory factor. J Cell Physiol.

Koudelka, S., Voas, M.G., Almeida, R.G., Baraban, M., Soetaert, J., Meyer, M.P., Talbot, W.S., and Lyons, D.A. (2016). Individual Neuronal Subtypes Exhibit Diversity in CNS Myelination Mediated by Synaptic Vesicle Release. *26*.

Kougioumtzidou, E., Shimizu, T., Hamilton, N.B., Tohyama, K., Sprengel, R., Monyer, H., Attwell, D., and Richardson, W.D. (2017). Signalling through AMPA receptors on

oligodendrocyte precursors promotes myelination by enhancing oligodendrocyte survival. Elife *6*, e28080.

Krämer, E., Schardt, A., and Nave, K. (2001). Membrane traffic in myelinating oligodendrocytes. Microscopy Research and Technique *52*, 656–671.

Krasnow, A.M., Ford, M.C., Valdivia, L.E., Wilson, S.W., and Attwell, D. (2018). Regulation of developing myelin sheath elongation by oligodendrocyte calcium transients in vivo. Nature Neuroscience *21*, 24–28.

Kukley, M., Capetillo-Zarate, E., and Dietrich, D. (2007). Vesicular glutamate release from axons in white matter. Nat Neurosci *10*, 311–320.

Kukley, M., Kiladze, M., Tognatta, R., Hans, M., Swandulla, D., Schramm, J., and Dietrich, D. (2008). Glial cells are born with synapses. Faseb J *22*, 2957–2969.

Kukley, M., Nishiyama, A., and Dietrich, D. (2010). The fate of synaptic input to NG2 glial cells: neurons specifically downregulate transmitter release onto differentiating oligodendroglial cells. *30*.

Küry, S., Woerden, G.M. van, Besnard, T., Onori, M.P., Latypova, X., Towne, M.C., Cho, M.T., Prescott, T.E., Ploeg, M.A., Sanders, S., et al. (2017). De Novo Mutations in Protein Kinase Genes CAMK2A and CAMK2B Cause Intellectual Disability. Am J Hum Genetics *101*, 768–788.

Labun, K., Montague, T.G., Gagnon, J.A., Thyme, S.B., and Valen, E. (2016). CHOPCHOP v2: a web tool for the next generation of CRISPR genome engineering. Nucleic Acids Res *44*, W272–W276.

Labun, K., Montague, T.G., Krause, M., Torres Cleuren, Y.N., Tjeldnes, H., and Valen, E. (2019). CHOPCHOP v3: expanding the CRISPR web toolbox beyond genome editing. Nucleic Acids Res *47*, W171–W174.

Lang, J., Maeda, Y., Bannerman, P., Xu, J., Horiuchi, M., Pleasure, D., and Guo, F. (2013). Adenomatous polyposis coli regulates oligodendroglial development. J Neurosci Official J Soc Neurosci *33*, 3113–3130.

Langseth, A.J., Munji, R.N., Choe, Y., Huynh, T., Pozniak, C.D., and Pleasure, S.J. (2010). Wnts influence the timing and efficiency of oligodendrocyte precursor cell generation in the telencephalon. J Neurosci Official J Soc Neurosci *30*, 13367–13372.

Lappe-Siefke, C., Goebbels, S., Gravel, M., Nicksch, E., Lee, J., Braun, P.E., Griffiths, I.R., and Nave, K.-A. (2003). Disruption of Cnp1 uncouples oligodendroglial functions in axonal support and myelination. Nat Genet *33*, 366–374.

Leal, G., Afonso, P.M., Salazar, I.L., and Duarte, C.B. (2015). Regulation of hippocampal synaptic plasticity by BDNF. Brain Res *1621*, 82–101.

Lebrun-Julien, F., Bachmann, L., and of …, N.C. (2014). Balanced mTORC1 activity in oligodendrocytes is required for accurate CNS myelination.

Lee, J., Duan, W., Long, J.M., Ingram, D.K., and Mattson, M.P. (2000). Dietary restriction increases the number of newly generated neural cells, and induces BDNF expression, in the dentate gyrus of rats. J Mol Neurosci *15*, 99–108.

Lee, S., Leach, M.K., Redmond, S.A., Chong, S.Y.C., Mellon, S.H., Tuck, S.J., Feng, Z.-Q., Corey, J.M., and Chan, J.R. (2012a). A culture system to study oligodendrocyte myelination processes using engineered nanofibers. Nat Methods *9*, 917–922.

Lee, S., Chong, S.Y.C., Tuck, S.J., Corey, J.M., and Chan, J.R. (2013). A rapid and reproducible assay for modeling myelination by oligodendrocytes using engineered nanofibers. Nat Protoc *8*, 771–782.

Lee, Y., Morrison, B.M., Li, Y., Lengacher, S., Farah, M.H., Hoffman, P.N., Liu, Y., Tsingalia, A., Jin, L., Zhang, P.-W., et al. (2012b). Oligodendroglia metabolically support axons and contribute to neurodegeneration. Nature *487*, 443.

Li, Q., Brus-Ramer, M., Martin, J., and McDonald, J. (2010). Electrical stimulation of the medullary pyramid promotes proliferation and differentiation of oligodendrocyte progenitor cells in the corticospinal tract of the adult rat. *479*.

Lin, S., and Bergles, D.E. (2003). Synaptic signaling between GABAergic interneurons and oligodendrocyte precursor cells in the hippocampus. Nat Neurosci *7*, 24–32.

Lin, S.-C., and Bergles, D.E. (2002). Physiological characteristics of NG2-expressing glial cells. J Neurocytol *31*, 537 ppl= – 549.

Lin, S., Huck, J.H.J., Roberts, J.D.B., Macklin, W.B., Somogyi, P., and Bergles, D.E. (2005). Climbing Fiber Innervation of NG2-Expressing Glia in the Mammalian Cerebellum. Neuron *46*, 773–785.

Lin, W.-J., Jiang, C., Sadahiro, M., Bozdagi, O., Vulchanova, L., Alberini, C.M., and Salton, S.R. (2015). VGF and Its C-Terminal Peptide TLQP-62 Regulate Memory Formation in Hippocampus via a BDNF-TrkB-Dependent Mechanism. The Journal of Neuroscience *35*, 10343–10356.

Liu, A., Li, J., Marin-Husstege, M., Kageyama, R., Fan, Y., Gelinas, C., and Casaccia-Bonnefil, P. (2006). A molecular insight of Hes5-dependent inhibition of myelin gene expression: old partners and new players. Embo J *25*, 4833–4842.

Liu, J., Dietz, K., DeLoyht, J.M., Pedre, X., Kelkar, D., Kaur, J., Vialou, V., Lobo, M., Dietz, D.M., Nestler, E.J., et al. (2012). Impaired adult myelination in the prefrontal cortex of socially isolated mice. Nature Neuroscience *15*, 1621.

Liu, Z., Hu, X., Cai, J., Liu, B., Peng, X., Wegner, M., and Qiu, M. (2007). Induction of oligodendrocyte differentiation by Olig2 and Sox10: Evidence for reciprocal interactions and dosage-dependent mechanisms. Dev Biol *302*, 683–693.

Logan, C.Y., and Nusse, R. (2004). THE WNT SIGNALING PATHWAY IN DEVELOPMENT AND DISEASE. Annu Rev Cell Dev Bi *20*, 781–810.

Lu, Q.R., Sun, T., Zhu, Z., Ma, N., Garcia, M., Stiles, C.D., and Rowitch, D.H. (2002). Common Developmental Requirement for Olig Function Indicates a Motor Neuron/Oligodendrocyte Connection. Cell *109*, 75–86.

Lundgaard, I., Luzhynskaya, A., Stockley, J., Wang, Z., Evans, K., Swire, M., Volbracht, K., Gautier, H., Franklin, R., ffrench-Constant, C., et al. (2013). Neuregulin and BDNF Induce a Switch to NMDA Receptor-Dependent Myelination by Oligodendrocytes. *11*.

Makinodan, M., Rosen, K.M., Ito, S., and Corfas, G. (2012). A Critical Period for Social Experience–Dependent Oligodendrocyte Maturation and Myelination. Science *337*, 1357–1360.

Makowiecki, K., Harvey, A.R., Sherrard, R.M., and Rodger, J. (2014). Low-Intensity Repetitive Transcranial Magnetic Stimulation Improves Abnormal Visual Cortical Circuit Topography and Upregulates BDNF in Mice. J Neurosci *34*, 10780–10792.

Marcus, J., and Popko, B. (2002). Galactolipids are molecular determinants of myelin development and axo–glial organization. Biochimica et Biophysica Acta (BBA) - General Subjects *1573*, 406–413.

Marques, S., Zeisel, A., Codeluppi, S., Bruggen, D. van, Falcão, A.M., Xiao, L., Li, H., Häring, M., Hochgerner, H., Romanov, R.A., et al. (2016). Oligodendrocyte heterogeneity in the mouse juvenile and adult central nervous system. Sci New York N Y *352*, 1326–1329.

Marques, S., Bruggen, D. van, and Castelo-Branco, G. (2019). Single-Cell RNA Sequencing of Oligodendrocyte Lineage Cells from the Mouse Central Nervous System. Methods Mol Biology Clifton N J *1936*, 1–21.

Matsumoto, S., Banine, F., Feistel, K., Foster, S., Xing, R., Struve, J., and Sherman, L.S. (2016). Brg1 directly regulates Olig2 transcription and is required for oligodendrocyte progenitor cell specification. Dev Biol *413*, 173–187.

Matthias, K., Kirchhoff, F., Seifert, G., Hüttmann, K., Matyash, M., Kettenmann, H., and Steinhäuser, C. (2003). Segregated Expression of AMPA-Type Glutamate Receptors and Glutamate Transporters Defines Distinct Astrocyte Populations in the Mouse Hippocampus. J Neurosci *23*, 1750–1758.

Mayford, M., Wang, J., Kandel, E.R., and O'Dell, T.J. (1995). CaMKII regulates the frequency-response function of hippocampal synapses for the production of both LTD and LTP. Cell *81*, 891–904.

Mayoral, S.R., Etxeberria, A., Shen, Y.-A.A., and Chan, J.R. (2018). Initiation of CNS Myelination in the Optic Nerve Is Dependent on Axon Caliber. Cell Reports *25*, 544-550.e3.

McKenzie, I.A., Ohayon, D., Li, H., Faria, J. de, Emery, B., Tohyama, K., and Richardson, W.D. (2014). Motor skill learning requires active central myelination. *346*.

Mei, F., Wang, H., Liu, S., Niu, J., Wang, L., He, Y., Etxeberria, A., Chan, J.R., and Xiao, L. (2013). Stage-specific deletion of Olig2 conveys opposing functions on differentiation and maturation of oligodendrocytes. J Neurosci Official J Soc Neurosci *33*, 8454–8462.

Mello, C.V., and Ribeiro, S. (1998). ZENK protein regulation by song in the brain of songbirds. J Comp Neurol *393*, 426–438.

Mensch, S., Baraban, M., Almeida, R., Czopka, T., Ausborn, J., Manira, A., and Lyons, D. (2015). Synaptic vesicle release regulates myelin sheath number of individual oligodendrocytes in vivo. *18*.

Mercer, T.R., Qureshi, I.A., Gokhan, S., Dinger, M.E., Li, G., Mattick, J.S., and Mehler, M.F. (2010). Long noncoding RNAs in neuronal-glial fate specification and oligodendrocyte lineage maturation. Bmc Neurosci *11*, 14.

Meyer, N., Richter, N., Fan, Z., Siemonsmeier, G., Pivneva, T., Jordan, P., Steinhäuser, C., Semtner, M., Nolte, C., and Kettenmann, H. (2018). Oligodendrocytes in the Mouse Corpus Callosum Maintain Axonal Function by Delivery of Glucose. Cell Reports *22*, 2383–2394.

Meyer-Franke, A., Kaplan, M.R., Pfieger, F.W., and Barres, B.A. (1995). Characterization of the signaling interactions that promote the survival and growth of developing retinal ganglion cells in culture. Neuron *15*, 805–819.

Michalski, J.-P., and Kothary, R. (2015). Oligodendrocytes in a Nutshell. Frontiers in Cellular Neuroscience *9*, 340.

Micheva, K.D., Wolman, D., Mensh, B.D., Pax, E., Buchanan, J., Smith, S.J., and Bock, D.D. (2016). A large fraction of neocortical myelin ensheathes axons of local inhibitory neurons. ELife *5*, e15784.

Micu, I., Jiang, Q., Coderre, E., Ridsdale, A., Zhang, L., Woulfe, J., Yin, X., Trapp, B.D., McRory, J.E., Rehak, R., et al. (2005). NMDA receptors mediate calcium accumulation in myelin during chemical ischaemia. Nature *439*, 988–992.

Micu, I., Plemel, J., Lachance, C., t, J., Jansen, A., Cummins, K., Minnen, J., and Stys, P. (2016). The molecular physiology of the axo-myelinic synapse. *276*.

Micu, I., Plemel, J.R., Caprariello, A.V., Nave, K.-A., and Stys, P.K. (2017). Axo-myelinic neurotransmission: a novel mode of cell signalling in the central nervous system. Nat Rev Neurosci *19*, 49–58.

Miller, R.H. (2002). Regulation of oligodendrocyte development in the vertebrate CNS. Prog Neurobiol *67*, 451–467.

Milner, R., Anderson, H.J., Rippon, R.F., McKay, J.S., Franklin, R.J.M., Marchionni, M.A., Reynolds, R., and Ffrench-Constant, C. (1997). Contrasting effects of mitogenic growth factors on oligodendrocyte precursor cell migration. Glia *19*, 85–90.

Mitew, S., Gobius, I., Fenlon, L.R., McDougall, S.J., Hawkes, D., Xing, Y.L., Bujalka, H., Gundlach, A.L., Richards, L.J., Kilpatrick, T.J., et al. (2018). Pharmacogenetic stimulation of neuronal activity increases myelination in an axon-specific manner. *9*.

Mizui, T., Takahashi, H., Sekino, Y., and Shirao, T. (2005). Overexpression of drebrin A in immature neurons induces the accumulation of F-actin and PSD-95 into dendritic filopodia, and the formation of large abnormal protrusions. Mol Cell Neurosci *30*, 149–157.

Mo, A., Mukamel, E.A., Davis, F.P., Luo, C., Henry, G.L., Picard, S., Urich, M.A., Nery, J.R., Sejnowski, T.J., Lister, R., et al. (2015). Epigenomic Signatures of Neuronal Diversity in the Mammalian Brain. Neuron *86*, 1369–1384.

Montague, T.G., Cruz, J.M., Gagnon, J.A., Church, G.M., and Valen, E. (2014). CHOPCHOP: a CRISPR/Cas9 and TALEN web tool for genome editing. Nucleic Acids Res *42*, W401–W407.

Moore, J.W., Joyner, R.W., Brill, M.H., Waxman, S.D., and Najar-Joa, M. (1978). Simulations of conduction in uniform myelinated fibers. Relative sensitivity to changes in nodal and internodal parameters. Biophys J *21*, 147–160.

Mori, F., Ljoka, C., Magni, E., Codecà, C., Kusayanagi, H., Monteleone, F., Sancesario, A., Bernardi, G., Koch, G., Foti, C., et al. (2011). Transcranial magnetic stimulation primes the effects of exercise therapy in multiple sclerosis. J Neurol *258*, 1281–1287.

Moyon, S., Huynh, J.L., Dutta, D., Zhang, F., Ma, D., Yoo, S., Lawrence, R., Wegner, M., John, G.R., Emery, B., et al. (2016). Functional Characterization of DNA Methylation in the Oligodendrocyte Lineage. Cell Reports *15*, 748–760.

Müller, M.B., Toschi, N., Kresse, A.E., Post, A., and Keck, M.E. (2000). Long-Term Repetitive Transcranial Magnetic Stimulation Increases the Expression of Brain-Derived Neurotrophic Factor and Cholecystokinin mRNA, but not Neuropeptide Tyrosine mRNA in Specific Areas of Rat Brain. Neuropsychopharmacol *23*, 205–215.

Müller-Dahlhaus, F., and Vlachos, A. (2013). Unraveling the cellular and molecular mechanisms of repetitive magnetic stimulation. Front Mol Neurosci *6*, 50.

Nagaraj, N., Wisniewski, J.R., Geiger, T., Cox, J., Kircher, M., Kelso, J., Pääbo, S., and Mann, M. (2011). Deep proteome and transcriptome mapping of a human cancer cell line. Mol Syst Biol *7*, 548.

Nagy, B., Hovhannisyan, A., Barzan, R., Chen, T.-J., and Kukley, M. (2017). Different patterns of neuronal activity trigger distinct responses of oligodendrocyte precursor cells in the corpus callosum. PLOS Biology *15*, e2001993.

Nait-Oumesmar, B., Picard-Riera, N., Kerninon, C., Decker, L., Seilhean, D., Höglinger, G.U., Hirsch, E.C., Reynolds, R., and Evercooren, A.B.-V. (2007). Activation of the subventricular zone in multiple sclerosis: Evidence for early glial progenitors. Proc National Acad Sci *104*, 4694–4699.

Nakagawa, T., Sasahara, M., Hayase, Y., Haneda, M., Yasuda, H., Kikkawa, R., Higashiyama, S., and Hazama, F. (1998). Neuronal and glial expression of heparin-binding EGF-like growth factor in central nervous system of prenatal and early postnatal rat. Dev Brain Res *108*, 263–272.

Nakatani, H., Martin, E., Hassani, H., Clavairoly, A., Maire, C.L., Viadieu, A., Kerninon, C., Delmasure, A., Frah, M., Weber, M., et al. (2013). Ascl1/Mash1 Promotes Brain Oligodendrogenesis during Myelination and Remyelination. J Neurosci *33*, 9752–9768.

Narayanan, S., Flores, A., and of …, W.F. (2009). Akt signals through the mammalian target of rapamycin pathway to regulate CNS myelination.

Narducci, R., Baroncelli, L., Sansevero, G., Begenisic, T., Prontera, C., Sale, A., Cenni, M.C., Berardi, N., and Maffei, L. (2018). Early impoverished environment delays the maturation of cerebral cortex. Sci Rep-Uk *8*, 1187.

Nave, K.-A. (2010). Myelination and the trophic support of long axons. Nature Reviews Neuroscience *11*, 275.

Nawaz, S., Sánchez, P., Schmitt, S., Snaidero, N., Mitkovski, M., Velte, C., Brückner, B.R., Alexopoulos, I., Czopka, T., Jung, S.Y., et al. (2015). Actin Filament Turnover Drives Leading Edge Growth during Myelin Sheath Formation in the Central Nervous System. Developmental Cell *34*, 139–151.

Nelson, J.W., Sklenar, J., Barnes, A.P., and Minnier, J. (2016). The START App: A Web-Based RNAseq Analysis and Visualization Resource. Bioinform Oxf Engl.

Nielsen, J.F., Sinkjaer, T., and Jakobsen, J. (1996). Treatment of spasticity with repetitive magnetic stimulation; a double-blind placebo-controlled study. Mult Scler *2*, 227–232.

Novitch, B.G., Chen, A.I., and Jessell, T.M. (2001). Coordinate Regulation of Motor Neuron Subtype Identity and Pan-Neuronal Properties by the bHLH Repressor Olig2. Neuron *31*, 773–789.

Oladehin, A., and Waters, R.S. (2001). Location and distribution of Fos protein expression in rat hippocampus following acute moderate aerobic exercise. Exp Brain Res *137*, 26–35.

Olivares, R., Montiel, J., and Aboitiz, F. (2001). Species Differences and Similarities in the Fine Structure of the Mammalian Corpus callosum. Brain Behav Evol *57*, 98–105.

Orduz, D., Maldonado, P.P., Balia, M., Vélez-Fort, M., Sars, V. de, Yanagawa, Y., Emiliani, V., and Angulo, M. (2015). Interneurons and oligodendrocyte progenitors form a structured synaptic network in the developing neocortex. ELife *4*, e06953.

Ortega, F., Gascón, S., Masserdotti, G., Deshpande, A., Simon, C., Fischer, J., Dimou, L., Lie, D.C., Schroeder, T., and Berninger, B. (2013). Oligodendrogliogenic and neurogenic adult subependymal zone neural stem cells constitute distinct lineages and exhibit differential responsiveness to Wnt signalling. Nat Cell Biol *15*, 602–613.

Ortiz, F.C., Habermacher, C., Graciarena, M., Houry, P.-Y., Nishiyama, A., Nait-Oumesmar, B., and Angulo, M. (2019). Neuronal activity in vivo enhances functional myelin repair. JCI Insight.

Ozgen, H., Baron, W., Hoekstra, D., and Kahya, N. (2016). Oligodendroglial membrane dynamics in relation to myelin biogenesis. Cellular and Molecular Life Sciences *73*, 3291–3310.

Pajevic, S., Basser, P.J., and Fields, R.D. (2013). Role of myelin plasticity in oscillations and synchrony of neuronal activity. Neuroscience *276*, 135–147.

Paula, M.L., Cui, Q., Hossain, S., Antel, J., and Almazan, G. (2014). The PTEN inhibitor bisperoxovanadium enhances myelination by amplifying IGF-1 signaling in rat and human oligodendrocyte progenitors. Glia *62*, 64–77.

Peckham, H., Giuffrida, L., Wood, R., Gonsalvez, D., Ferner, A., Kilpatrick, T.J., Murray, S.S., and Xiao, J. (2015). Fyn is an intermediate kinase that BDNF utilizes to promote oligodendrocyte myelination. Glia *64*, 255–269.

Pencea, V., Bingaman, K.D., Wiegand, S.J., and Luskin, M.B. (2001). Infusion of Brain-Derived Neurotrophic Factor into the Lateral Ventricle of the Adult Rat Leads to New Neurons in the Parenchyma of the Striatum, Septum, Thalamus, and Hypothalamus. J Neurosci *21*, 6706–6717.

Perge, J.A., Niven, J.E., Mugnaini, E., Balasubramanian, V., and Sterling, P. (2012). Why Do Axons Differ in Caliber? The Journal of Neuroscience *32*, 626–638.

Perkins, E., Suminaite, D., and Jackson, M. (2016). Cerebellar ataxias: β-III spectrin's interactions suggest common pathogenic pathways. J Physiology *594*, 4661–4676.

Perlman, K., Couturier, C.P., Yaqubi, M., Tanti, A., Cui, Q.-L., Pernin, F., Stratton, J.A., Ragoussis, J., Healy, L., Petrecca, K., et al. (2020). Developmental trajectory of oligodendrocyte progenitor cells in the human brain revealed by single cell RNA sequencing. Glia *68*, 1291–1303.

Pierre, K., Pellerin, L., Debernardi, R., Riederer, B.M., and Magistretti, P.J. (2000). Cell-specific localization of monocarboxylate transporters, MCT1 and MCT2, in the adult mouse brain revealed by double immunohistochemical labeling and confocal microscopy. Neuroscience *100*, 617–627.

Pol, S.U., Polanco, J.J., Seidman, R.A., O'Bara, M.A., Shayya, H.J., Dietz, K.C., and Sim, F.J. (2017). Network-Based Genomic Analysis of Human Oligodendrocyte Progenitor Differentiation. Stem Cell Reports *9*, 710–723.

Praag, H. van, Kempermann, G., and Gage, F.H. (1999). Running increases cell proliferation and neurogenesis in the adult mouse dentate gyrus. Nat Neurosci *2*, 266–270.

Praag, H. van, Shubert, T., Zhao, C., and Gage, F.H. (2005). Exercise Enhances Learning and Hippocampal Neurogenesis in Aged Mice. J Neurosci *25*, 8680–8685.

PRESTOZ, L., CHATZOPOULOU, E., LEMKINE, G., SPASSKY, N., LEBRAS, B., KAGAWA, T., IKENAKA, K., ZALC, B., and THOMAS, J.-L. (2004). Control of axonophilic migration of oligodendrocyte precursor cells by Eph–ephrin interaction. Neuron Glia Biol *1*, 73–83.

Qi, Y., Cai, J., Wu, Y., Wu, R., Lee, J., Fu, H., Rao, M., Sussel, L., Rubenstein, J., and Qiu, M. (2001). Control of oligodendrocyte differentiation by the Nkx2.2 homeodomain transcription factor. Development (Cambridge, England) *128*, 2723–2733.

Rafiki, A., Boulland, J.L., Halestrap, A.P., Ottersen, O.P., and Bergersen, L. (2003). Highly differential expression of the monocarboxylate transporters MCT2 and MCT4 in the developing rat brain. Neuroscience *122*, 677–688.

Raman, M., Chen, W., and Cobb, M.H. (2007). Differential regulation and properties of MAPKs. Oncogene *26*, 3100–3112.

Ransom, B.R., Yamate, C.L., Black, J.A., and Waxman, S.G. (1985). Rat optic nerve: Disruption of gliogenesis with 5-azacytidine during early postnatal development. Brain Res *337*, 41–49.

Readhead, C., Popko, B., Takahashi, N., Shine, D.H., Saavedra, R.A., Sidman, R.L., and Hood, L. (1987). Expression of a myelin basic protein gene in transgenic shiverer mice: Correction of the dysmyelinating phenotype. Cell *48*, 703–712.

Reddy, A.S., O'Brien, D., Pisat, N., Weichselbaum, C.T., Sakers, K., Lisci, M., Dalal, J.S., and Dougherty, J.D. (2017). A Comprehensive Analysis of Cell Type–Specific Nuclear RNA From Neurons and Glia of the Brain. Biological Psychiatry *81*.

Rhodes, J.S., Praag, H. van, Jeffrey, S., Girard, I., Mitchell, G.S., Garland, T., and Gage, F.H. (2003). Exercise Increases Hippocampal Neurogenesis to High Levels but Does Not Improve Spatial Learning in Mice Bred for Increased Voluntary Wheel Running. Behav Neurosci *117*, 1006–1016.

Richardson, W.D., Kessaris, N., and Pringle, N. (2006). Oligodendrocyte wars. Nature Reviews Neuroscience *7*, 11–18.

Roach, A., Boylan, K., Horvath, S., Prusiner, S., Hood, L., Roach, A., Boylan, K., Horvath, S., Prusiner, S., and Hood, L. (1983). Characterization of cloned cDNA representing rat myelin basic protein: Absence of expression in brain of shiverer mutant mice. Cell.

Roch, K.G.L., Johnson, J.R., Florens, L., Zhou, Y., Santrosyan, A., Grainger, M., Yan, S.F., Williamson, K.C., Holder, A.A., Carucci, D.J., et al. (2004). Global analysis of transcript and protein levels across the Plasmodium falciparum life cycle. Genome Res *14*, 2308–2318.

Rosenberg, S.S., Kelland, E.E., Tokar, E., Torre, A.R.D. la, and Chan, J.R. (2008). The geometric and spatial constraints of the microenvironment induce oligodendrocyte differentiation. P Natl Acad Sci Usa *105*, 14662–14667.

Saab, A.S., and Nave, K.-A. (2017). Myelin dynamics: protecting and shaping neuronal functions. Current Opinion in Neurobiology *47*, 104–112.

Saab, A.S., Tzvetanova, I.D., and Nave, K.-A. (2013). The role of myelin and oligodendrocytes in axonal energy metabolism. *23*.

Saab, A.S., Tzvetavona, I.D., Trevisiol, A., Baltan, S., Dibaj, P., Kusch, K., Möbius, W., Goetze, B., Jahn, H.M., Huang, W., et al. (2016). Oligodendroglial NMDA Receptors Regulate Glucose Import and Axonal Energy Metabolism. *91*.

Salami, M., Itami, C., Tsumoto, T., and Kimura, F. (2003). Change of conduction velocity by regional myelination yields constant latency irrespective of distance between thalamus and cortex. Proc National Acad Sci *100*, 6174–6179.

Samanta, J., and Kessler, J.A. (2004). Interactions between ID and OLIG proteins mediate the inhibitory effects of BMP4 on oligodendroglial differentiation. Development *131*, 4131–4142.

Sanz, E., Yang, L., Su, T., Morris, D.R., McKnight, G.S., and Amieux, P.S. (2009a). Cell-type-specific isolation of ribosome-associated mRNA from complex tissues. P Natl Acad Sci Usa *106*, 13939–13944.

Sanz, E., Yang, L., Su, T., Morris, D.R., McKnight, G.S., and Amieux, P.S. (2009b). Cell-type-specific isolation of ribosome-associated mRNA from complex tissues.pdf. PNAS.

Sanz, E., Bean, J.C., Carey, D.P., Quintana, A., and McKnight, G.S. (2019). RiboTag: Ribosomal Tagging Strategy to Analyze Cell-Type-Specific mRNA Expression In Vivo. Curr Protoc Neurosci *88*, e77.

Schirmer, L., Velmeshev, D., Holmqvist, S., Kaufmann, M., Werneburg, S., Jung, D., Vistnes, S., Stockley, J.H., Young, A., Steindel, M., et al. (2019). Neuronal vulnerability and multilineage diversity in multiple sclerosis. Nature *573*, 75–82.

Schnädelbach, O., Özen, Í., Blaschuk, O.W., Gour, B.J., Meyer, R.L., and Fawcett, J.W. (2001). N-Cadherin Is Involved in Axon-Oligodendrocyte Contact and Myelination. Mol Cell Neurosci *17*, 1084–1093.

Scholz, J., Klein, M.C., Behrens, T.E.J., and Johansen-Berg, H. (2009). Training induces changes in white-matter architecture. Nat Neurosci *12*, 1370–1371.

Schotte, A., Janssen, P.F.M., Megens, A.A.H.P., and Leysen, J.E. (1993). Occupancy of central neurotransmitter receptors by risperidone, clozapine and haloperidol, measured ex vivo by quantitative autoradiography. Brain Res *631*, 191–202.

Serwanski, D.R., Rasmussen, A.L., Brunquell, C.B., Perkins, S.S., and Nishiyama, A. (2018). Sequential Contribution of Parenchymal and Neural Stem Cell-Derived Oligodendrocyte Precursor Cells toward Remyelination. Neurogl *1*, 8.

Shigeoka, T., Jung, H., Jung, J., Turner-Bridger, B., Ohk, J., Lin, J.Q., Amieux, P.S., and Holt, C.E. (2016). Dynamic Axonal Translation in Developing and Mature Visual Circuits. Cell *166*, 181–192.

Shin, D., Shin, J.-Y., McManus, M.T., PtÃ¡cÌŒek, L.J., and Fu, Y.-H. (2009). Dicerablation in oligodendrocytes provokes neuronal impairment in mice. Ann Neurol *66*, 843–857.

Shirao, T., and Obata, K. (1986). Immunochemical homology of 3 developmentally regulated brain proteins and their developmental change in neuronal distribution. Dev Brain Res *29*, 233–244.

Sim, F.J., McClain, C.R., Schanz, S.J., Protack, T.L., Windrem, M.S., and Goldman, S.A. (2011). CD140a identifies a population of highly myelinogenic, migration-competent and efficiently engrafting human oligodendrocyte progenitor cells. Nat Biotechnol *29*, 934–941.

Simon, C., Götz, M., and Dimou, L. (2011). Progenitors in the adult cerebral cortex: Cell cycle properties and regulation by physiological stimuli and injury. Glia *59*, 869–881.

Simons, M., Krämer, E.-M., Macchi, P., Rathke-Hartlieb, S., Trotter, J., Nave, K.-A., and Schulz, J.B. (2002). Overexpression of the myelin proteolipid protein leads to accumulation of cholesterol and proteolipid protein in endosomes/lysosomes. The Journal of Cell Biology *157*, 327–336.

Simpson, P.B., and Armstrong, R.C. (1999). Intracellular signals and cytoskeletal elements involved in oligodendrocyte progenitor migration. Glia *26*, 22–35.

Sinclair, J.L., Fischl, M.J., Alexandrova, O., Heβ, M., Grothe, B., Leibold, C., and Kopp-Scheinpflug, C. (2017). Sound-Evoked Activity Influences Myelination of Brainstem Axons in the Trapezoid Body. J Neurosci *37*, 8239–8255.

Snaidero, N., and Simons, M. (2014). Myelination at a glance. Journal of Cell Science *127*, 2999–3004.

Snaidero, N., Möbius, W., Czopka, T., Hekking, L., Mathisen, C., Verkleij, D., Goebbels, S., Edgar, J., Merkler, D., Lyons, D.A., et al. (2014). Myelin Membrane Wrapping of CNS Axons by PI(3,4,5)P3-Dependent Polarized Growth at the Inner Tongue. *156*.

Sobczak, I., Galabova-Kovacs, G., Sadzak, I., Kren, A., Christofori, G., and Baccarini, M. (2008). B-Raf is required for ERK activation and tumor progression in a mouse model of pancreatic beta-cell carcinogenesis. Oncogene *27*, 4779–4787.

Sohn, J., Natale, J., Chew, L.-J., Belachew, S., Cheng, Y., Aguirre, A., Lytle, J., Nait-Oumesmar, B., Kerninon, C., Kanai-Azuma, M., et al. (2006). Identification of Sox17 as a Transcription Factor That Regulates Oligodendrocyte Development. J Neurosci *26*, 9722–9735.

Sontheimer, H., Trotter, J., Schachner, M., and Kettenmann, H. (1989). Channel expression correlates with differentiation stage during the development of Oligodendrocytes from their precursor cells in culture. Neuron *2*, 1135–1145.

Spitzer, S.O., Sitnikov, S., Kamen, Y., Evans, K.A., Kronenberg-Versteeg, D., Dietmann, S., Faria, O. de, Agathou, S., and Káradóttir, R.T. (2019). Oligodendrocyte Progenitor Cells Become Regionally Diverse and Heterogeneous with Age. Neuron *101*, 459-471.e5.

Stankewich, M.C., Gwynn, B., Ardito, T., Ji, L., Kim, J., Robledo, R.F., Lux, S.E., Peters, L.L., and Morrow, J.S. (2010). Targeted deletion of III spectrin impairs synaptogenesis and generates ataxic and seizure phenotypes. Proc National Acad Sci *107*, 6022–6027.

Stariha, R.L., Kikuchi, S., Siow, Y.L., Pelech, S.L., Kim, M., and Kim, S.U. (2002). Role of Extracellular Signal-Regulated Protein Kinases 1 and 2 in Oligodendroglial Process Extension. J Neurochem *68*, 945–953.

Stedehouder, J., Brizee, D., Shpak, G., and Kushner, S.A. (2018). Activity-Dependent Myelination of Parvalbumin Interneurons Mediated by Axonal Morphological Plasticity. J Neurosci Official J Soc Neurosci *38*, 3631–3642.

Stephenson, J.R., Wang, X., Perfitt, T.L., Parrish, W.P., Shonesy, B.C., Marks, C.R., Mortlock, D.P., Nakagawa, T., Sutcliffe, J.S., and Colbran, R.J. (2017). A Novel Human CAMK2A Mutation Disrupts Dendritic Morphology and Synaptic Transmission, and Causes ASD-Related Behaviors. J Neurosci *37*, 2216–2233.

Stevens, B., Porta, S., Haak, L.L., Gallo, V., and Fields, R. (2002). Adenosine: a neuron-glial transmitter promoting myelination in the CNS in response to action potentials. *36*.

Stolt, C., Rehberg, S., Ader, M., and & … L.-P. (2002). Terminal differentiation of myelin-forming oligodendrocytes depends on the transcription factor Sox10.

Stolt, C.C., Schlierf, A., Lommes, P., Hillgärtner, S., Werner, T., Kosian, T., Sock, E., Kessaris, N., Richardson, W.D., Lefebvre, V., et al. (2006). SoxD Proteins Influence Multiple Stages of Oligodendrocyte Development and Modulate SoxE Protein Function. Dev Cell *11*, 697–709.

Strelau, J., and Unsicker, K. (1999). GDNF family members and their receptors: Expression and functions in two oligodendroglial cell lines representing distinct stages of oligodendroglial development. Glia *26*, 291–301.

Sturrock, R.R. (1980). MYELINATION OF THE MOUSE CORPUS CALLOSUM. Neuropath Appl Neuro *6*, 415–420.

Stys, P.K. (2011). The axo-myelinic synapse. Trends Neurosci *34*, 393–400.

Sugimoto, Y., Taniguchi, M., Yagi, T., Akagi, Y., Nojyo, Y., and Tamamaki, N. (2001). Guidance of glial precursor cell migration by secreted cues in the developing optic nerve. Dev Camb Engl *128*, 3321–3330.

Sun, L.O., Mulinyawe, S.B., Collins, H.Y., Ibrahim, A., Li, Q., Simon, D.J., Tessier-Lavigne, M., and Barres, B.A. (2018). Spatiotemporal Control of CNS Myelination by Oligodendrocyte Programmed Cell Death through the TFEB-PUMA Axis. Cell *175*, 1811-1826.e21.

Susuki, K., Raphael, A.R., Ogawa, Y., Stankewich, M.C., Peles, E., Talbot, W.S., and Rasband, M.N. (2011). Schwann cell spectrins modulate peripheral nerve myelination. Proc National Acad Sci *108*, 8009–8014.

Susuki, K., Zollinger, D.R., Chang, K.-J., Zhang, C., Huang, C.Y.-M., Tsai, C.-R., Galiano, M.R., Liu, Y., Benusa, S.D., Yermakov, L.M., et al. (2018). Glial βII Spectrin Contributes to Paranode Formation and Maintenance. J Neurosci *38*, 6063–6075.

Suzuki, N., Fukushi, M., Kosaki, K., Doyle, A.D., Vega, S. de, Yoshizaki, K., Akazawa, C., Arikawa-Hirasawa, E., and Yamada, Y. (2012). Teneurin-4 is a novel regulator of oligodendrocyte differentiation and myelination of small-diameter axons in the CNS. J Neurosci Official J Soc Neurosci *32*, 11586–11599.

Swiss, V.A., Nguyen, T., Dugas, J., Ibrahim, A., Barres, B., Androulakis, I.P., and Casaccia, P. (2011). Identification of a Gene Regulatory Network Necessary for the Initiation of Oligodendrocyte Differentiation. Plos One *6*, e18088.

Tait, S., Gunn-Moore, F., Collinson, M.J., Huang, J., Lubetzki, C., Pedraza, L., Sherman, D.L., Colman, D.R., and Brophy, P.J. (2000). An Oligodendrocyte Cell Adhesion Molecule at the Site of Assembly of the Paranodal Axo-Glial Junction. The Journal of Cell Biology *150*, 657–666.

Takahashi, H., Sekino, Y., Tanaka, S., Mizui, T., Kishi, S., and Shirao, T. (2003). Drebrin-Dependent Actin Clustering in Dendritic Filopodia Governs Synaptic Targeting of Postsynaptic Density-95 and Dendritic Spine Morphogenesis. J Neurosci *23*, 6586–6595.

Takeuchi, H., Sekiguchi, A., Taki, Y., Yokoyama, S., Yomogida, Y., Komuro, N., Yamanouchi, T., Suzuki, S., and Kawashima, R. (2010). Training of Working Memory Impacts Structural Connectivity. J Neurosci *30*, 3297–3303.

Tang, A., Thickbroom, G., and Rodger, J. (2017). Repetitive Transcranial Magnetic Stimulation of the Brain. Neurosci *23*, 82–94.

Taveggia, C., Zanazzi, G., Petrylak, A., Yano, H., Rosenbluth, J., Einheber, S., Xu, X., Esper, R.M., Loeb, J.A., Shrager, P., et al. (2005). Neuregulin-1 Type III Determines the Ensheathment Fate of Axons. Neuron *47*, 681–694.

Taveggia, C., Thaker, P., Petrylak, A., Caporaso, G.L., Toews, A., Falls, D.L., Einheber, S., and Salzer, J.L. (2007). Type III neuregulin-1 promotes oligodendrocyte myelination. Glia *56*, 284–293.

Tawk, M., Makoukji, J., Belle, M., Fonte, C., Trousson, A., Hawkins, T., Li, H., Ghandour, S., Schumacher, M., and Massaad, C. (2011). Wnt/ -Catenin Signaling Is an Essential and Direct Driver of Myelin Gene Expression and Myelinogenesis. J Neurosci *31*, 3729–3742.

Tebaldi, T., Re, A., Viero, G., Pegoretti, I., Passerini, A., Blanzieri, E., and Quattrone, A. (2012). Widespread uncoupling between transcriptome and translatome variations after a stimulus in mammalian cells. Bmc Genomics *13*, 220.

Tiane, A., Schepers, M., Rombaut, B., Hupperts, R., Prickaerts, J., Hellings, N., Hove, D. van den, and Vanmierlo, T. (2019). From OPC to Oligodendrocyte: An Epigenetic Journey. Cells *8*, 1236.

Titterness, A.K., Wiebe, E., Kwasnica, A., Keyes, G., and Christie, B.R. (2011). Voluntary exercise does not enhance long-term potentiation in the adolescent female dentate gyrus. Neuroscience *183*, 25–31.

Tomassy, G.S., Berger, D.R., Chen, H.-H., Kasthuri, N., Hayworth, K.J., Vercelli, A., Seung, H.S., Lichtman, J.W., and Arlotta, P. (2014). Distinct profiles of myelin distribution along single axons of pyramidal neurons in the neocortex. Sci New York N Y *344*, 319–324.

Tran, N.M., Shekhar, K., Whitney, I.E., Jacobi, A., Benhar, I., Hong, G., Yan, W., Adiconis, X., Arnold, M.E., Lee, J.M., et al. (2019). Single-Cell Profiles of Retinal Ganglion Cells Differing in Resilience to Injury Reveal Neuroprotective Genes. Neuron *104*, 1039-1055.e12.

Trapp, B.D., Nishiyama, A., Cheng, D., and Macklin, W. (1997). Differentiation and Death of Premyelinating Oligodendrocytes in Developing Rodent Brain. J Cell Biol *137*, 459–468.

Tsai, H.-H., Tessier-Lavigne, M., and Miller, R.H. (2003). Netrin 1 mediates spinal cord oligodendrocyte precursor dispersal. Development *130*, 2095–2105.

Tsai, H.-H., Niu, J., Munji, R., Davalos, D., Chang, J., Zhang, H., Tien, A.-C., Kuo, C.J., Chan, J.R., Daneman, R., et al. (2016). Oligodendrocyte precursors migrate along vasculature in the developing nervous system. Science *351*, 379–384.

Tyler, W.A., Gangoli, N., Gokina, P., Kim, H.A., Covey, M., Levison, S.W., and Wood, T.L. (2009). Activation of the Mammalian Target of Rapamycin (mTOR) Is Essential for Oligodendrocyte Differentiation. J Neurosci *29*, 6367–6378.

Tyler, W.A., Jain, M.R., Cifelli, S.E., Li, Q., Ku, L., Feng, Y., Li, H., and Wood, T.L. (2011). Proteomic identification of novel targets regulated by the mammalian target of rapamycin pathway during oligodendrocyte differentiation. Glia *59*, 1754–1769.

Vallstedt, A., Klos, J.M., and Ericson, J. (2005). Multiple Dorsoventral Origins of Oligodendrocyte Generation in the Spinal Cord and Hindbrain. Neuron *45*, 55–67.

Varshney, G.K., Pei, W., LaFave, M.C., Idol, J., Xu, L., Gallardo, V., Carrington, B., Bishop, K., Jones, M., Li, M., et al. (2015). High-throughput gene targeting and phenotyping in zebrafish using CRISPR/Cas9. Genome Res *25*, 1030–1042.

Vélez-Fort, M., Maldonado, P.P., Butt, A.M., Audinat, E., and Angulo, M.C. (2010). Postnatal switch from synaptic to extrasynaptic transmission between interneurons and NG2 cells. J Neurosci Official J Soc Neurosci *30*, 6921–6929.

Venezia, A.C., Guth, L.M., Sapp, R.M., Spangenburg, E.E., and Roth, S.M. (2016). Sex-dependent and independent effects of long-term voluntary wheel running on Bdnf mRNA and protein expression. Physiol Behav *156*, 8–15.

Venkatesh, H.S., Johung, T.B., Caretti, V., Noll, A., Tang, Y., Nagaraja, S., Gibson, E.M., Mount, C.W., Polepalli, J., Mitra, S.S., et al. (2015). Neuronal Activity Promotes Glioma Growth through Neuroligin-3 Secretion. Cell *161*, 803–816.

Viganò, F., Schneider, S., Cimino, M., Bonfanti, E., Gelosa, P., Sironi, L., Abbracchio, M.P., and Dimou, L. (2016). GPR17 expressing NG2-Glia: Oligodendrocyte progenitors serving as a reserve pool after injury. Glia *64*, 287–299.

Vinkers, D.J., Gussekloo, J., and Westendorp, R.G.J. (2003). Leisure Activities and the Risk of Dementia. New Engl J Medicine *349*, 1290–1292.

Voas, M.G., Lyons, D.A., Naylor, S.G., Arana, N., Rasband, M.N., and Talbot, W.S. (2007). αII-Spectrin Is Essential for Assembly of the Nodes of Ranvier in Myelinated Axons. Curr Biol *17*, 562–568.

Voskuhl, R.R., Itoh, N., Tassoni, A., Matsukawa, M.A., Ren, E., Tse, V., Jang, E., Suen, T.T., and Itoh, Y. (2019). Gene expression in oligodendrocytes during remyelination reveals cholesterol homeostasis as a therapeutic target in multiple sclerosis. P Natl Acad Sci Usa *116*, 10130–10139.

Waggener, C.T., Dupree, J.L., Elgersma, Y., and Fuss, B. (2013). CaMKIIβ regulates oligodendrocyte maturation and CNS myelination. J Neurosci Official J Soc Neurosci *33*, 10453–10458.

Wahl, S., McLane, L., and of …, B.-K. (2014). Mammalian target of rapamycin promotes oligodendrocyte differentiation, initiation and extent of CNS myelination.

Wake, H., Lee, P.R., and Fields, D.R. (2011). Control of Local Protein Synthesis and Initial Events in Myelination by Action Potentials. *333*.

Wang, H., Moyano, A.L., Ma, Z., Deng, Y., Lin, Y., Zhao, C., Zhang, L., Jiang, M., He, X., Ma, Z., et al. (2017). miR-219 Cooperates with miR-338 in Myelination and Promotes Myelin Repair in the CNS. Dev Cell *40*, 566-582.e5.

Wang, S., Sdrulla, A., Johnson, J.E., Yokota, Y., and Barres, B.A. (2001). A role for the helix-loop-helix protein Id2 in the control of oligodendrocyte development. Neuron *29*, 603–614.

Waxman, S.G. (1980). Determinants of conduction velocity in myelinated nerve fibers. Muscle Nerve *3*, 141–150.

Wei, Q., Miskimins, W.K., and Miskimins, R. (2005). Stage-specific Expression of Myelin Basic Protein in Oligodendrocytes Involves Nkx2.2-mediated Repression That Is Relieved by the Sp1 Transcription Factor. J Biol Chem *280*, 16284–16294.

Weng, Q., Chen, Y., Wang, H., Xu, X., Yang, B., He, Q., Shou, W., Chen, Y., Higashi, Y., van den Berghe, V., et al. (2012). Dual-Mode Modulation of Smad Signaling by Smad-Interacting Protein Sip1 Is Required for Myelination in the Central Nervous System. Neuron *73*, 713–728.

Werner, H.B., Kuhlmann, K., Shen, S., Uecker, M., Schardt, A., Dimova, K., Orfaniotou, F., Dhaunchak, A., Brinkmann, B.G., Möbius, W., et al. (2007). Proteolipid Protein Is Required for Transport of Sirtuin 2 into CNS Myelin. The Journal of Neuroscience *27*, 7717–7730.

Wilkins, A., Chandran, S., and Compston, A. (2001). A role for oligodendrocyte-derived IGF-1 in trophic support of cortical neurons. Glia *36*, 48–57.

Wilkins, A., Majed, H., Layfield, R., Compston, A., and Chandran, S. (2003). Oligodendrocytes Promote Neuronal Survival and Axonal Length by Distinct Intracellular Mechanisms: A Novel Role for Oligodendrocyte-Derived Glial Cell Line-Derived Neurotrophic Factor. Journal of Neuroscience *23*, 4967–4974.

Williamson, J.M., and Lyons, D.A. (2018). Myelin Dynamics Throughout Life: An Ever-Changing Landscape? Front Cell Neurosci *12*, 424.

Wong, A.W., Xiao, J., Kemper, D., Kilpatrick, T.J., and Murray, S.S. (2013). Oligodendroglial expression of TrkB independently regulates myelination and progenitor cell proliferation. J Neurosci Official J Soc Neurosci *33*, 4947–4957.

Wu, L.M.N., Williams, A., Delaney, A., Sherman, D.L., and Brophy, P.J. (2012). Increasing internodal distance in myelinated nerves accelerates nerve conduction to a flat maximum. Curr Biology Cb *22*, 1957–1961.

Wu, R.S., Lam, I.I., Clay, H., Duong, D.N., Deo, R.C., and Coughlin, S.R. (2018). A Rapid Method for Directed Gene Knockout for Screening in G0 Zebrafish. Developmental Cell *46*, 112-125.e4.

Xiao, J., Wong, A.W., Willingham, M.M., Buuse, M. van den, Kilpatrick, T.J., and Murray, S.S. (2011). Brain-Derived Neurotrophic Factor Promotes Central Nervous System Myelination via a Direct Effect upon Oligodendrocytes. Neurosignals *18*, 186–202.

Xiao, J., Ferner, A.H., Wong, A.W., Denham, M., Kilpatrick, T.J., and Murray, S.S. (2012). Extracellular signal-regulated kinase 1/2 signaling promotes oligodendrocyte myelination in vitro. J Neurochem *122*, 1167–1180.

Xiao, L., Ohayon, D., McKenzie, I., Sinclair-Wilson, A., Wright, J., Fudge, A., Emery, B., Li, H., and Richardson, W. (2016). Rapid production of new oligodendrocytes is required in the earliest stages of motor-skill learning. *19*.

Xing, Y.L., Röth, P.T., Stratton, J.A.S., Chuang, B.H.A., Danne, J., Ellis, S.L., Ng, S.W., Kilpatrick, T.J., and Merson, T.D. (2014). Adult Neural Precursor Cells from the Subventricular Zone Contribute Significantly to Oligodendrocyte Regeneration and Remyelination. J Neurosci *34*, 14128–14146.

Ye, F., Chen, Y., Hoang, T., Montgomery, R.L., Zhao, X., Bu, H., Hu, T., Taketo, M.M., Es, J.H. van, Clevers, H., et al. (2009). HDAC1 and HDAC2 regulate oligodendrocyte differentiation by disrupting the beta-catenin-TCF interaction. Nature Neuroscience *12*, 829–838.

Yim, S.H., Hammer, J.A., and Quarles, R.H. (2001). Differences in signal transduction pathways by which platelet-derived and fibroblast growth factors activate extracellular signal-regulated kinase in differentiating oligodendrocytes. J Neurochem *76*, 1925–1934.

Younes-Rapozo, V., Felgueiras, L.O.R., Viana, N.L., Fierro, I.M., Barja-Fidalgo, C., Manhães, A.C., and Barradas, P.C. (2009). A role for the MAPK/ERK pathway in oligodendroglial differentiation in vitro: stage specific effects on cell branching. Int J Dev Neurosci *27*, 757–768.

Young, K.M., Psachoulia, K., Tripathi, R.B., Dunn, S.-J., Cossell, L., Attwell, D., Tohyama, K., and Richardson, W.D. (2013). Oligodendrocyte Dynamics in the Healthy Adult CNS: Evidence for Myelin Remodeling. *77*.

Yu, Y., Chen, Y., Kim, B., Wang, H., Zhao, C., He, X., Liu, L., Liu, W., Wu, L., Mao, M., et al. (2013). Olig2 Targets Chromatin Remodelers to Enhancers to Initiate Oligodendrocyte Differentiation. Cell *152*, 248–261.

Zangenehpour, S., and Chaudhuri, A. (2002). Differential induction and decay curves of c-fos and zif268 revealed through dual activity maps. Mol Brain Res *109*, 221–225.

Zeller, N., Behar, T., Dubois-Dalcq, M., and Lazzarini, R. (1985). The timely expression of myelin basic protein gene in cultured rat brain oligodendrocytes is independent of continuous neuronal influences. J Neurosci *5*, 2955–2962.

Zhang, C., Susuki, K., Zollinger, D., Dupree, J., and Rasband, M.N. (2013). Membrane domain organization of myelinated axons requires βII spectrin. J Gen Physiology *142*, 1426OIA45.

Zhang, N., Xing, M., Wang, Y., Tao, H., and Cheng, Y. (2015a). Repetitive transcranial magnetic stimulation enhances spatial learning and synaptic plasticity via the VEGF and BDNF–NMDAR pathways in a rat model of vascular dementia. Neuroscience *311*, 284–291.

Zhang, Y., Chen, K., Sloan, S., Bennett, M., Scholze, A., O'Keeffe, S., Phatnani, H., Guarnieri, P., Caneda, C., Ruderisch, N., et al. (2014a). An RNA-Sequencing Transcriptome and Splicing Database of Glia, Neurons, and Vascular Cells of the Cerebral Cortex. *34*.

Zhang, Y., Sloan, S.A., Clarke, L.E., Caneda, C., Plaza, C.A., Blumenthal, P.D., Vogel, H., Steinberg, G.K., Edwards, M.S.B., Li, G., et al. (2015b). Purification and Characterization of Progenitor and Mature Human Astrocytes Reveals Transcriptional and Functional Differences with Mouse. Neuron *89*, 37–53.

Zhang, Z., Jhaveri, D.J., Marshall, V.M., Bauer, D.C., Edson, J., Narayanan, R.K., Robinson, G.J., Lundberg, A.E., Bartlett, P.F., Wray, N.R., et al. (2014b). A Comparative Study of Techniques for Differential Expression Analysis on RNA-Seq Data. PLoS ONE *9*, e103207.

Zhao, X., He, X., Han, X., Yu, Y., Ye, F., Chen, Y., Hoang, T., Xu, X., Mi, Q.-S., Xin, M., et al. (2010). MicroRNA-mediated control of oligodendrocyte differentiation. Neuron *65*, 612–626.

Zhao, X., Dai, J., Ma, Y., Mi, Y., Cui, D., Ju, G., Macklin, W.B., and Jin, W. (2014). Dynamics of ten-eleven translocation hydroxylase family proteins and 5-hydroxymethylcytosine in oligodendrocyte differentiation. Glia *62*, 914–926.

Zheng, J., Sun, X., Ma, C., Li, B., and Luo, F. (2019). Voluntary wheel running promotes myelination in the motor cortex through Wnt signaling in mice. Mol Brain *12*, 85.

Zhou, Q., and Anderson, D.J. (2002). The bHLH Transcription Factors OLIG2 and OLIG1 Couple Neuronal and Glial Subtype Specification. Cell *109*, 61–73.

Zhou, Q., Choi, G., and Anderson, D.J. (2001). The bHLH transcription factor Olig2 promotes oligodendrocyte differentiation in collaboration with Nkx2.2. Neuron *31*, 791–807.

Zhu, X., Hill, R.A., Dietrich, D., Komitova, M., Suzuki, R., and Nishiyama, A. (2011). Age-dependent fate and lineage restriction of single NG2 cells. Dev Camb Engl *138*, 745–753.

Zhu, X., Zuo, H., Maher, B.J., Serwanski, D.R., LoTurco, J.J., Lu, R.Q., and Nishiyama, A. (2012). Olig2-dependent developmental fate switch of NG2 cells. Development *139*, 2299–2307.

Ziskin, J., Nishiyama, A., Rubio, M., Fukaya, M., and Bergles, D. (2007). Vesicular release of glutamate from unmyelinated axons in white matter. *10*.

Zou, Y., Jiang, W., Wang, J., Li, Z., Zhang, J., and of …, B.-J. (2014). Oligodendrocyte precursor cell-intrinsic effect of Rheb1 controls differentiation and mediates mTORC1-dependent myelination in brain.

Zuchero, B.J., Fu, M.-M., Sloan, S.A., Ibrahim, A., Olson, A., Zaremba, A., Dugas, J.C., Wienbar, S., Caprariello, A.V., Kantor, C., et al. (2015). CNS Myelin Wrapping Is Driven by Actin Disassembly. Developmental Cell *34*, 152–167.